

**Patterns of Expression of Oligodendrocyte Specific Proteins
During Development of the Mouse Brain**

By

ZhiCheng Zhou

A thesis submitted to the Faculty of Graduate Studies of

The University of Manitoba

in partial fulfillment of the requirements of the degree of

MASTER OF SCIENCE

Department of Pathology

Faculty of Medicine

University of Manitoba

Winnipeg, Manitoba

Copyright ©2008 by ZhiCheng Zhou

**THE UNIVERSITY OF MANITOBA
FACULTY OF GRADUATE STUDIES

COPYRIGHT PERMISSION**

**Patterns of Expression of Oligodendrocyte Specific Proteins
During Development of the Mouse Brain**

BY

ZhiCheng Zhou

**A Thesis/Practicum submitted to the Faculty of Graduate Studies of The University of
Manitoba in partial fulfillment of the requirement of the degree**

Of

Master of Science

ZhiCheng Zhou © 2008

Permission has been granted to the University of Manitoba Libraries to lend a copy of this thesis/practicum, to Library and Archives Canada (LAC) to lend a copy of this thesis/practicum, and to LAC's agent (UMI/ProQuest) to microfilm, sell copies and to publish an abstract of this thesis/practicum.

This reproduction or copy of this thesis has been made available by authority of the copyright owner solely for the purpose of private study and research, and may only be reproduced and copied as permitted by copyright laws or with express written authorization from the copyright owner.

ACKNOWLEDGEMENTS

I offer my sincere thanks to Dr. Emma Frost, Assistant Professor of Department of Pathology, Human Anatomy and Cell Biology, and Biochemistry and Medical Genetics, for her valuable supervision, constant guidance, enthusiasm and encouragement in my studies in pursuit of my Master's Degree in Science. Not only did she allow me to enter into the research field, but she provided a most excellent learning experience. I appreciate her sharing knowledge and expertise with me. She showed great patience with me during my academic pursuits.

My thanks also go to Dr. Mary Lynn Duckworth, Associate Professor of Department of Physiology and Dr. Cindy Ellison, Assistant Professor of Department of Pathology and Immunology, for serving on my advisory committee and providing valuable suggestions for the project and thesis.

Special recognition is extended to Jan Mustapha for her experimental assistance and inspirational friendship. In addition, I would like to express my gratitude to the rest of the 531 lab who have not been mentioned here by name, but have furthered my educational progress. Further, Joan Gordon, who has coached me in English skills, deserves my commendation.

Most of all, heartfelt thanks go to my husband, Lan Xu, my dear parents, JiQuan Zhou and GuoYing Jiang. Their encouragement and unwavering belief in me through countless obstacles have been invaluable.

This research project was funded by the Dr. Paul H.T. Thorlakson Foundation and the Children's Hospital Foundation of Manitoba.

ABSTRACT

Oligodendrocytes (OL), the CNS myelinating cell, originate in discrete areas of the developing brain. Myelination is preceded by migration, proliferation, and differentiation. Platelet-derived growth factor AA (PDGF) is a critical regulator of OL progenitor (OP) development. This project investigates the regulatory role of PDGF in OPs migration, and maps expression patterns of PDGF and its receptor during the mouse brain development. In addition, this study investigates the intracellular signaling pathways involved in OP migration. This study shows that PDGF-R α immunoreactivity is restricted to the expected location of migrating OPs at the earliest stage, and spreads out as the brain develops. In contrast, PDGF immunoreactivity is localized throughout the developing mouse brain. In addition, this study shows that transient exposure to PDGF can induce OP migration for up to 72 hours without affecting cell proliferation and cell death. Further, PDGF induced OP migration is regulated via extracellular regulated kinase signaling.

TABLE OF CONTENTS

Acknowledgements	i
Abstract	ii
Table of Contents	iii
List of Figures	vii
List of Table	ix
List of Abbreviations	x
Chapter I. Introduction	1
The Nervous System	2
Myelination	5
The Differences between Schwann Cells and Oligodendrocytes.....	6
Mechanism.....	8
Structure.....	10
<i>The Structure of the Node of Ranvier</i>	10
<i>Myelin Proteins</i>	11
<i>Proteolipid Protein (PLP)</i>	12
<i>Myelin Basic Protein (MBP)</i>	12
<i>Other Myelin Protein</i>	13
Nature or Function of the Myelin Sheath	16
Disorder of myelination	18
Dysmyelination.....	18

Demyelination.....	19
Oligodendrocyte Origin and Lineage.....	20
Five Stages.....	21
Factors Regulating Oligodendrocyte.....	24
<i>PDGF</i>	24
<i>CXCL1</i>	27
Chapter II. Objectives and Hypotheses.....	29
Rationale and Objectives.....	30
Hypotheses.....	31
Chapter III. Materials and Methods.....	32
Materials.....	33
Animal Source.....	33
Chemicals.....	33
Methods.....	34
Cryosectioning.....	34
Immunohistochemistry.....	36
CXCL1 Staining.....	36
Oligodendrocyte Isolation.....	37
Agarose Drop Migration Assay.....	39
Proliferation Assay.....	40
Activated Caspase-3 Staining.....	41
Western Blot.....	42
Statistical Analysis.....	43

Chapter IV. Regulation of OP Migration.....	44
Introduction.....	45
Migration Assay.....	48
The Effect of Short Term Exposure (30 minutes) PDGF-A on OPs Migration.....	49
The Change of OP Cell Density in Response to Transient and Continuous Exposure to PDGF-A.....	50
The Effect of the OP Proliferation Inhibitor, AMPA, on OPs Migration.....	51
The Effect of ERK Signaling in PDGF-A Induced OPs Migration.....	52
Western Blot.....	54
Activated Caspase-3 Staining.....	57
The Effect of PDGF-A Withdrawal on OPs Death.....	57
Proliferation Assay.....	59
The Effect of Transient PDGF-A Exposure on OPs Proliferation.....	59
Results.....	60
Chapter V. PDGF Ligand and Receptor Expression in the Developing Mouse	
Brain.....	62
Introduction.....	63
PDGF-A and PDGF-Rα Expression in the Mouse Brain.....	65
PDGF-A Expression Pictures from E11 to E19.....	66
PDGF-R α Expression Pictures from E11 to P7.....	80
Results.....	108
Chapter VI. CXCL1 Expression in the Developing Mouse Brain.....	109
Introduction.....	110

CXCL1 Expression in the Mouse Brain.....	111
CXCL1 Expression Pictures from P2 to P7.....	113
Results.....	125
Chapter VII. Discussion.....	126
Transient Exposure to PDGF-A Induces OPs Migration for up to 72 Hours.....	129
PDGF-A Withdrawal.....	130
ERK Signaling Regulates PDGF Induced OPs Migration.....	131
PDGF Ligand and Receptor Expression in the Developing Mouse Brain.....	132
CXCL1 Expression in the Developing Mouse Brain.....	134
Chapter VIII. Conclusions.....	136
Chapter IX. Future Directions.....	139
Chapter X. References.....	141

List of Figures

Figure 1.1. Oligodendrocyte (OL) and it myelinates axons of the neurons.....	4
Figure 1.2. Myelinated axon in the PNS (A) and CNS (B).....	7
Figure 1.3. Myelin in the CNS.....	14
Figure 1.4. The structure of the compact myelin.....	15
Figure 1.5. The OL lineage.....	23
Figure 4.1. Schematic view of the MAPK signaling pathway.....	47
Figure 4.2. Effect of short term exposure (30 minutes) to PDGF-A on OPs migration....	49
Figure 4.3. Change of OP cell density in response to transient and continuous exposure to PDGF-A.....	50
Figure 4.4. Effect of the OP proliferation inhibitor, AMPA, on OPs migration.....	51
Figure 4.5. Effect of the ERK signaling inhibitor, U0126, on OPs migration.....	53
Figure 4.6. ERK phosphorylation in OPs.....	55
Figure 4.7. Activated caspase-3 in OPs.....	58
Figure 4.8. Transient PDGF-A exposure on OPs proliferation.....	59
Figure 5.1. PDGF-A expression at E11.5 in the mouse brain.....	66
Figure 5.2. PDGF-A expression at E12.5 in the mouse brain.....	68
Figure 5.3. PDGF-A expression at E14.5 in the mouse brain.....	70
Figure 5.4. PDGF-A expression at E16.5 in the mouse brain.....	72
Figure 5.5. PDGF-A expression at E17.5 in the mouse brain.....	74
Figure 5.6. PDGF-A expression at E18.5 in the mouse brain.....	76
Figure 5.7. PDGF-A expression at E19.5 in the mouse brain.....	78
Figure 5.8. PDGF-R α expression at E11.5 in the mouse brain.....	80

Figure 5.9. PDGF-R α expression at E12.5 in the mouse brain.....	82
Figure 5.10. PDGF-R α expression at E13.5 in the mouse brain.....	84
Figure 5.11. PDGF-R α expression at E14.5 in the mouse brain.....	86
Figure 5.12. PDGF-R α expression at E16.5 in the mouse brain.....	88
Figure 5.13. PDGF-R α expression at E17.5 in the mouse brain.....	90
Figure 5.14. PDGF-R α expression at E18.5 in the mouse brain.....	92
Figure 5.15. PDGF-R α expression at E19.5 in the mouse brain.....	94
Figure 5.16. PDGF-R α expression at P2 in the mouse brain.....	96
Figure 5.17. PDGF-R α expression at P3 in the mouse brain.....	98
Figure 5.18. PDGF-R α expression at P4 in the mouse brain.....	100
Figure 5.19. PDGF-R α expression at P5 in the mouse brain.....	102
Figure 5.20. PDGF-R α expression at P6 in the mouse brain.....	104
Figure 5.21. PDGF-R α expression at P7 in the mouse brain.....	106
Figure 6.1. CXCL1 expression at P2 in the mouse brain.....	113
Figure 6.2. CXCL1 expression at P3 in the mouse brain.....	115
Figure 6.3. CXCL1 expression at P4 in the mouse brain.....	117
Figure 6.4. CXCL1 expression at P5 in the mouse brain.....	119
Figure 6.5. CXCL1 expression at P6 in the mouse brain.....	121
Figure 6.6. CXCL1 expression at P7 in the mouse brain.....	123

List of Table

Table 1.1. Receptor specifically binding to the five different isoforms of PDGF.....25

List of Abbreviations

AEC	3-amino-9-ethyl-carbazole
AMPA	alpha-amino-3-hydroxy-5-methyl-4-isoxazolepropionic acid
BrdU	bromodeoxyuridine
BSA	bovine serum albumin
C	cysteine
°C	degrees Celsius
CNPase	2', 3'-cyclic nucleotide 3'-phosphohydrolase
CNS	central nervous system
CO ₂	carbon dioxide
CXCL1	chemokine (C-X-C motif) ligand 1
CXCR2	CXC receptor type 2
DAPI	4'6- diamidino-2-phenylindole
DFG	Dulbecco's Modified Eagle's Medium with 5000U penicillin and streptomycin, 4mM L-Glutamine and 10% fetal bovine serum
DMEM	Dulbecco's Modified Eagle's Medium
DMF	N,N-Dimethylformamide
E8	embryonic day 8
ERK	extracellular regulated kinase
FBS	fetal bovine serum
FITC	fluorescein isothiocyanate
FGF	fibroblast growth factor
GAP	guanosine triphosphatase activating protein
GAPDH	glyceraldehyde-3-phosphate dehydrogenase
GGF	glial growth factor
GM	germinal matrix
Grb2	growth factor receptor binding protein 2
GTPase	guanosine triphosphatase
HRP	horseradish peroxidase
IL-8	interleukin-8
JNK	c-jun NH2-terminal protein kinase
MAG	myelin-associated glycoprotein
MAPK	mitogen activated protein kinase
MBP	myelin basic protein
MEK	MAP/ extracellular-related kinase
MEME	Minimum Essential Medium Eagle
MHC	myosin heavy chain
ML	metachromatic leukodystrophy
MLC	myosin light chain
MLCK	myosin light chain kinase
MOG	myelin oligodendrocyte glycoprotein
MPK	MAPK phosphatase
MS	multiple sclerosis
NDS	normal donkey serum
NGS	normal goat serum

OL	oligodendrocyte
OP	oligodendrocyte progenitor
OSP	OL specific protein
P1	postnatal day 1
PBS	phosphate buffered saline
PD098059	2'-amino-3'-methoxyflavone
PDGF	platelet-derived growth factor
PDGF-A	platelet-derived growth factor AA
PDGF-R α	platelet-derived growth factor receptor alpha
PDL	poly-D-lysine
pERK	phosphorylated extracellular regulated kinase
PI ₃ -kinase	phosphatidylinositol 3'-kinase
PLC- γ	phospholipase C- γ
PLP	proteolipid protein
PNS	peripheral nervous system
rpm	revolutions per minute
RTK	receptor tyrosine kinase
SDF-1 α	stromal cell-derived factor-1 alpha
SoS	son of sevenless
SVZ	subventricular zone
T3	Tri-iodothyroxine
T4	thyroxine
TBS-T	Tris-buffered saline containing 0.5% Tween-20
U0126	1,4-diamino-2,3-dicyano-1,4-bis (2-aminophenylthio)-butadiene

Chapter I

Introduction

The Nervous System

A healthy nervous system is characterized by some critical factors, such as the precisely constructed organization and the efficient transduction of the nerve impulses along the axon. Therefore, clearly understanding the organization of the brain is essential in studying its functions.

The nervous system is a complex network. It encompasses the peripheral nervous system (PNS) and the central nervous system (CNS), both of which closely interact, thus enabling the PNS to transmit messages or signals to and from the CNS.

Two principal cell types of the nervous system are neurons and glial cells. In the human brain, there are billions of neurons that process information and convey signals. Most neurons have a tapered extension of cell body called dendrites and one long, cylindrical process called an axon. The neurons are primarily the functional circuit. They transmit signals from one to the other, with dendrites receiving information from other neurons. The neuronal processes, or axons, transmit information away from the cell body. Translated from Greek, “glia” means “glue”. Glial cells are a major cellular component of the nervous system, ten times more in number than neurons in the human brain (Ndubaku and de Bellard, 2008).

Historically, glial cells were so called because they occupy most of the spaces between neurons.

For many years, glial cells were regarded as the supportive cells for neurons, providing structural and metabolic support, responding to nervous system infection and damage, and producing the insulating myelin sheath. In the last 20 years,

however, glial cells have been found to play a variety of important roles in brain development. For example, glial cells regulate neuronal migration during early development, shape the vital scaffold for neuronal structure and play significant roles in synaptic formation, structure and nerve impulse transmission (Ndubaku and de Bellard, 2008).

There are three types of glial cells: OLs, microglial cells and astrocytes, each of which has a distinct morphology and characteristic functions. Astrocytes are star-shaped, hence the name “astrocyte”. Microglial cells are also stellate but much smaller, and function as the immune cells of the CNS. OLs are octopus-shaped, having fewer branches than axons have dendrites. “Oligodendro” is historically known in Greek as “a tree with fewer and smaller branches”.

This research project is a study and investigation into a specific part of the nervous system, which in its complexity is still not well understood. The cell of choice for this study is the OL, in particular the patterns of OL protein expression from embryonic to postnatal stage in the mouse brain were studied. OLs myelinate the axon of the neurons to produce insulating sheaths (Figure 1.1). The wrapping of the axon provides a physical basis for rapid communication between neurons by hastening the speed of the nerve impulse or action potential to reach its destination.

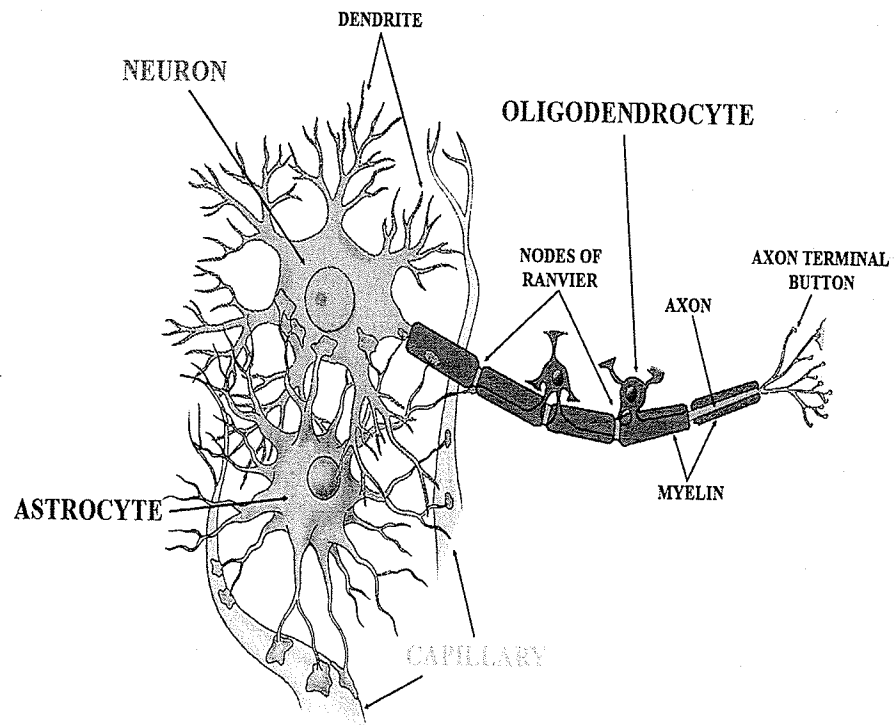


Figure 1.1. OL and it myelinates axons of the neurons. Diagram is drawn by Dr.

Emma Frost.

OL is octopus-shaped, having several processes.

Its plasma membrane spirally wraps around the portions of the axons to form the concentric multilayer of myelin.

Myelination

As mentioned, a healthy nervous system is characterized by the efficient nerve impulse or action potential conduction along the axon, and the effective conduction of nerve impulse is facilitated by a mechanism known as saltatory conductance, which will be explored in more detail below. An intact myelin system is crucial in preventing a loss of electric impulse along the myelinated axon, thereby facilitating the efficient conduction of effective nerve impulses from neuron to neuron. In this way, myelination is essential for the normal function of a healthy nervous system.

Myelination is a developmental process and the entire procedure varies among species. In most vertebrates, myelination of the CNS occurs after birth (Miller, 2002). For instance, myelination in a horse is almost completed by postnatal day 45 (Szalay, 2001), whereas during human brain development, it is considerably extended till the third decade of life (Fields, 2008).

Myelin exists only in vertebrates, both in the PNS and CNS (Fields, 2008).

White matter is the area where myelinated axons predominate. It is so named because many axons are coated with myelin sheaths that are mostly lipid, resulting in a fatty, white appearance.

In the nervous system, the two most abundant cells, Schwann cells and OLs, are responsible for generating the myelin sheath in the PNS and CNS respectively (Ndubaku and de Bellard, 2008). Both cells express specific proteins and lipids to assemble the myelin sheath, which are composed of multiple layers of compacted cell

membrane wrapped around the axon (Dyer, 2002; Fields, 2008). Some of the differences between those two cells will be highlighted below.

The Differences between Schwann Cells and OLs

The two differences between the two myelin-forming cells are summarized below:

1. An individual Schwann cell can only wrap around one single axon at a time. On the contrary, several processes of an OL extend out from the cell until reaching an axon and enveloping around a segment of it. Hence, one single OL is able to ensheath up to 50 axons (Bjartmar et al., 1994), all of which have different neuronal origins (Figure 1.2).

2. Schwann cells exit the cell cycle during the final maturation stage of the lineage. However, Schwann cell has the ability to reenter the cell cycle and de-differentiate (Zujovic et al., 2007). Once reconnecting with axons, Schwann cell can redifferentiate and remyelinate (Zujovic et al., 2007). In contrast, OL does not have such feature.

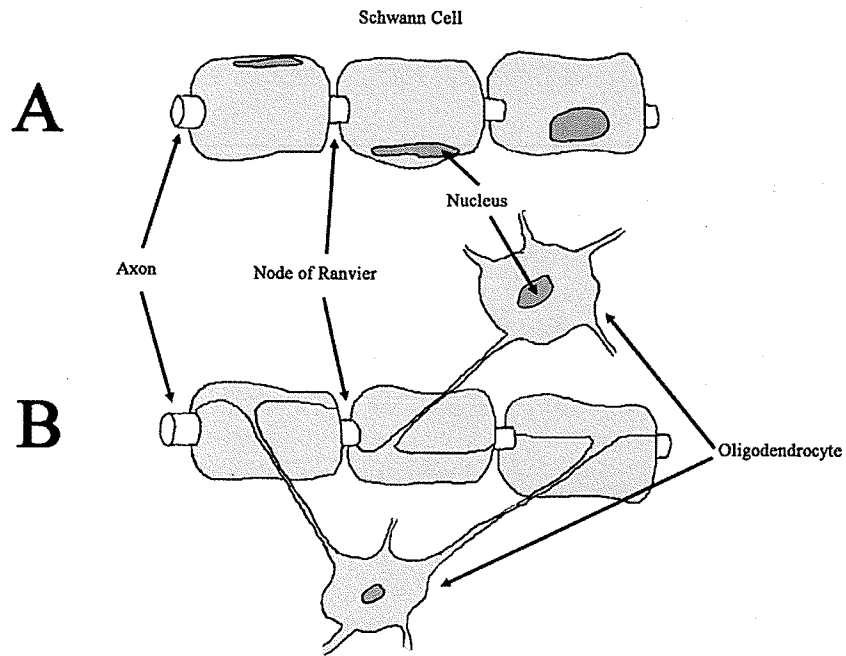


Figure 1.2. Myelinated axon in the PNS (A) and CNS (B). Diagram is drawn by Dr. Emma Frost.

The myelin sheath is a segmented, discontinuous layer. The exposed area between two adjoining segments of an axon is called the node of Ranvier.

Panel A: In the PNS, several Schwann cells wrap around a single axon.

Panel B: In the CNS, one single OL wraps more than one axon, all of which have different neuronal origins.

Mechanism

As mentioned, myelination is critical for a healthy nervous system. It is apparent that careful molecular orchestration plays a pivotal role in assembling the myelin. However, the mechanism of myelination still remains unclear. There are many unanswered questions: how does the complex process work? What are the regulatory signals? How do these signals regulate the different stages? These questions need to be individually answered to fully understand the regulatory mechanisms involved.

The following sequential steps are known to be crucial:

1. OLs migrate to the axons to be myelinated at the appropriate developmental time;
2. OLs proliferate and polarize the pathways for transporting the extensions of the OL plasma membrane to the axon, ensuring the delivery of myelin components to the glial axon contact site;
3. OL processes adhere to the axon and deliver newly synthesized myelin specific lipids and proteins;
4. OL processes spiral around the axon with the recognition of the space to be myelinated;
5. Myelin membrane compaction occurs due to specific lipids and proteins interactions.

It is acknowledged that OLs migration, proliferation and differentiation are crucial to the success of these multiple steps (Baumann and Pham-Dinh, 2001).

The myelination is known to occur in a rostral to caudal direction in the human brain (Kinney et al., 1988; Looney and Elberger, 1986). Conversely, Vincze found that myelination took place first in the caudal area in the mouse corpus callosum (Vincze et al., 2008).

Furthermore, neurons themselves have been found to regulate membrane trafficking in OLs by reducing endocytosis and increasing transportation of proteolipid protein (PLP), the major myelin protein, to the plasma membrane (Trajkovic et al., 2006). Likewise, OLs and myelin may also stimulate neurons development and maturation by increasing the axonal caliber (Windebank et al., 1985; Vincze et al., 2008).

In addition, other factors are known to modulate myelin development. For example, experiments by Zalc and Fields indicated that nerve impulse activity is important to myelin formation in optic nerve development, and the firing pattern of axons may influence myelination (Zalc and Fields, 2000).

There is also some evidence suggesting that environmental factors might influence myelination. For instance, pregnant rats were exposed to a restraint stress once a day during the late gestation. This stress leads to hypermyelination in the offspring of rats (Wiggins and Gottesfeld, 1986). As well, the myelinated axons are increased in the corpus callosum of rats when raised in an enriched environment (Juraska and Kopcik, 1988).

Structure

In myelinated neurons, most of the axon is wrapped by myelin. Unlike other membranes, myelin has elevated lipid content, containing 70% lipids and 30% proteins (Baumann and Pham-Dinh, 2001). For comparison, mitochondrial inner membrane contains 76% protein and only 24% lipid. Plasma membranes of human red blood cells and mouse liver contain nearly equal amounts of proteins 44, 49% and lipids 43, 52% respectively.

The Structure of the Node of Ranvier

Electron microscopy is a useful tool to better understand the delicate structure of the myelin. The myelin sheath is interrupted at regular intervals where the axolemma, the axonal membrane, is exposed. These exposed portions between adjoining portions of the myelin sheath are termed the nodes of Ranvier where sodium ion channels are clustered. Kaplan et al showed that OLs are required to induce sodium channel clustering (Kaplan et al., 1997). The myelin structure between two nodes is called an internode where multi layers of compact myelin are wrapped (Figure 1.3.). The internodes are sealed by compacted myelin sheath, thereby restricting current flow at the nodes of Ranvier (Fields, 2008).

Accordingly, the segmental structure allows the nerve impulses or action potentials to propagate by jumping from node to node or skipping the myelinated areas. This type of impulse transduction is known as saltatory conductance (Huxley and Stampfli, 1949). “Saltatory” stems from a Latin word which means “to leap or

to dance”. More detail about the saltatory conductance will be discussed in the “nature or function of the myelin sheath”.

In addition, two other specialized areas of the myelin sheath have been identified:

1. The adjacent paranode where the myelin adheres to the axon by cell-adhesion molecules.
2. The juxtaparanode where the potassium ion channels are located.

The compact myelin sheath when viewed transversely, is composed of tight junctions and adherent junctions (Dyer, 2002). The former are where three major constituent proteins are located: 2, 3- cyclic nucleotide 3'- phosphohydrolase (CNPase), actin filaments and tubules, all of which contribute to the construction of cytoskeletal veins of the compact myelin sheath (Dyer, 2002). The latter, containing PLP and myelin basic protein (MBP), are the areas where the major and minor dense lines localize (Dyer, 2002). The cytoplasmic interfaces combine to form the major dense lines and two extracellular faces constitute the minor dense lines (Baumann and Pham-Dinh, 2001) (Figure 1.4.).

Myelin Proteins

The two major structural proteins of myelin are PLP (and isoform DM-20) and MBP. PLP is synthesized in the endoplasmic reticulum and then transported to the plasma membrane by vesicular transport (Simons and Trotter, 2007). On the contrary, MBP is synthesized at the myelin membrane by local mRNAs translation,

which may prevent non specific adhesion to the membranes (Simons and Trotter, 2007).

PLP

PLP constitutes 50% of myelin proteins (Baumann and Pham-Dinh, 2001). PLP binds to other PLP proteins which reside in the next loop of the myelin spirals. The network of PLPs results in the close apposition of the outer membranes of adjoining myelin sheath. Mutations involving PLP gives rise to the Jimpy mouse, in which OL death and dysmyelination occur. In this mouse, the myelin sheaths are thinner than normal and the myelin compaction is abnormal (Campagnoni and Skoff, 2001). The Jimpy mouse is regarded as a model of Pelizaeus-Merzbacher disease, where mental and motor coordination are disrupted (Mikoshiha et al., 1991). However, even without PLP expression, OLs are still capable of assembling myelin sheaths, indicating PLP is not critical for the formation of myelin (Garbern, 2007). However, it is critical for the normal structure of myelin.

MBP

MBP is the second most abundant myelin protein, comprising 30% of the myelin proteins (Baumann and Pham-Dinh, 2001). MBPs are located at the cytoplasmic side of the membrane. They interact with lipids, which are also at the cytoplasmic side of the membrane, to stabilize the myelin. Correspondingly, a MBP

mutation results in the Shiverer mouse, in which the major dense line is missing (Privat et al., 1979).

It is likely that highly positive charged MBPs binding a negatively charged cytoplasmic membrane is critical for compact myelin formation (Harauz et al., 2004). Fitzner demonstrated that MBP plays a role in forming the myelin lipid bilayer by increasing lipid packing (Fitzner et al., 2006). MBP may act as a lipid coupler which either brings the different layers of myelin together or clusters the lipid bilayer to help facilitate myelin sheath formation (Fitzner et al., 2006).

Other Myelin Protein

In the CNS myelin, OL specific protein (OSP), also known as Claudin-11, is the third most abundant myelin protein, representing 7% of the myelin proteins. It is required to form the tight junctions (Bajramovic et al., 2008; Dyer, 2002).

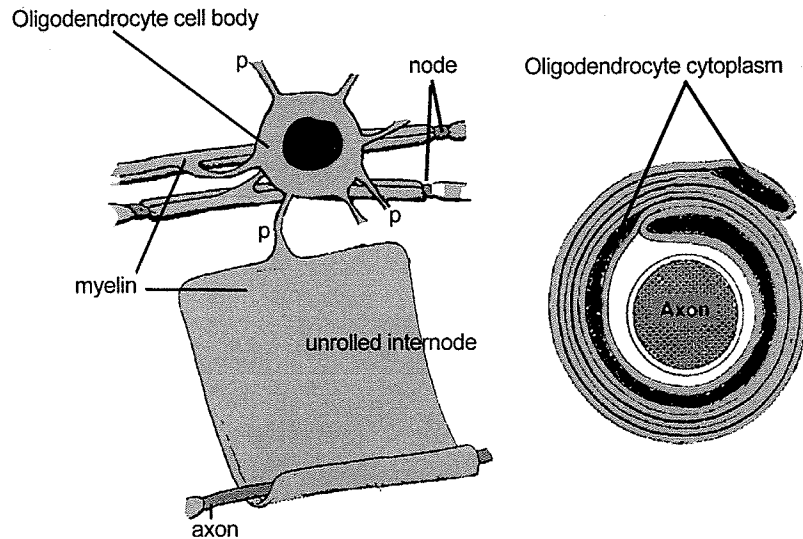


Figure 1.3. Myelin in the CNS. Diagram is drawn by Dr. Emma Frost.

Several processes (P) of an OL extend out from the cell, each process gives rise to an extension that wraps around a segment of the axon to form an internode resulting in a multiple layers appearance. Most of the internode is composed of firmly wrapped membranes and OL cytoplasm. The bare axon between the internodes is the node of Ranvier.

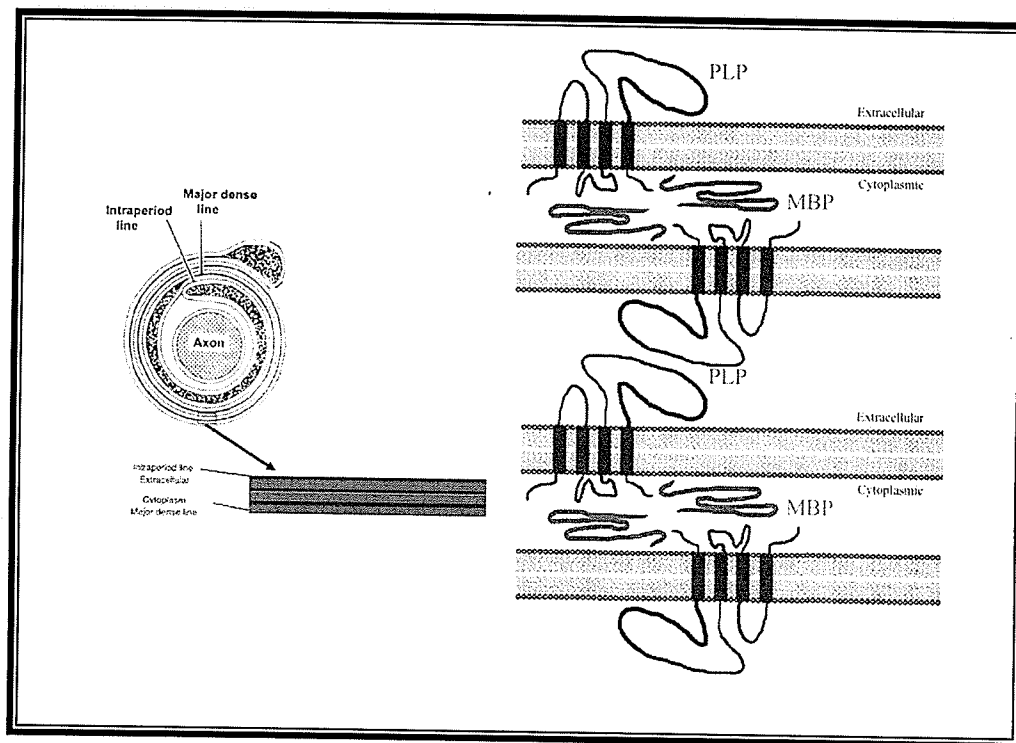


Figure 1.4. The structure of the compact myelin. Diagram is drawn by Dr. Emma Frost.

Myelin sheath is a lipid bilayer which contains several large proteins. MBP locates at the cytoplasmic site between the lipid bilayer. Two cytoplasmic sites fuse together to form the major dense line (red). PLP locates at the extracellular surface of the lipid bilayer, and two extracellular surfaces form the intraperiodic line (blue).

Nature or Function of the Myelin Sheath

The myelin sheath's unique structure and composition, as described, is essential to build a membrane with high electrical resistance and low capacitance to prevent current loss during nerve impulse conduction. Furthermore, in contrast to the invertebrate nervous system where the fast nerve conduction is achieved by increased axonal diameter, the myelin sheath has three main advantages: high-speed conduction, fidelity of transmitting signaling over long distance and space economy. The saltatory conductance contributes to all of these (Baumann and Pham-Dinh, 2001).

As stated, the mechanism by which myelinated axons conduct nerve impulse is saltatory conduction. In contrast, the propagation speed of unmyelinated axons is directly proportional to the axon diameter, thereby, nerve impulse progresses in a slow and continuous manner (Zalc et al., 2008). In addition, the signal may get lost or lose its strength as it travels through the unmyelinated axon. For example, it takes longer for a signal of an unmyelinated axon of a heat sensor in the finger to travel to the brain, than that of the myelinated axons of the pain receptor. Myelinated axons conduct nerve impulse 50 to 100 times faster than non-myelinated axons which have the same diameter (Zalc et al., 2008).

Further, by saltatory conductance, fewer ions enter or leave the axon during membrane potential changes and less energy is required by the sodium-potassium exchange pump. Hence, energy is saved for the action potential conduction. By adding faster nerve transmission, the myelin sheaths are able to achieve an efficient and effective action potential conduction.

The myelin not only hastens the speed of nerve impulse, but also regulates it by several features, such as the diameter of the axon, the thickness of the myelin sheath, the number and the structure of nodes of Ranvier, as well as the distribution of ion channels (Fields, 2008).

New findings also indicate that myelin has additional functions besides being an insulator. For instance, the myelin sheath maintains the ionic balance in the periaxonal space by distributing channels for ions such as sodium, potassium and chloride (Dyer, 2002). It also plays a role in maintaining axonal integrity (Simons and Trotter, 2007). In addition, it maintains the axon caliber to ensure normal conduction of the action potential by acting as a water exchange pump (Dyer, 2002). Myelin, on the other hand, is also capable of inhibiting axonal growth and regeneration (Simons and Trotter, 2007; Baumann and Pham-Dinh, 2001). Moreover, myelin proteins such as Nogo-A and myelin-associated glycoprotein (MAG) modulate synapse formation by suppressing axon sprouting (Chen et al., 2000; McKerracher et al., 1994).

In humans, the myelin function facilitates cognitive development, and the learning and memory development of young children (Zalc and Fields, 2000; Fields, 2008). It is known that decision-making skills are not fully developed in adolescence. This observation could be explained by incomplete myelination of the frontal lobes, which regulate higher reasoning, until the early twenties (Giedd, 2004). In addition, numerous disorders of the brain associated with dysfunctional

myelination, further prove the functional importance of myelin; this will be explored in greater detail below.

Disorder of Myelination

To properly acknowledge the importance of the myelin, it is worthwhile examining neurological disorders. For example, incorrect myelination, leading to failure to conduct nerve impulses, may lead to paralysis, sensory-motor dysfunction, cognitive impairment, mental retardation and even death (Fields, 2008).

There are two major disorders of myelin: dysmyelination and demyelination. The dysmyelinating disorders are characterized by abnormality in myelin formation, resulting in dysfunctional myelin. In most cases, heritable conditions affect the biosynthesis and formation of myelin, causing the dysmyelination disorders. Demyelinating disorders are characterized by the damage or loss of the myelin sheath. Often the cause is unknown, however, autoimmune, toxic, metabolic, infectious or traumatic conditions are factors that are associated with demyelination. A variety of nervous system and psychiatric disorders, then, are related to the abnormal myelin sheath formation or damaged myelin.

Dysmyelination

The leukodystrophies are a group of rare CNS diseases affecting myelin, the major component of white matter (Lyon et al., 2006). Metachromatic leukodystrophy (ML), the most common form of leukodystrophy, is an autosomal recessive disorder with the incidence of 1 per 40,000 to 100,000 (Lyon et al., 2006).

ML is caused by lack of activity of the lysosomal enzyme, arylsulfatase, resulting in the accumulation of sulfatides, which in turn cause myelin breakdown (Lyon et al., 2006). Both central and peripheral white matter can be involved. The histopathologic finding is diffuse, confluent loss of myelin that is most advanced in the cerebrum. Most patients suffer the onset in infancy, usually between 18 and 24 months (Lyon et al., 2006). Death occurs by the end of the first decade (Lyon et al., 2006). However, two other onset forms exist: juvenile and adult (Lyon et al., 2006). Gait abnormalities, ataxia, nystagmus, hypotonia, diffuse spasticity and pathologic reflexes are common symptoms.

Pelizaeus-Merzbacher disease, making up 6.5% of all leukodystrophies, is an X linked myelin disorder, showing a total absence of myelin (Koeppen et al., 2002). Mutation of the PLP gene has been shown to be the cause of Pelizaeus-Merzbacher disease (Lyon et al., 2006). This rare CNS disease progresses slowly (Garbern, 2007). The patients present symptoms in the neonatal period with classic signs including ataxia, nystagmus, spastic quadriparesis and cognitive delay in early childhood (Lyon et al., 2006; Garbern, 2007). Affected individuals may survive into the second to fourth decades of life (Lyon et al., 2006).

Demyelination

Multiple sclerosis (MS) is the most well known neurological disorder of the white matter, characterized by multiple areas of demyelination within the CNS. 40% of MS patients show impaired cognitive ability (Kujala et al., 1997). The pathological findings include inflammation, astrocyte scarring, loss of OLs and

consequent destruction of myelin (Storch and Lassmann, 1997; Omari et al., 2006). Although the pathogenesis of demyelination is not well understood, it is agreed that T lymphocytes, mediating an immune response against the myelin, trigger the disease (Storch and Lassmann, 1997).

Recently, damaged myelin has also been discovered in the brains of normal aged individuals, and of schizophrenic patients (Miller, 2007). Several experiments have proved that the length of myelinated axons decreases with age in the human brain (Hinman and Abraham, 2007).

Schizophrenia, major depression and bipolar disorder fall in the realm of psychiatric disorders. Hakak used gene expression studies analyzing thousands of genes from schizophrenia brains. He found 35 myelin genes were abnormally regulated (Hakak et al., 2001). Post mortem studies of brain tissue from patients suffering from schizophrenia, major depression and bipolar disorder found a decreased number of mRNA transcripts of myelin genes and genes modulating OLs (Tkachev et al., 2003; Aston et al., 2005).

Oligodendrocyte Origin and Lineage

OPs initially appear in discrete areas of the developing CNS, such as the embryonic telecephalon (Rakic and Zecevic, 2003; Menn et al., 2006), the ganglionic eminences (Kessar et al., 2006) and the sub-ventricular or sub-ependymal zone (Miller, 1996). These areas consist of highly proliferative precursor cells, which ultimately produce neural and glial progenitor cells.

OPs migrate extensive distances from the site of origin to their final location where they will myelinate the axon. Subsequently, OPs start to proliferate and generate a sufficient population of cells, prior to differentiating into mature OLs. The mature OLs are capable of populating putative white matter tracts, such as the corpus callosum (Levison and Goldman, 1993). Thereby, OPs disperse extensively radially and tangentially throughout the brain (Suzuki and Goldman, 2003). To date, the mechanisms underlying these developmental stages are not well understood.

Experiments on the adult brain reveal that adult SVZ continues to be a source of neurons and OPs (Menn et al., 2006). Menn and his colleagues used SVZ type B cells or astrocytes to generate OLs and neurons successfully in vivo and in vitro. More importantly, the number of OPs derived from the adult SVZ type B cells increased significantly. These OPs were found within or around the demyelination areas, suggesting that adult SVZ type B cells contribute to repair myelin after the development of a demyelinating lesion (Menn et al., 2006).

Five Stages

In the developing rat CNS, at least five developmental stages are identified based on morphology, behavioral characteristic and antigenic expression (Figure 1.5.) (Armstrong, 1998). OLs originate as progenitors, with a simple bi-polar morphology. The progenitors are highly migratory and actively proliferating. As the cell differentiates, it undergoes a vast morphological change to form a large network with multiple branching processes. At this stage, the cell has reduced

proliferative capacity, yet is not generating myelin. The cell eventually differentiates into a mature, myelin sheath-producing OL.

Different antigenic markers are used to identify the different stages of the lineage. OL pre-progenitor cells express high levels of PDGF receptor alpha (PDGF-R α) (Pringle and Richardson, 1993), or the proteoglycan NG2 (Nishiyama et al., 1996), OPs also express cell surface ganglioside which is recognized by the monoclonal antibody A2B5, (Raff et al., 1983) or the single ganglioside G_{D3} (Levi et al., 1987).

Eventually, with the differentiation of OP, another cell surface ganglioside, termed O4 is expressed. As the cell differentiates into pre-myelinating OLs, some surface or intracellular antigens disappear and new ones are acquired. Although expression of A2B5 and G_{D3} is lost, O4 expression is still maintained, and another ganglioside is newly expressed, termed O1. Furthermore, the pre-myelinating OLs express myelin proteins, for example PLP and its isoform DM-20 (Fruttiger et al., 1999) and MBP (Lin et al., 2006). Later markers are MAG and myelin oligodendrocyte glycoprotein (MOG), at the final stage of differentiation (Li et al., 1994; Duchala et al., 1995). Different stages of the OL lineage can be identified by these specific cell markers.

Most OPs expressing proteoglycan NG2 differentiate into mature myelinating OLs, but some remain at the immature stage and the rest undergo programmed cell death (Polito and Reynolds, 2005; Bozzali and Wrabetz, 2004).

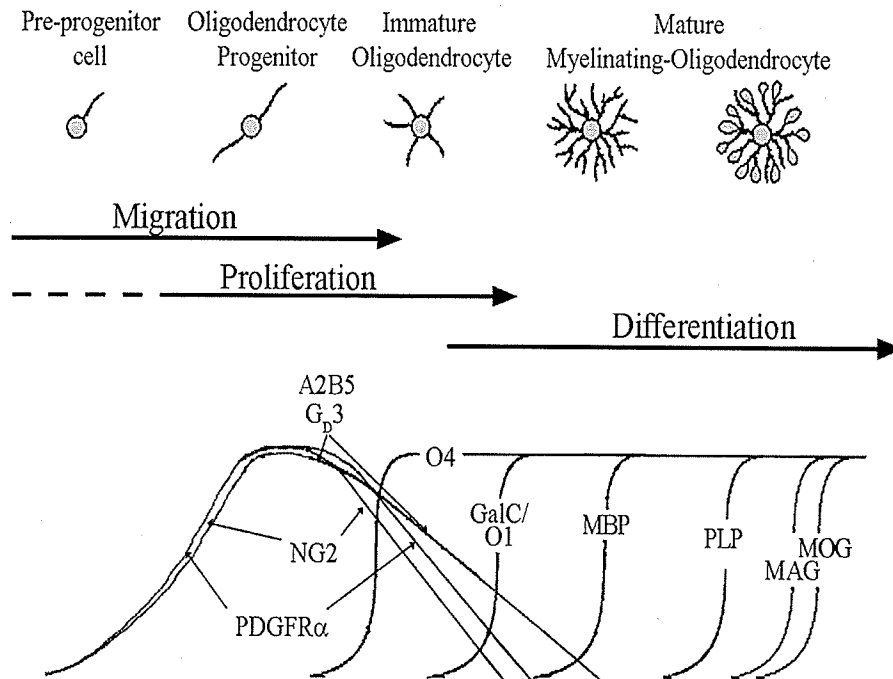


Figure 1.5. The OL lineage. Diagram is drawn by Dr. Emma Frost.

The names of the cell type are listed at the top, from the pre-progenitor cell, oligodendrocyte progenitor, immature oligodendrocyte to the mature myelinating-oligodendrocyte (left to the right).

The morphological change develops from very simple to complex. The three behavioral characteristics are: migration, proliferation and differentiation. The different antigenic markers are used to identify different stage of lineage. OPs express PDGF-R α , NG2, A2B5 and G_p3. As those markers decline, some other markers take over, such as O4, O1, and myelin proteins: MBP and PLP. Late markers comprise MOG and MAG, at the late stage of the differentiation.

Factors Regulating Oligodendrocyte

OL development is carefully orchestrated on the basis of a complex series of migration, proliferation and differentiation events. A broad range of growth factors have been postulated to regulate the development of OLs, including fibroblast growth factor-2 (FGF-2), glial growth factor-2 (GGF-2) and PDGF-A (Frost et al., 2003; Miller, 2007).

PDGF

Among these growth factors, the most significant and best characterized is PDGF-A. PDGF is so called because it was originally isolated from platelets and has been found to play an important role in vascular biology (Soriano, 1997). PDGF was one of the growth factors which was first characterized as well as being the most studied. Study of PDGF has led to an understanding of many different signaling pathways.

In the CNS, PDGF-A is synthesized widely by different cells such as neurons, astrocytes and OLs (Fruttiger et al., 1999; Heldin and Westermark, 1999). PDGFs are homodimers or heterodimers consisting of two polypeptide chains (Fredriksson et al., 2004). There are five different isoforms: AA, AB, BB, CC and DD (Fredriksson et al., 2004). These isoforms achieve their effects via plasma membrane receptors: the alpha and beta isoforms (PDGF-R α and PDGF-R β), which may combine to form homo or hetero dimers: $\alpha\alpha$, $\alpha\beta$ and $\beta\beta$ (Soriano, 1997). PDGF-R α can bind to both

PDGF-A and PDGF-B, while PDGF-R β only binds PDGF dimer containing B chains (see table 1.1.) (Pringle et al., 1992).

Receptor \ Ligand	AA	AB	BB	CC	DD
$\alpha\alpha$	√	√	√	√	
$\alpha\beta$		√	√	√	
$\beta\beta$			√		√

Table 1.1. Receptor specifically binding to the five different isoforms of PDGF (Fredriksson et al., 2004)

These receptors are members of the tyrosine kinase receptor family. Binding to the receptors by extracellular ligand-binding domains activates an intracellular tyrosine kinase domain triggering a series of events known as the tyrosine kinase cascade:

1. Receptor dimerization activates tyrosine kinase;
2. Autophosphorylation of tyrosine residue occurs both inside and outside the kinase domain, leading to elevated catalytic efficiencies of the kinases and creating docking sites for SH2 domains;
3. Binding of SH2 domain and further initiation of signal transmission. A number of SH2 domain containing proteins are able to bind to either PDGF-R α or PDGF-R β , such as phosphatidylinositol 3'-kinase (PI₃-kinase) and phospholipase C - γ (PLC- γ) and a guanosine triphosphatase (GTPase) activating protein (GAP)

for Ras. (Pringle et al., 1992; Oumesmar et al., 1997; Klinghoffer et al., 2001; Heldin and Westermark, 1999).

During OPs development, PDGF is known to be a potent mitogen which promotes proliferation. It also regulates precursor motility and survival (Tsai et al., 2002; Frost et al., 2003; Barres et al., 1993). PDGF has been shown to be essential for normal myelination of the CNS during brain development (Soriano, 1997). PDGF is also involved in the regulation of OPs migration, differentiation and survival (Calver et al., 1998; Armstrong et al., 1991; Frost et al., 1996; Frost et al., 2008; Barres et al., 1993; Noble et al., 1988). Over-expression of PDGF in a transgenic mouse results in the hyperproliferation of OPs (Calver et al., 1998). Experiments using knockout mouse models proved that PDGF-A, but not PDGF-B, is necessary in spinal cord development (Fruttiger et al., 1999). PDGF-A knockout mouse embryos have severely reduced numbers of PDGF-R α positive OPs at different sites, such as the spinal cord, optic nerve, cerebellum and those embryos that survive postnatally are severely hypo-myelinated (Fruttiger et al., 1999). The PDGF-R α knockout phenotype is severe and includes mesodermal and neural crest cell migration defects, leading to death between embryonic day 8 (E8) and E16 (Soriano, 1997). In addition, PDGF-R α knockout mice exhibit subepidermal blebs, skeletal abnormalities and bleeding (Soriano, 1997). PDGF-R α is considered to be the only PDGF receptor expressed by OL. Further studies are required to identify the role of the B, C and D isoforms of PDGF in OL lineage regulation.

PDGF is not the only extracellular signaling molecule that is important in regulating the development of OL. PDGF might act in concert with other environmental signals to influence OPs behavior. Chemokine (C-X-C motif) ligand 1 (CXCL1) is such a candidate (Robinson et al., 1998; Tsai et al., 2002).

CXCL1

Chemokines or chemoattractant cytokines are a family of proteins that primarily regulates leukocyte migration (Amiri and Richmond, 2003). Chemokines are categorized into four groups: CXC, CC, C and CX₃C, which are based on the location of the first two of four conserved cysteine (C) residues within the mature proteins (Amiri and Richmond, 2003). The CXC chemokines are defined as one amino acid residue separating the first two conserved cysteines. The CC chemokines have adjacent conserved cysteines at the first two residues. The C chemokines lack the first two conserved cysteine residues while the CX₃C has three amino acid residues separating the first two cysteines (Amiri and Richmond, 2003).

The first isolated chemokine family member CXCL1, which is a homologue of interleukin-8 (IL-8), is a high affinity ligand for the CXC receptor type 2 (CXCR2). CXCL1 has proved to have a range of functions, such as modulating inflammation, angiogenesis, wound healing and tumorigenesis (Amiri and Richmond, 2003). In addition, CXCL1 is the first chemokine that was identified as having a proliferative effect on rat OPs (Robinson et al., 1998). Robinson et al discovered that CXCL1

expression is correlated with OPs proliferation (Robinson et al., 1998), which significantly increased knowledge of the local control of OPs proliferation.

In combination with PDGF, CXCL1 regulates myelination by inhibiting OPs migration as well as promoting cell proliferation, both of which are mediated through the interaction with its receptor CXCR2, suggesting that both CXCL1 and CXCR2 contribute to the modulation of normal myelination (Robinson et al., 1998; Tsai et al., 2002). More detail about CXCL1 regulation of OP will be discussed in Chapter VI.

Chapter II

Objectives and Hypotheses

Rationale and Objectives

Many previous studies have demonstrated that PDGF-A plays a significant role in the distribution of OPs during brain development (Calver et al., 1998; Armstrong et al., 1991; Frost et al., 1996; Frost et al 2008; Barres et al., 1993; Noble et al., 1988). The growth factor, PDGF-A acts as not only a powerful motogen for OPs, but also an important factor regulating OPs migration, proliferation, differentiation and survival (Calver et al., 1998; Armstrong et al., 1991; Frost et al., 1996; Frost et al 2008; Barres et al., 1993; Noble et al., 1988). In addition, the chemokine, CXCL1 synergizes with PDGF-A to regulate OPs migration, proliferation and myelination (Robinson et al., 1998; Tsai et al., 2002; Fillpovic and Zecevic, 2008). Furthermore, it has previously been thought that there is a gradient of PDGF-A concentrations drawing OPs away from their site of origin. However the presence of a concentration gradient has never been experimentally identified. In addition, previous studies have indicated that PDGF-A is expressed throughout the developing brain (Calver et al., 1998; Hutchins and Jefferson, 1992; Miller, 2002). Therefore, the main objectives of this research project are:

1. To clarify the role of PDGF-A in regulating OPs migration.
2. To map the expression patterns of PDGF-A and its receptor PDGF-R α during development of the mouse brain.
3. To map the expression patterns of CXCL1 and its receptor CXCR2 during development of the mouse brain.

Hypotheses

The underlying hypotheses of the research project are:

1. PDGF-A regulates OP migration via extracellular regulated kinase (ERK) signaling.
2. PDGF-R α expression is restricted to the location of OPs in the CNS, and its ligand PDGF-A is expressed throughout embryonic brain development.
3. CXCL1 expression is ubiquitous throughout the postnatal stage as brain develops and the expression of its receptor CXCR2 is similar to PDGF-R α .

Chapter III
Materials and Methods

Materials

Animal Source

This project was performed using pregnant adult and postnatal C57BL/6 mice, and postnatal day 1(P1) Sprague-Dawley rats, purchased from the Central Animal Care Services, Faculty of Medicine, University of Manitoba (Winnipeg, Manitoba, Canada). All animal experiments were conducted under University of Manitoba Protocol Management and Review Committee approved animal use protocols and conformed to the Canadian Council on Animal Care.

Chemicals

Unless otherwise specified, all chemicals were purchased from Sigma-Aldrich, Inc. (St. Louis, MO, U.S.A) and were of analytical grade. OCT cryocompound was from Fisher Scientific Company (Ottawa, ON, Canada). PDGF-A was from Research & Diagnostics Systems, Inc. (Minneapolis, MN, U.S.A). Bromodeoxyuridine (BrdU) was from Boehringer Ingelheim GmbH (Ingelheim, Germany). Monoclonal anti-BrdU antibody was from Becton, Dickinson and Company (Mississauga, ON, Canada). Rabbit polyclonal anti-activated caspase-3 was from BioVision, Inc. (Mountain View, CA, U.S.A). Rabbit anti-PDGF-R α , rabbit anti-PDGF-A and goat anti-GRO α were purchased from Santa Cruz Biotechnology, Inc. (Santa Cruz, CA., USA). Secondary antibodies were from Jackson ImmunoResearch Laboratories, Inc. (West Grove, PA, U.S.A), using fluorescein isothiocyanate (FITC) conjugated goat anti-rabbit, FITC conjugated

F(ab')₂ fragment donkey anti-mouse IgG (H+L), peroxidase conjugated donkey anti-goat IgG and horseradish peroxidase (HRP)-conjugated secondary antibody. Antibody serum used for Western blot: polyclonal anti-phospho- ERK1/ERK2 was from Research & Diagnostics Systems, Inc. (Minneapolis, MN, U.S.A); polyclonal anti-glyceraldehyde-3-phosphate dehydrogenase (GAPDH) was from GenWay Biotech, Inc. (San Diego, CA, U.S.A). The pharmacological inhibitors used were 1,4-diamino-2,3-dicyano-1,4-bis(2-aminophenylthio)-butadiene (U0126) from EMD Chemicals Inc. (San Diego, CA, U.S.A) and alpha-amino-3-hydroxy-5-methyl-4-isoxazolepropionic acid (AMPA) from AXXORA, LLC (San Diego, CA, U.S.A). Chemilucifer ECL detection system was from Millipore Corporation (Temecula, CA, U.S.A). L-glutamine was from Invitrogen Canada Inc. (Burlington, ON, Canada). Fetal bovine serum (FBS) was from Thermo Fisher Scientific Inc. (Waltham, MA, U.S.A). Trypan blue solution was from Mediatech, Inc. (Manassas, VA, U.S.A). Methanol, alcohol, 30% hydrogen peroxide and 10% buffered formalin were from Fisher Scientific Company (Ottawa, ON, Canada).

Methods

Cryosectioning

The experimental mice were sacrificed at specific days post-conception by CO₂ asphyxiation. Death was verified by the absence of both respiration and heart beat, and a lack of response to tail and foot pinch. The mice were then pinned and the

thoraxes were opened. The right atria were snipped, and 50 ml phosphate buffered saline (PBS) containing 10 U/ml heparin and 10% buffered formalin were injected through the left ventricle to circulate through the entire vascular system which was operated by a syringe. PBS was followed by 50 ml of 10% buffered formalin, to fix the entire animal. After fixation, the uterine horns were exposed, removed in their entirety and placed into a petri dish (Fisher Scientific Company). The uterine muscle layers and the amniotic membranes were removed and the embryos were put in 10% buffered formalin for 48 hours fixation at 4°C. The embryos were then incubated in 20% followed by 30% sucrose in PBS for 2-3 days at 4°C; thereafter, the heads were dissected from the bodies, embedded in OCT cryocompound, quickly frozen on dry ice and stored at -80°C until sectioned. The postnatal mice were sacrificed as described above. The mice heads were then dissected from the bodies and fixed in 10% buffered formalin for 48 hours at 4°C. After fixation, the heads were soaked in 20% followed by 30% sucrose in PBS for 2-3 days at 4°C, thereafter, embedded in OCT cryocompound, quickly frozen on dry ice and stored at -80°C until sectioned.

During cryosectioning, the heads were mounted on the cryostat chuck. From olfactory bulb to brain stem, 12 µm sections were cut coronally on a Shandon cryotome® SME cryostat (Thermo Fisher Scientific Inc., Waltham, MA, U.S.A). One exception is E11.5 head which was cut sagittally. Serial sections were mounted on superfrost® microscope slides (Fisher Scientific Company) and stored at -80°C until stained.

Immunohistochemistry

Serial sections were immunostained for PDGF-R α and PDGF-A. The primary antibodies were visualized by fluorescently conjugated secondary antibodies. The slides were taken through the following steps: blocking with 20% normal goat serum (NGS) in PBS for 20 minutes, incubating rabbit anti-PDGF-R α – 1:50 dilution in PBS and 5% NGS for 60 minutes or rabbit anti-PDGF-A – 1:100 dilution in PBS and 5% NGS for 4 hours, goat anti-rabbit FITC conjugated antibody – 1:100 dilution in PBS for 30 minutes, nuclear staining 4'6-diamidino-2-phenylindole (DAPI) – 1:500 dilution in PBS for 5 minutes.

Negative control sections were incubated in either primary antibody alone, or secondary antibody alone, to demonstrate non-specific binding.

Images were then photographed using an Inverted Olympus IX51 with c-mounted Retiga 2000 RV monochrome camera with EXFO X- Cite metal halide fluorescence system. Image Pro 6.0 was used to capture images.

CXCL1 staining

Serial sections were stained for CXCL1 and visualized using 3-amino-9-ethyl-carbazole (AEC) staining. AEC is an enzyme reaction that deposits a reddish brown precipitation on the antibody, enhancing the signal. It provides a more stable visualization than fluorochromes.

The slides were treated in 100% methanol for 5 minutes, blocked with 5% normal donkey serum (NDS) in PBS for 30 minutes, followed by primary antibody,

goat anti-GRO α - 1:200 dilution in 5% NDS and PBS for 60 minutes and corresponding secondary antibody peroxidase conjugated donkey anti-goat IgG - 1:2500 dilution in PBS for 30 minutes.

50 mM acetate buffer was prepared as follow: 115 μ l glacial acetic acid in 100 ml deionized water to make 0.2M acetic acid; mixing together of 7.4 ml of 0.2 M acetic acid, 544 mg sodium acetate trihydrate and 75 ml deionized water to make up the 50 mM acetate buffer. After that, AEC was added to 1 ml N,N-Dimethylformamide (DMF), then diluted 1:20 in prepared 50 mM acetate buffer. Add 30% hydrogen peroxide - 1:20 dilution into AEC, DMF and acetate buffer immediately before adding to the sections, allowing color to develop. Finally, the sections were mounted in aqueous mounting medium.

Oligodendrocyte Isolation

OPs were obtained from P1 rat brain. The pups were anesthetized and decapitated. The heads were then pinned and sprayed with 70% ethanol. The brains were removed and placed into a tissue culture plastic petri dish containing Minimum Essential Medium Eagle (MEME). Working under a dissecting microscope (Fisher Scientific Company), cerebral cortexes were dissected and the meninges were removed. The clean hemispheres were then transferred into a 50 ml centrifuge tube (Corning Inc., Corning, NY, U.S.A) containing fresh MEME, thereafter, the tissue was triturated with an 18-gauge needle followed by a 21-gauge needle. The solution was then transferred to a 70 μ m cell strainer (Becton,

Dickinson and Company, Mississauga, ON, Canada) on the top of a 50 ml centrifuge tube. Cells were then centrifuged at 1000-1200 revolutions per minute (rpm) for 5 minutes and resuspended in DFG – Dulbecco's Modified Eagle's Medium (DMEM) supplemented with 5000U penicillin and streptomycin, 4mM L-glutamine and 10% FBS. The cells were then plated into 75 ml tissue culture flasks (Becton, Dickinson and Company, Mississauga, ON, Canada), which were coated with poly-D-lysine (PDL) (5µg/ml). DFG medium was changed every three days.

Approximately 7-10 days after plating, OPs and microglia were removed by shaking the flasks at 250 rpm (New Brunswick Scientific Co., Inc., Edison, NJ, U.S.A). The medium was replaced with the fresh DGF after a two hour preliminary shake, followed by a further 16-20 hours shake. The supernatant was placed in a non-coated tissue culture plastic petri dish for 25-40 minutes at 37°C, 7.5% CO₂ to allow the differential adhesion of microglial cells. The supernatant was then centrifuged at 1000-1200 rpm for 5 minutes, resuspended in Sato's modification of DMEM, the components of which were 5 µg/ml bovine insulin, 100 µg/ml bovine serum albumin (BSA) fraction V, 50 µg/ml human transferrin, 66 ng/ml progesterone, 5 ng/ml sodium selenite, 400 ng/ml thyroxine (T4) and 400 ng/ml Tri-iodothyroxine (T3). After gentle trituration, 10 µl of a 1:3 dilution of Trypan blue solution was added to 10 µl of the cell suspension, followed by cell counting using a haemocytometer (Glaswarenfabrik Karl Hecht KG, Sondheim, Germany).

Agarose Drop Migration Assay

Weigh out agarose to make 1% agarose in PBS and dissolve the solution in a microwave oven. OLs were obtained from day 1 rat pups, as described in OL isolation. Approximately 50,000 OPs per well were mixed with 1% agarose in PBS. Both cell suspensions and 1% agarose were transferred to a clean microfuge tube (Fisher Scientific Company) to make a final 0.3% agarose solution. Cell suspensions were then triturated thoroughly in 0.3% agarose, containing 10% FBS. Immediately, 1.5 μ l of cell suspension was plated at the centre of wells of 24 well tissue culture plates (MJS Biolynx Inc., Brockville, ON, Canada) which were precoated with PDL. The plates were then placed on the ice for no more than 3 minutes to allow the agarose drop to set, followed by carefully adding Sato with 0.5% FBS around the drops. After 24 hours incubation at 37°C, the supernatant was removed and replaced with defined medium containing test reagents.

The response of cells to PDGF-A in both the presence and absence of inhibitory reagents were tested. Cells were pretreated with inhibitory reagents, AMPA and U0126 at the specified concentrations for 1 to 2 hours prior to incubating in PDGF-A. The exposure times designed for PDGF-A were 30, 60, and 120 minutes, after which, the supernatant was carefully removed and replaced with serum and PDGF-A free Sato medium for 3 to 5 minutes. The medium was again replaced with serum and PDGF-A free Sato medium for the duration of the experiment.

The cells migrated away from the agarose drop in a corona and the distance was measured between the edge of the drop and the leading edge of the migrating cells

(Frost et al., 2000). The measurement was taken at 0, 90, 180 and 270° around the drop every 24 hour for 3 days, using a calibrated eyepiece graticule, in which the width of one square is equivalent to 162 μm .

Proliferation Assay

OLs were obtained from day 1 rat pups, as described in OL isolation. Twelve mm glass coverslips (Fisher Scientific Company) were coated with PDL, and 25,000 cells were plated on each coverslip. The cells were settled on the coverslips in Sato medium with 1% FBS at 37°C for 2 hours. After which time, the cells were washed using serum free Sato medium. The supernatant was then replaced with Sato medium containing 10 ng/ml PDGF-A. After 30, 60 and 120 minutes, the supernatant was removed and the coverslips washed twice with serum and PDGF-A free Sato medium. Subsequently, serum and PDGF-A free Sato medium was replaced again for 24 hours. Ten μM BrdU was then added to each well for the final 2 hours of the experiment.

The immunodetection of incorporated BrdU was assayed as follows: the cells were washed with cold HEPES buffered Minimal Essential Medium, fixed in 100% methanol at -20°C for 10 minutes, followed by treatment with 0.2% paraformaldehyde for 1 minute, 0.07 M NaOH for 7 minutes and another treatment with 2% paraformaldehyde for 3 minutes. Cells were then incubated with anti-BrdU monoclonal antibody at 0.25 $\mu\text{g/ml}$ in PBS for 60 minutes, followed by incubation in

donkey anti-mouse IgG (H+L) F(ab')₂ FITC conjugate and counter staining with DAPI.

Cell proliferation was assessed as the percentage of DAPI positive that were also BrdU positive. At least 100 cells per coverslip were counted with 3 to 4 coverslips per experiment, using an Olympus inverted IX70 microscope. For each coverslip, 5 randomly selected fields of view were counted at 10 × magnification. Total cell numbers were assessed from DAPI staining; and BrdU positive cell numbers, as assessed by fluorescent conjugated primary antibody, were recorded. Counts for each coverslip were averaged, and then the experiments were averaged to get the final data.

Activated Caspase-3 Staining

OLs were isolated and plated on the glass coverslips, as described in OL isolation and proliferation assay. After the initial PDGF-A exposure, cells were incubated in serum free Sato medium for 24 to 72 hours, after which, cells were fixed in 4% paraformaldehyde for 10 minutes. Cells were then washed twice with 1% saponin in PBS and blocked in 10% NGS. Cells were incubated in rabbit polyclonal anti-activated caspase-3 (1:20) for 1 hour and visualized using goat anti-rabbit conjugated with FITC (1:100) for 20 minutes. DAPI was then used to counter stain nuclei.

At least 3 coverslips were prepared for each experiment. For each coverslip, 7 randomly selected fields of view were counted at 10 × magnification. Total cell

numbers were recorded by counting DAPI staining; and caspase-3 positive cell numbers by counting fluorescent conjugated primary antibody, using a Zeiss Axio Imager Z1 inverted microscope with AxioCam monochrome digital camera and software. Counts for each coverslip were averaged, and then the experiments were averaged to obtain the final data.

Western Blot

OLs were obtained from day 1 rat pups, as described in OL isolation. OPs were pretreated with PDGF-A in the presence or absence of pharmacological inhibitor. Cells were treated with U0126 at the specified concentration for 30 minutes prior to a 30 minute exposure to 10 ng/ml PDGF-A. Cells were then lysed with Laemmli sample buffer and boiled at 100°C for no more than 5 minutes. Samples were stored at -80°C until analyzed. 2X sample buffer were composed of 80 ml 0.125 M Tris HCL buffer (pH6.8), 20 ml glycerol, 10 ml 2-mercaptoethanol, 4g sodium dodecyl sulfate and 1 mg bromophenol blue.

15-20 µl samples were loaded onto a 12% SDS-PAGE gel and electrophoresed for 2 hours at 100 volts. The proteins were transferred to PVDF membranes (GE Healthcare Bio-Sciences Corp., Piscataway, NJ, U.S.A), using a Panther Semidry electroblotter (Thermo Fisher Scientific Owl Separation Systems, Rochester, NY, U.S.A) at 40 mA overnight. After the transfer, blots were blocked for 1 hour with 5% skim milk in Tris-buffered saline containing 0.5% Tween-20 (TBS-T), with agitation at room temperature. The blots were then incubated at 4°C overnight with

the primary antibody, using an appropriate dilution in 5% skim milk in TBS-T (phosphorylated extracellular regulated kinase (pERK), 1:10,000; total ERK, 1:10,000; GAPDH, 1:1,000). After that, the blots were treated with HRP-conjugated secondary antibody in TBS-T for 1 hour at room temperature. By using the ECL detection kit, a luminol-HRP-chemiluminescence reaction was used to enhance the secondary signal. Finally, blots were exposed to X-ray film (Kodak Graphic Communications Company, Burnaby, BC, Canada) to visualize protein bands.

Statistical Analysis

One-way analysis of variance was used to analyze differences between migration curves, followed by Dunnett's t-test post hoc analysis. The student t-test was used to test the differences between means of cell count experiments.

Chapter IV

Regulation of OP Migration

Introduction

In the CNS, OPs initially appear in discrete areas of the developing CNS, such as the embryonic telecephalon (Rakic and Zecevic, 2003; Menn et al., 2006), the ganglionic eminences (Kessaris et al., 2006) and the SVZ or sub-ependymal zone (Miller, 1996). OP development then occurs in sequential steps, whereby OPs migrate, proliferate, and differentiate into mature OLs. Migration, in which OPs migrate extensively from their site of origin to colonize the entire CNS, is a critical step in myelination (Levison, Chuang et al., 1993; Kakita and Goldman, 1999).

A number of growth factors mediate OL development. Many studies have revealed that PDGF plays a significant role in OL development both in vivo and in vitro (Calver et al., 1998; Armstrong et al., 1991; Frost et al., 1996; Frost et al 2008; Barres et al., 1993; Noble et al., 1988). Not only is PDGF-A a powerful motogen for OPs, but also an important growth factor to promote the migration, proliferation, differentiation and survival (Calver et al., 1998; Armstrong et al., 1991; Frost et al., 1996; Frost et al 2008; Barres et al., 1993; Noble et al., 1988). Further, Soriano and Fruttiger provided persuasive evidence, using the PDGF-A and PDGF-R α knockout mice, that PDGF is pivotal to normal myelination (Soriano, 1997; Fruttiger et al., 1999).

As stated previously, five different PDGF isoforms exert their effects by activating two receptors: PDGF-R α and PDGF-R β . Both are tyrosine kinase receptors. Ligand binding results in the activation of several different intracellular signaling pathways, including PI₃-kinase, mitogen activated protein kinase (MAPK)

and PLC γ . Among these, the MAPK pathway has been demonstrated to play an important roles in OL development, such as cell growth, proliferation and death (Stariha and Kim, 2001; Wang et al., 2003).

ERK, c-jun NH2-terminal protein kinase (JNK) and p38 MAPK constitute three members of the MAPK family (Stariha and Kim, 2001; Wang et al., 2003). ERK is activated by the tyrosine kinase receptor signaling pathway composed of sequential kinases activation: Ras, Raf, MAP/ extracellular-related kinase (MEK), ERK, (Figure 4.1.) (Stariha and Kim, 2001). Further, ERK is the best characterized MAPK member in mammals and one of the major downstream signaling pathways. In addition, it has two isoforms: 44 KDa ERK1 and 42 KDa ERK2 (Stariha and Kim, 2001; Wang et al., 2003).

To date, the mechanism regulating OL development remains unclear. Therefore, this study was undertaken to clearly investigate the role of PDGF and ERK pathway underlying OL migration, using migration assay, Western blot analysis and immunohistochemistry, etc.

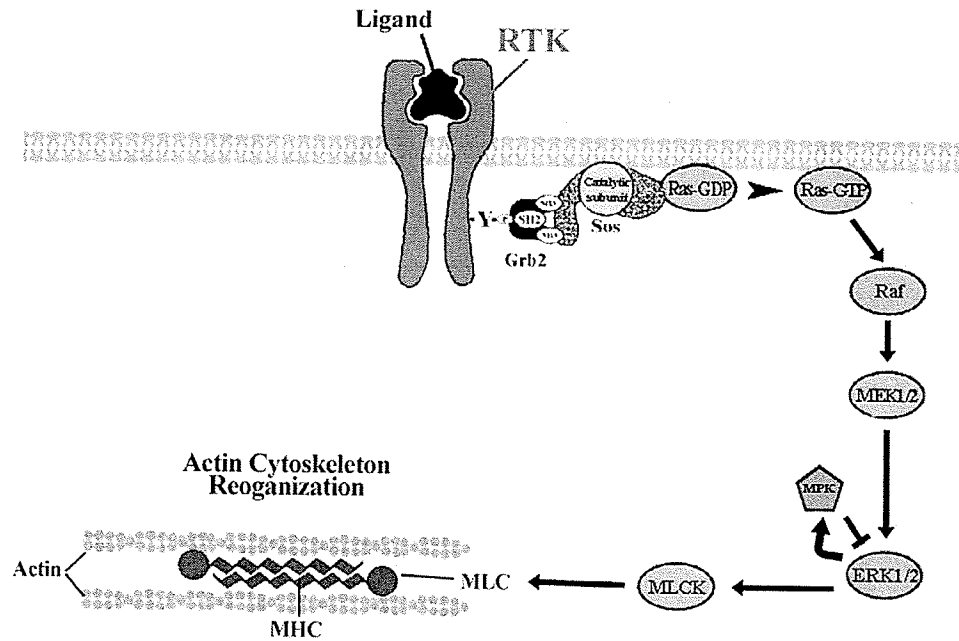


Figure 4.1. Schematic view of the MAPK signaling pathway. Figure is drawn by Dr. Emma Frost. (RTK: receptor tyrosine kinase. MHC: myosin heavy chain. MLC: myosin light chain. MLCK: myosin light chain kinase. MPK: MAPK phosphatase) ERK1/2 is triggered by PDGF binding to its receptor. The binding of PDGF ligand and receptor results in a series of events.

1. Growth factor receptor binding protein 2 (Grb2) binds to the receptor through the SH2 domain.
2. Son of sevenless (SoS) is activated through SH3 domain.
3. Ras-GDP converts to Ras-GTP by SoS acting as the exchange factor.
4. Activated Ras-GTP phosphorylates Raf.
5. Raf, in turn, activates MEK1/2.
6. MEK1/2 phosphorylates ERK1/2.
7. Actin cytoskeleton is reorganized, leading to the cell migration.

Migration Assay

The agarose drop migration assay was used to investigate OPs migration in response to PDGF-A in both the presence and absence of inhibitory reagents. The inhibitory reagents: AMPA and U0126 at the specified concentrations were used to pretreat cells for 1 to 2 hours prior to incubating in PDGF-A. The exposure times for PDGF-A were 30, 60, 120 minutes respectively, after which time, the supernatant was carefully removed and replaced with serum and PDGF-A free Sato medium for 3 to 5 minutes. Then the medium was again replaced with serum and PDGF-A free Sato medium for the duration of the experiment.

The cells migrated away from the drop in a corona and the distance was measured between the edge of the drop and the leading edge of migrating cells (Frost et al., 2000). The measurement was taken at 0, 90, 180 and 270° around the drop every 24 hour for 3 days, using a calibrated eyepiece graticule, in which the width of one square is equivalent to 162 μm .

In this study, OPs migratory distance was analyzed when OPs were exposed to PDGF-A transiently and continuously. In addition, the measurement was taken when OPs were pretreated with the OP proliferation inhibitor, AMPA and ERK signaling inhibitor, U0126.

The Effect of Short Term Exposure (30 minutes) PDGF-A on OPs Migration

Exposure to PDGF-A at 10 ng/ml for 30 minutes resulted in $917.0 \pm 8.6 \mu\text{m}$ migration, compared to $973.3 \pm 6.6 \mu\text{m}$ migration when the cells were exposed to PDGF-A continuously (Figure. 4.2.).

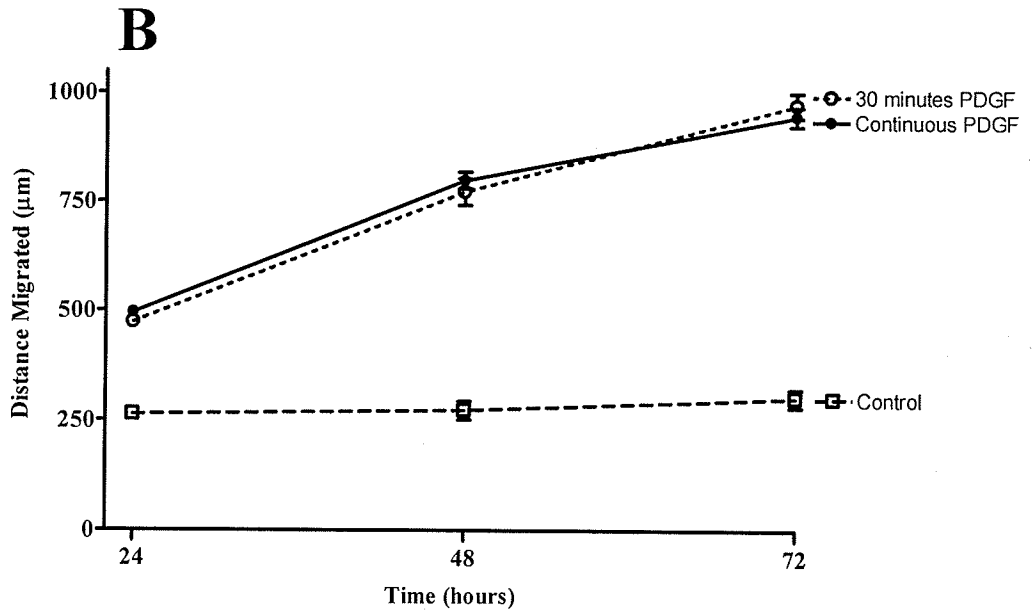


Figure 4.2. Effect of short term exposure (30 minutes) to PDGF-A on OPs migration. OPs which were exposed to 10ng/ml PDGF-A for 30 minutes (open circles and dashed line), migrate to the same extent as OPs continuously exposed to PDGF-A (closed circles). Control (no PDGF) was shown as open squares and dashed lines.

The Change of OP Cell Density in Response to Transient and Continuous Exposure to PDGF-A

OPs showed a lower cell density when exposed to PDGF-A for only 30 minutes, as compared to continuous exposure to PDGF-A (Figure 4.3.).

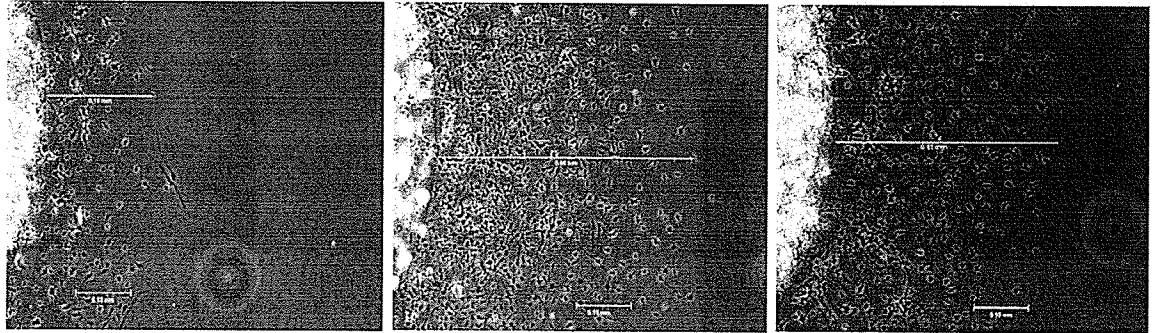


Figure 4.3. Change of OP cell density in response to transient and continuous exposure to PDGF-A. (bar = 0.1 mm)

Left panel: Control OPs were untreated and the measurement was taken 48 hours later.

Middle panel: The measurement was taken 48 hours after OPs were treated with 10 ng/ml PDGF-A continuously.

Right panel: The measurement was taken 48 hours after OPs were treated with 10 ng/ml PDGF-A for 30 minutes.

The Effect of the OPs Proliferation Inhibitor, AMPA, on OPs Migration

It was important to determine whether PDGF induced OP migration was not related to OPs proliferation. For this purpose, the OP proliferation inhibitor, AMPA at 200 μM was used. Using the proliferation assay, it was confirmed that AMPA inhibits OP proliferation (Frost et al., 2008). In the presence of AMPA prior to continuous exposure to PDGF-A, the migration was measured as 849.72 ± 13 μm , while 828.09 ± 30.6 μm for the cells continuously exposed to PDGF-A. (Figure 4.4.).

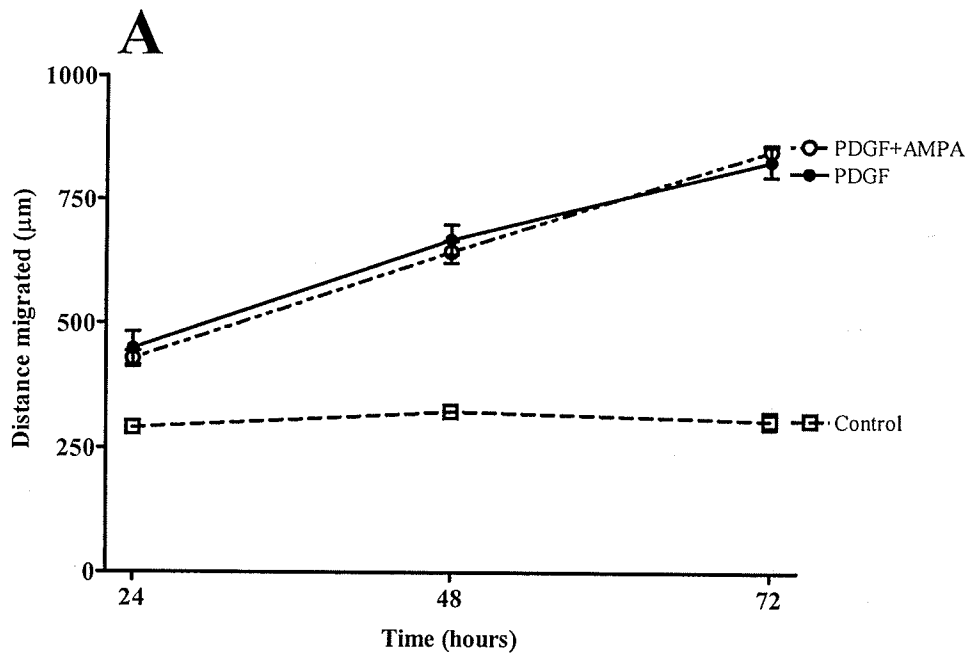


Figure 4.4. Effect of the OP proliferation inhibitor, AMPA, on OPs migration. AMPA, which inhibits OP proliferation, does not have an effect on OPs migration in the presence of PDGF-A (open circles and dashed line), as compared to treatment with only PDGF-A (closed circle). Control (no PDGF) was shown as open squares and dashed lines.

The Effect of ERK Signaling in PDGF-A Induced OPs Migration

A widely used inhibitor of ERK signaling is 2'- amino - 3'- methoxyflavone (PD098059). Previous studies revealed that PD098059 does not inhibit PDGF-A induced OP migration (Simpson and Armstrong, 1999; Frost et al., 2008). Further, PD098059 only inhibits the activation of MEK-1 (Alessi et al., 1995). On the contrary, U0126, a dual ERK signaling inhibitor, acts to selectively inhibit MEK-1 and MEK-2 phosphorylation and the activation of ERKs (Newton et al., 2000). Moreover, U0126 has a 100 fold higher potency in inhibiting ERK signaling than PD098059 (Newton et al., 2000; Favata et al., 1998). In addition, U0126 does not cause OP death (Frost et al., 2008).

Therefore, in this study, U0126 was used to assess the contribution of ERK signaling to OPs migration. OPs migration was $672 \pm 18 \mu\text{m}$ in the presence of a $5.0 \mu\text{M}$ U0126 pretreatment prior to 30 minutes exposure to 10 ng/ml PDGF-A, compared to $483 \pm 83 \mu\text{m}$ following a $10.0 \mu\text{M}$ U0126 pretreatment (Figure 4.5.). Migration was $878 \pm 48 \mu\text{m}$ when the cells were exposed to PDGF-A for 30 minutes.

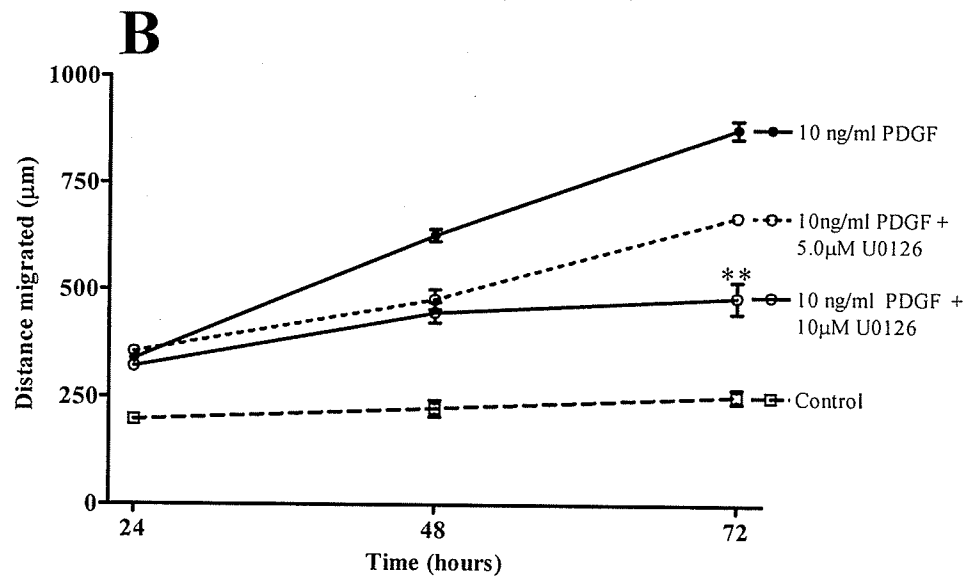


Figure 4.5. Effect of the ERK signaling inhibitor, U0126, on OPs migration

PDGF-A (10 ng/ml) induced OP migration was significantly reduced by using U0126 at both 5.0 µM (open circles and dashed line) and 10.0 µM (open circles and solid line), as compared to OPs exposed to 10 ng/ml PDGF-A alone for 30 minutes (closed circle). Control (no PDGF) was shown as open squares and dashed line.

** P < 0.01 as compared to continuous exposure to PDGF-A.

Western Blot

Western blot analysis was carried out in order to investigate ERK phosphorylation in OPs in response to a 30 minutes of exposure to PDGF-A in the presence or absence of pharmacological inhibitors.

Figure 4.6.A shows that the activated form of ERK, pERK was activated after OPs were treated with PDGF-A alone. Control OPs without the PDGF-A treatment also show ERK activation, but, the band is only faintly discernible (Figure 4.6.A. Lane 1). The level of pERK was increased 24 hours after a 30 minutes exposure to 10 ng/ml PDGF-A (Figure 4.6.A. Lane 2). The levels of pERK remained elevated 72 hours following a 30 minutes exposure to PDGF-A (Figure 4.6.A. Lane 3-5). In contrast, the total ERK, in response to the growth factor, was unchanged.

Further, pERK activation was studied after OPs were treated with both PDGF-A and a pharmacological inhibitor (Figure 4.6.B). Control (untreated) OPs showed low level of ERK activation (Figure 4.6.B. Lane 1), compared to the increased levels of pERK when OPs were harvested immediately or 24 hours after a 30 minutes exposure to 10ng/ml PDGF-A (Figure 4.6.B. Lane 2-3). On the contrary, the levels of pERK were lower when OPs were pretreated with U0126 (Figure 4.6.B. Lane 4-5).

The relative band densities of OPs showed a significant decrease when OPs were pretreated with U0126 prior to the PDGF-A exposure (Figure 4.6.C).

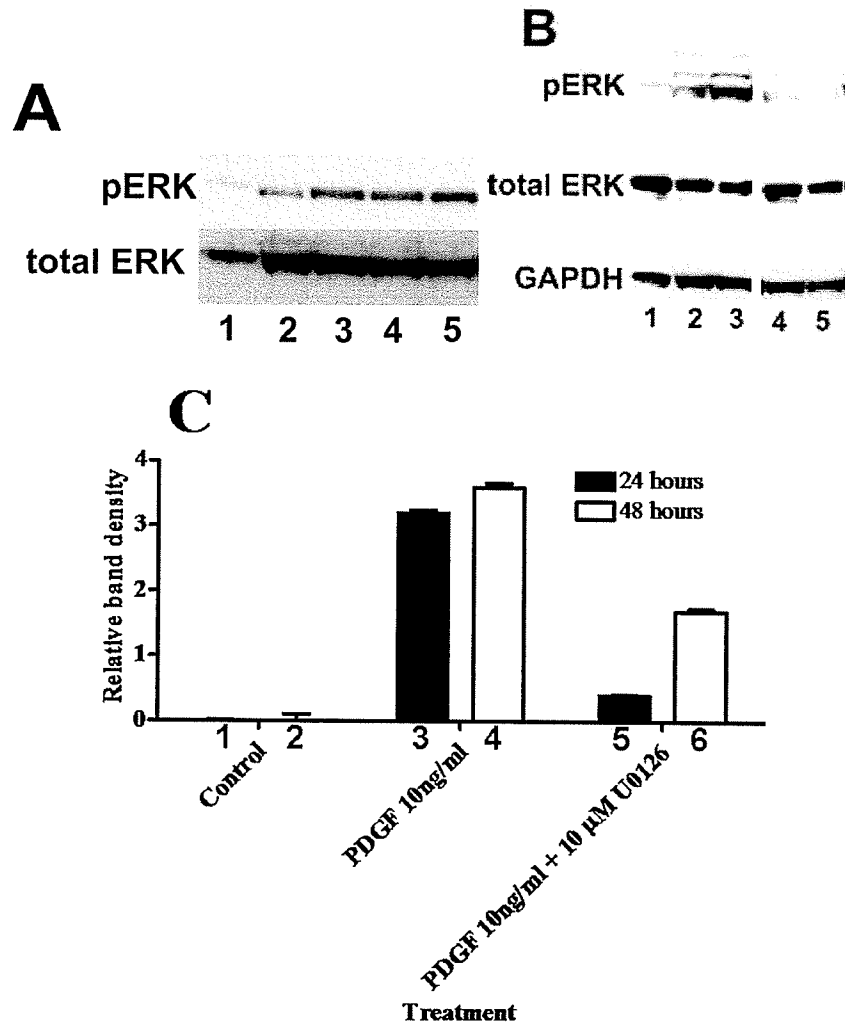


Figure 4.6. ERK phosphorylation in OPs

(A) ERK phosphorylation was analyzed after a 30 minutes PDGF-A treatment.

Lane 1- Control OPs were untreated.

Lane 2- OPs were harvested 24 hours after a 30 minutes exposure to 10 ng/ml PDGF-A.

Lane 3-5 Replicates of cells were harvested 72 hours after a 30 minutes exposure to 10 ng/ml PDGF-A.

(B) ERK phosphorylation was analyzed after a 30 minutes PDGF-A treatment in the presence of pharmacological inhibitor.

Lane 1- Control OPs were untreated.

Lane 2- OPs were harvested immediately after a 30 minutes exposure to 10 ng/ml
PDGF-A.

Lane 3- OPs were harvested 24 hours after a 30 minutes exposure to 10 ng/ml
PDGF-A.

Lane 4- OPs were pretreated with U0126 for 30 minutes prior to 30 minutes
PDGF-A treatment and then harvested immediately.

Lane 5- OPs were pretreated with U0126 for 30 minutes prior to 30 minutes
PDGF-A treatment and then harvested 24 hours later.

(C) Relative density values for the pERK protein bands were obtained by testing three
different cell preparations

Lane 1- Control OPs were harvested 24 hours later.

Lane 2- Control OPs were harvested 48 hours later.

Lane 3- OPs were harvested 24 hours after a 30 minutes exposure to 10 ng/ml
PDGF-A

Lane 4- OPs were harvested 48 hours after a 30 minutes exposure to 10 ng/ml
PDGF-A

Lane 5- OPs were pretreated with U0126 for 30 minutes prior to 30 minutes
PDGF-A treatment and then harvested 24 hours later.

Lane 6- OPs were pretreated with U0126 for 30 minutes prior to 30 minutes
PDGF-A treatment and then harvested 48 hours later.

Activated Caspase-3 Staining

The Effect of PDGF-A Withdrawal on OPs Death

A previous study indicated that PDGF withdrawal resulted in increased OP death (Tokumoto et al., 1999). In order to examine the effect of PDGF-A withdrawal after transient PDGF-A treatment, a cell death assay was performed, using activated caspase-3 staining. As an important caspase, caspase-3 can be activated by both intrinsic and extrinsic apoptotic pathways (Budihardjo et al., 1999).

Based on the randomly selected fields of view, 100 cells per coverslip were counted with 3 to 4 replicates. Total cell numbers were recorded by counting DAPI staining; and caspase-3 positive cell numbers by counting fluorescent conjugated primary antibody. This study assesses the extent of cell death 72 hours after a 30 minutes exposure to 10 ng/ml PDGF-A. As measured by immunoreactivity, $15.8 \pm 1.5\%$ cells were detected as positive for activated caspase-3 (Figure 4.7.). In contrast to the control data (data not shown here), the data showed no significant increase of cell death.



Figure 4.7. Activated caspase-3 in OPs

Very few cells were positive caspase-3 cells (green) 72 hours after OPs were exposed to 10 ng/ml PDGF-A for 30 minutes. The cells were counter stained with DAPI (blue).

Proliferation Assay

The Effect of Transient PDGF-A Exposure on OPs Proliferation

Transient exposure to PDGF-A (10 ng/ml) for 30, 60 and 120 minutes and 24 hours of continuous exposure resulted in $15.84 \pm 3.7\%$, $15.33 \pm 2.1\%$, $19.23 \pm 1.9\%$ and $65.49 \pm 2.6\%$ BrdU positive cells, respectively (Figure 4.8.).

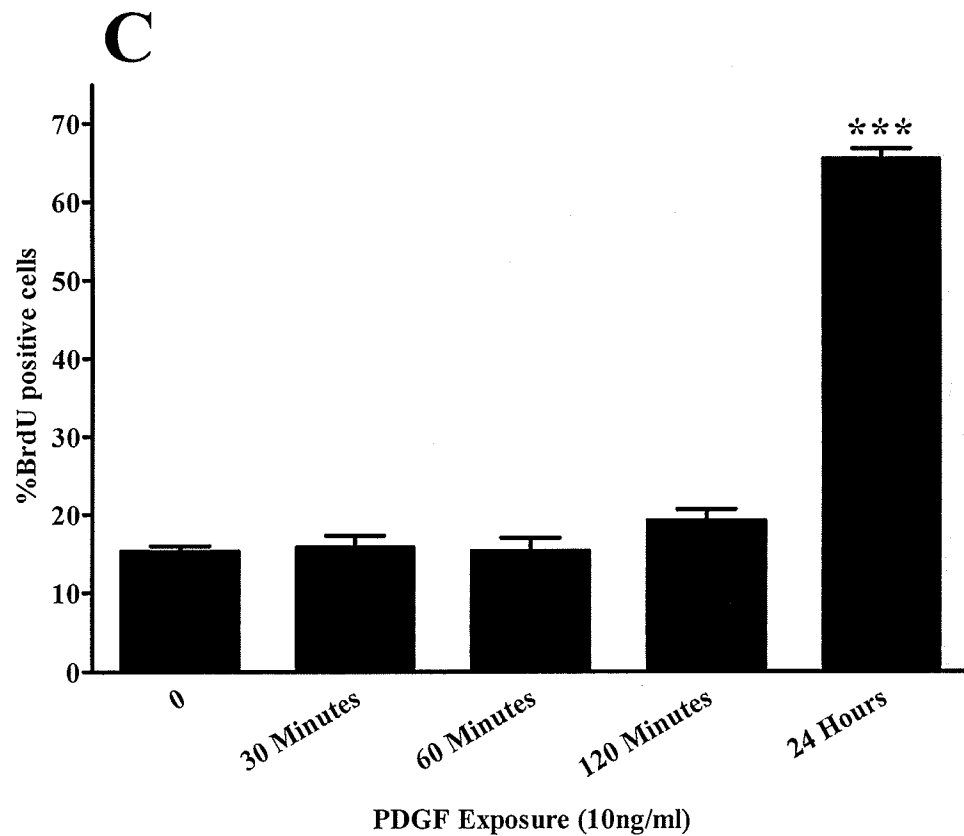


Figure 4.8. Transient PDGF-A exposure on OPs proliferation

Transient 10 ng/ml PDGF-A exposure for up to 120 minutes does not have an effect on OPs proliferation.

*** P < 0.005 as compared to untreated cells.

Results

OPs, exposed to PDGF-A (10 ng/ml) for 30 minutes, migrate to the same extent as cells exposed to PDGF-A (10 ng/ml) continuously for the duration of the experiment. Further, transient exposure to PDGF-A (10 ng/ml) for up to 120 minutes does not induce OPs proliferation, as compared to the PDGF-A incubation for 24 hours which does induce proliferation. This was also confirmed by AMPA, which proved that inhibition of OPs proliferation does not affect OPs migration in response to PDGF-A. However, the cell density revealed to be lower when OPs were exposed to PDGF-A for only 30 minutes. Together, short term exposure to PDGF-A is sufficient to stimulate OPs migration for up to 72 hours without inducing OPs proliferation.

The extent of cell death 72 hours after 30 minutes exposure to PDGF-A was determined by activated caspase-3 staining. Very few cells, $15.8 \pm 1.5\%$ cells, were measured as positive for activated caspase-3, indicating PDGF withdrawal has no effect on cell death. The results presented here confirm that PDGF is a critical factor stimulating OP migration without affecting OP proliferation and cell death.

In order to assess the ERK signaling in PDGF-A induced OPs migration, ERK phosphorylation in OPs in response to a 30 minutes PDGF-A treatment was examined, using Western blot analysis. The level of pERK activation was increased 24 hours after transient PDGF-A exposure, and remained at the same level for the following 48 hours.

The study further investigated the effect of ERK signaling by using its inhibitor U0126. As shown, OPs migration was reduced by 23.3% in the presence of 5.0 μ M U 0126, and 45.0% in the presence of 10.0 μ M U 0126. The above studies strongly suggest that ERK signaling pathway is crucial in PDGF-A induced OPs migration.

Chapter V

PDGF Ligand and Receptor Expression in the Developing Mouse Brain

Introduction

PDGF exists as disulfide-bonded homodimers or heterodimers consisting of two polypeptide chains. There are five isoforms AA, AB, BB, CC and DD (Fredriksson et al., 2004). There are two PDGF Receptors, the alpha and beta isoforms, PDGF-R α and PDGF-R β , which form homodimers or heterodimers: $\alpha\alpha$, $\alpha\beta$ and $\beta\beta$. They are members of the tyrosine kinase receptor family and activate numerous different intracellular signaling pathways (Heldin and Westermark, 1999). The distinct functions of each PDGF isoforms is achieved by different affinities to different receptors, and the nature of the ligand (i.e. homodimer or heterodimer) binding to receptors (Heldin and Westermark, 1999). Receptor dimerization occurs after ligand binding, and results in phosphorylation of the cytoplasmic tail (Heldin and Westermark, 1999).

During CNS development, PDGF is synthesized by astrocytes, neurons, as well as OLs (Fruttiger et al., 1999; Heldin and Westermark, 1999). As described, many studies have showed that both PDGF-A and PDGF-R α are essential in regulating OL development both in vivo and in vitro (Calver et al., 1998; Armstrong et al., 1991; Frost et al., 1996; Frost et al 2008; Barres et al., 1993; Noble et al., 1988; Fruttiger et al., 1999; Soriano, 1997).

In the intact mouse CNS, PDGF-A is ubiquitously distributed both in the spinal cord at E15 and brain at E11, E13, E15 (Calver et al., 1998; Hutchins and Jefferson, 1992; Miller, 2002). There is a slight difference in the temporal expression of PDGF-A and PDGF-R α . In the mouse brain, PDGF-A mRNA expression in

neurons first appears at E15, whereas, in the mouse spinal cord, its expression is first seen at E12 (Heldin and Westermark, 1999). Hutchins and Jefferson, however, showed that PDGF-A positive cells are detected throughout the ventricular zone at E11 in the developing mouse brain and at E12 in the mouse spinal cord (Hutchins and Jefferson, 1992). In the mouse brain, a transient expression of PDGF-R α protein is found in the neuronal tube at E9, while its expression in the brain and spinal cord appears at E13 (Heldin and Westermark, 1999). Another study in rats, found that PDGF-R α positive cells are present in the forebrain at E16 and increase in numbers until P10 (Pringle et al., 1992).

It is important to note that previous studies on protein expression have not provided a complete picture. For example, the study by Hutchins and Jefferson did not investigate the expression of PDGF between E11 to P7, the most important stage of OL development, but only chose three time points at E11, E13 and E15 (Hutchins and Jefferson, 1992).

To fully understand the role of PDGF-A and its receptor PDGF-R α , it is necessary to examine PDGF-A and PDGF-R α expression at all stages of brain development relevant to OP development. The morphological development of the mouse brain changes significantly between E11 and the adult mouse. Those changes occurring within a single day may affect the development of OL significantly. This study, therefore, will provide data that is both novel and comprehensive, providing critical information for the future studies related to the roles of other proteins in the regulation of different stages of the OL development.

PDGF-A and PDGF-R α Expression in the Mouse Brain

In order to investigate the temporal-spatial expression of PDGF ligand and receptor α in the developing mouse brain, sequential sections of mice brains from E11.5 to P7 were stained and analyzed for expression of two most significant proteins: PDGF-R α and PDGF-A. Cryostat sections of mouse brain stained with PDGF-A or PDGF-R α were visualized by FITC conjugated secondary antibody.

The sections were photographed under bright-field and epifluorescence microscopy. The images were pseudocolored in Image Pro 6.0. The age of the tissue is denoted at the lower right and the higher magnification images are derived from the boxes in phase contrast images.

The proteins expression was analyzed throughout the brain, including SVZ, lateral ganglion eminence and cortical regions. Representative pictures are shown as follows.

PDGF-A Expression Pictures from E11 to E19

Figure 5.1. PDGF-A expression at E11.5 in the mouse brain:

Panel 1 – Phase contrast photomicrograph of an E11 mouse brain section (10×).

Areas shown at higher magnification are labeled A-D. Bar = 500 μm.

Panel 2 – Immunohistochemistry showing PDGF-A (green) expression in the different regions of mouse brain (60×). Cells are counterstained with DAPI (blue).

A – Area from ventricular zone of frontal cortex showing extensive PDGF-A

expression. B – Area from mesencephalon showing PDGF-A expression. C – The conjunction of superior colliculus and mesencephalon showing PDGF-A expression.

D – Area from cerebellum showing PDGF-A expression. Bar = 50 μm.

E11.5

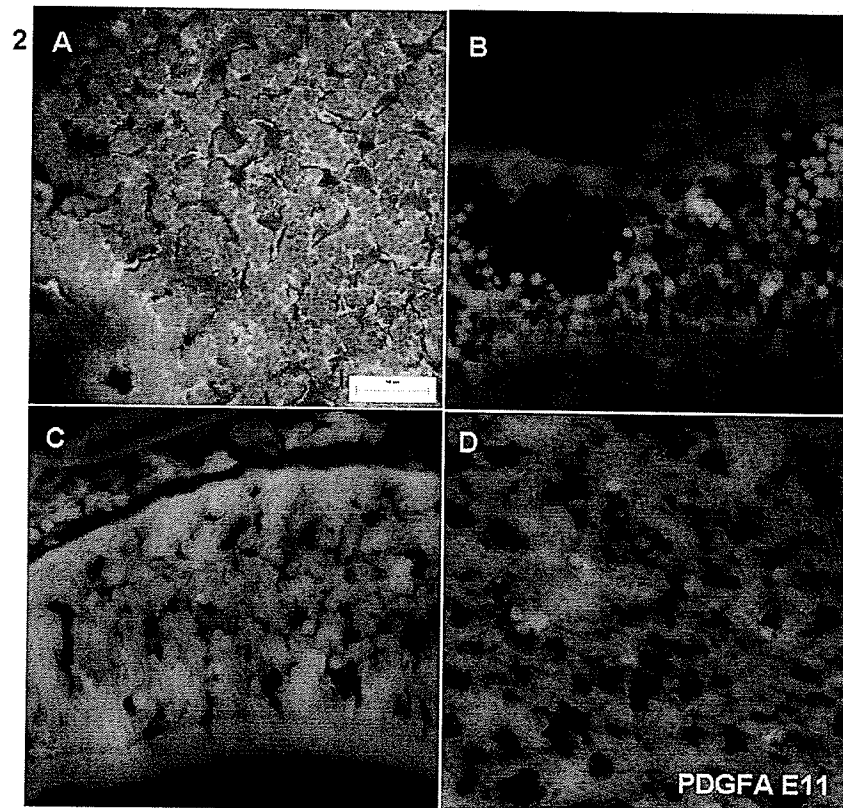
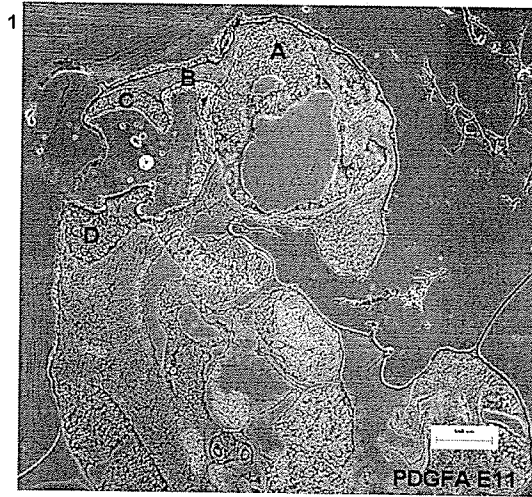


Figure 5.2. PDGF-A expression at E12.5 in the mouse brain:

Panel 1 – Phase contrast photomicrograph of an E12 mouse brain section showing one region of the brain: posterior (10×). Areas shown at higher magnification are labeled A-D. Bar = 500 μm.

Panel 2 – Immunohistochemistry showing PDGF-A (green) expression in the different regions of mouse brain (60×). Cells are counterstained with DAPI (blue).

A and B – Area from mesencephalic tegmentum showing PDGF-A expression. C

and D – The conjunction of superior colliculus and mesencephalon showing PDGF-A expression. Bar = 50 μm.

E12.5

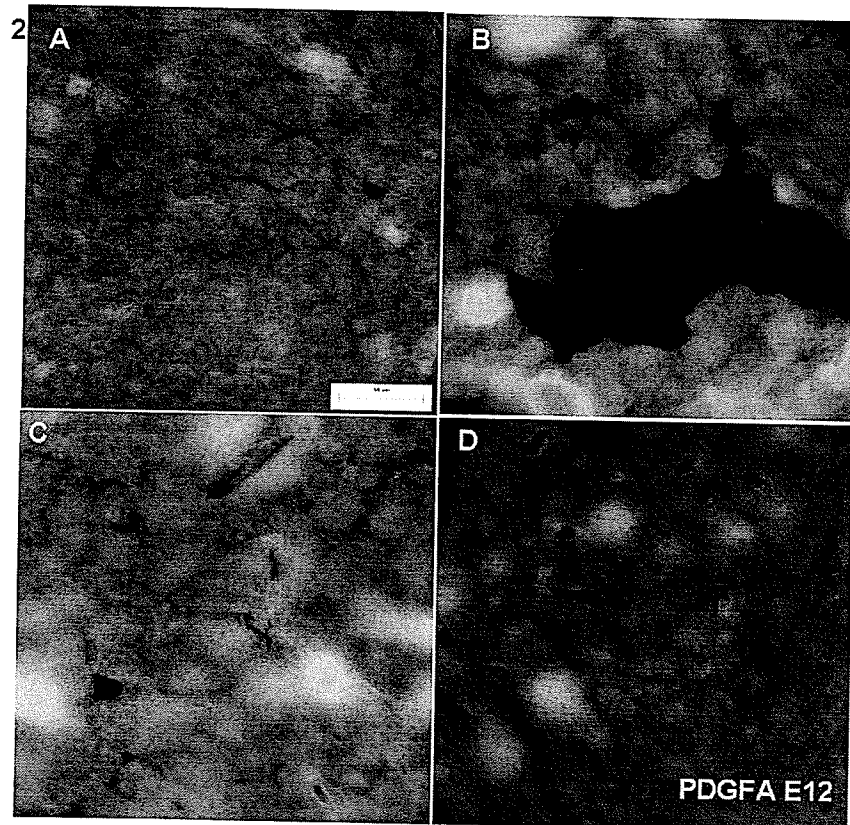
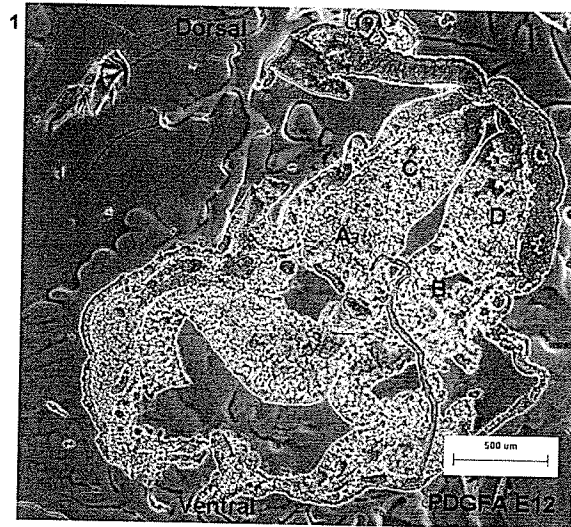


Figure 5.3. PDGF-A expression at E14.5 in the mouse brain:

Panel 1 – Phase contrast photomicrograph of an E14 mouse brain section showing three regions of the brain: in the middle (left and middle panels) and posterior (right panel) (10×). Areas shown at higher magnification are labeled A-D. Bar = 500 μm .

Panel 2 – Immunohistochemistry showing PDGF-A (green) expression in the different regions of mouse brain (60×). Cells are counterstained with DAPI (blue). A – Area from amygdala showing PDGF-A expression. B – Area from dorsal thalamus showing PDGF-A expression. C – Area from dorsal thalamus showing PDGF-A expression. D – Area from amygdala besides lateral ventricle showing PDGF-A expression. Bar = 50 μm .

E14.5

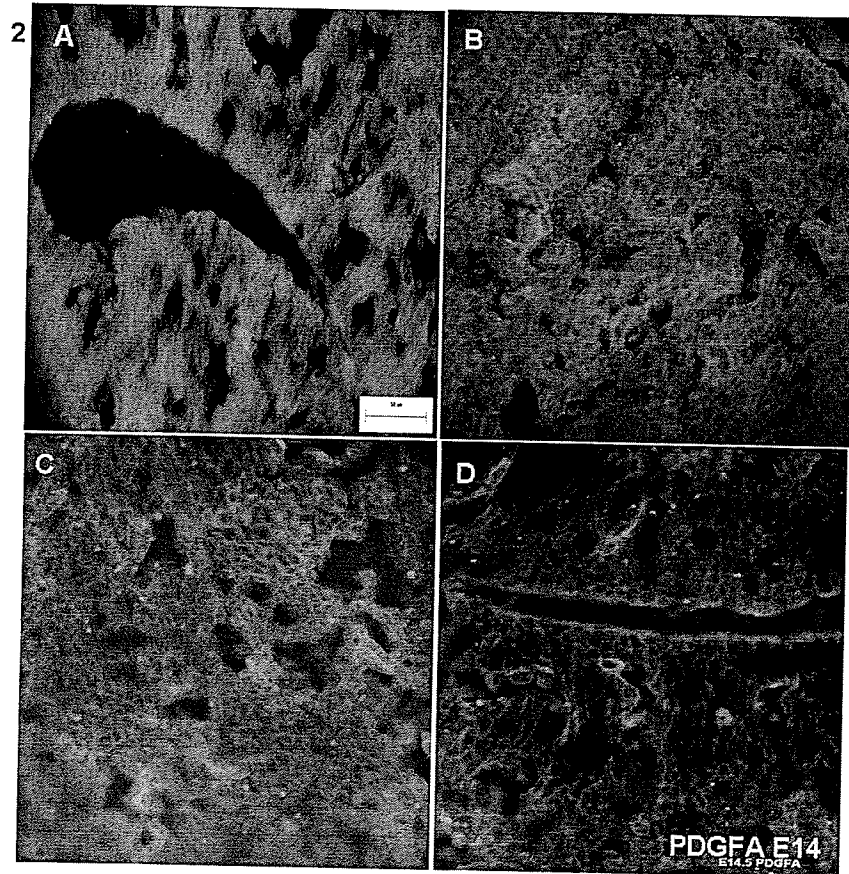
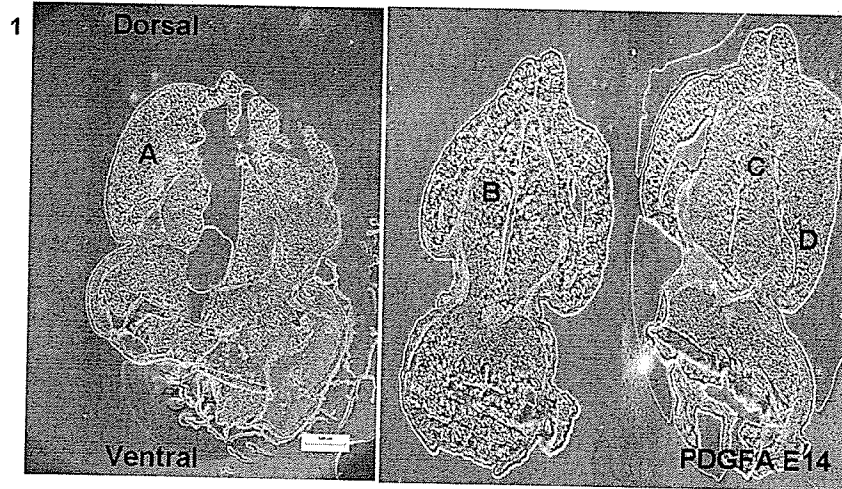


Figure 5.4. PDGF-A expression at E16.5 in the mouse brain:

Panel 1 – Phase contrast photomicrograph of an E16 mouse brain section showing four regions of the brain: anterior (top left and top right panels), in the middle (bottom left panel) and posterior (bottom right panel) (10×). Areas shown at higher magnification are labeled A-D. Bar = 500 μm .

Panel 2 – Immunohistochemistry showing PDGF-A (green) expression in the different regions of mouse brain (60×). Cells are counterstained with DAPI (blue).

A – Area from subventricular zone (olfactory bulb) showing PDGF-A expression. B – Area from subventricular zone (olfactory bulb) showing PDGF-A expression. C – Area from diagonal band, vertical limb showing PDGF-A expression. D – The conjunction of lateral lemniscus and medial cerebellar peduncle showing PDGF-A expression. Bar = 50 μm .

E16.5

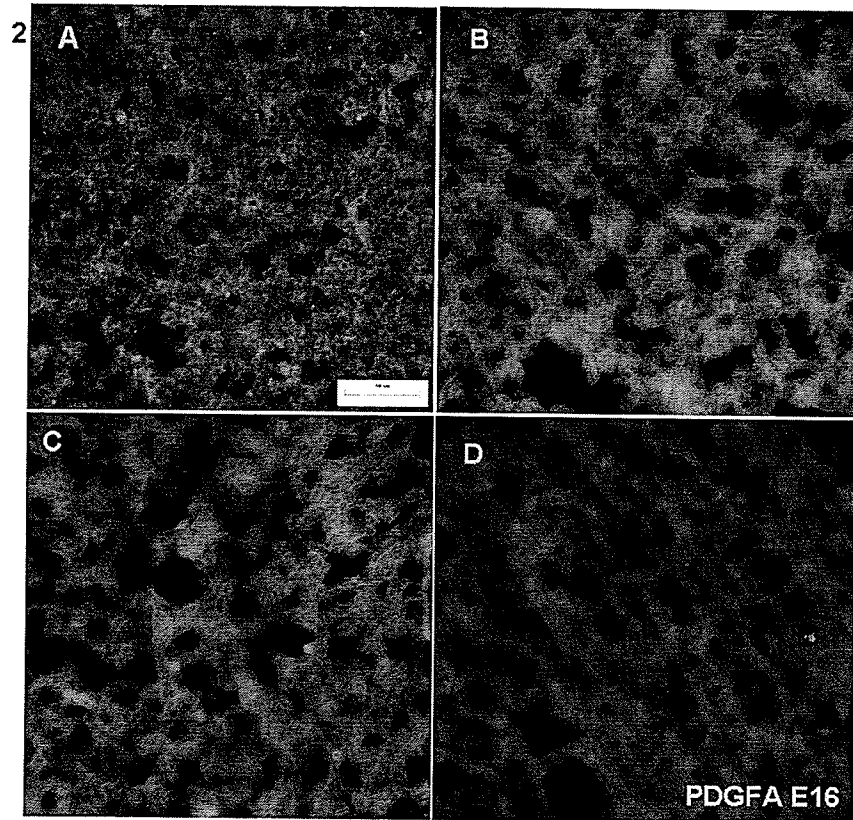
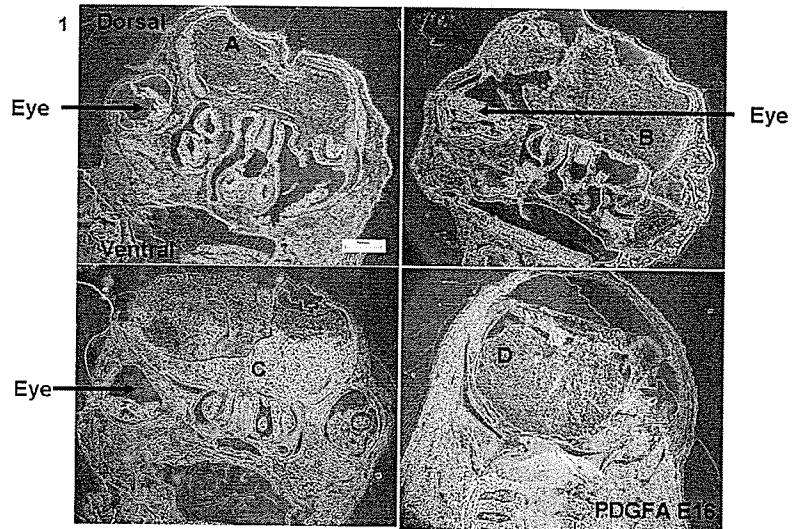


Figure 5.5. PDGF-A expression at E17.5 in the mouse brain:

Panel 1 – Phase contrast photomicrograph of an E17 mouse brain section showing four regions of the brain: anterior (top left panel), in the middle (top right and bottom left panels) and posterior (bottom right panel) (10×). Areas shown at higher magnification are labeled A-D. Bar = 500 μ m.

Panel 2 – Immunohistochemistry showing PDGF-A (green) expression in the different regions of mouse brain (60×). Cells are counterstained with DAPI (blue).

A – Area from subventricular zone (olfactory bulb) showing PDGF-A expression. B

– Area from subventricular zone besides lateral ventricle showing PDGF-A

expression. C – Area from caudate putamen showing PDGF-A expression. D –

Area from hippocampal area besides lateral ventricle showing PDGF-A expression.

Bar = 50 μ m.

E17.5

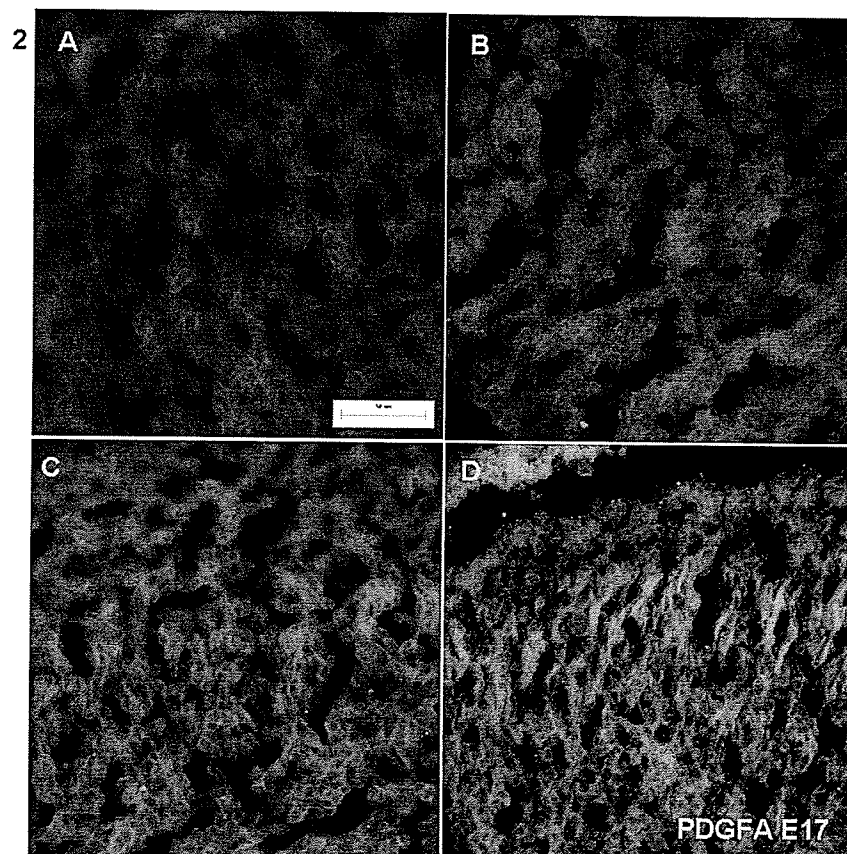
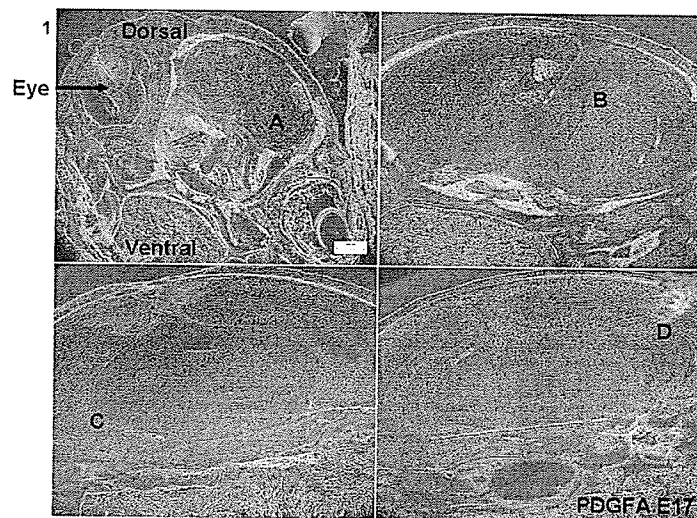


Figure 5.6. PDGF-A expression at E18.5 in the mouse brain:

Panel 1 – Phase contrast photomicrograph of an E18 mouse brain section showing four regions of the brain: in the middle (top left, top right and bottom left panels) and posterior (bottom right panel) (10×). Areas shown at higher magnification are labeled A-D. Bar = 500 μm .

Panel 2 – Immunohistochemistry showing PDGF-A (green) expression in the different regions of mouse brain (60×). Cells are counterstained with DAPI (blue).

A – Medial preoptic area showing PDGF-A expression. B – Hippocampal area besides lateral ventricle showing PDGF-A expression. C – The conjunction of cortical plate and subplate showing PDGF-A expression. D – Area from posteromedial cortical amygdaloid nucleus showing PDGF-A expression. Bar = 50 μm .

E18.5

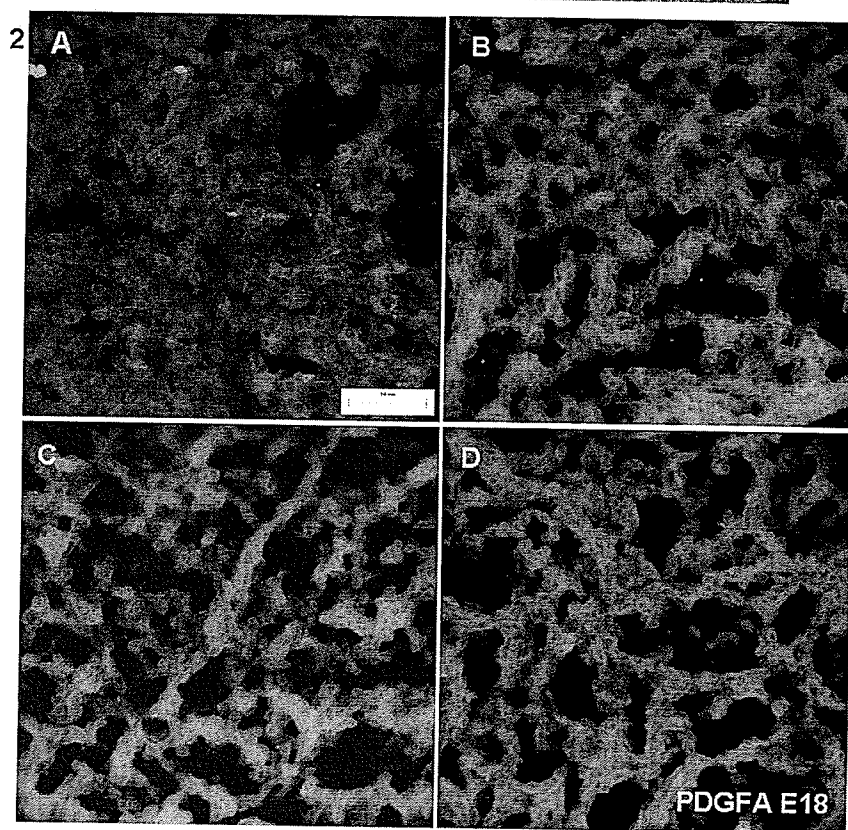
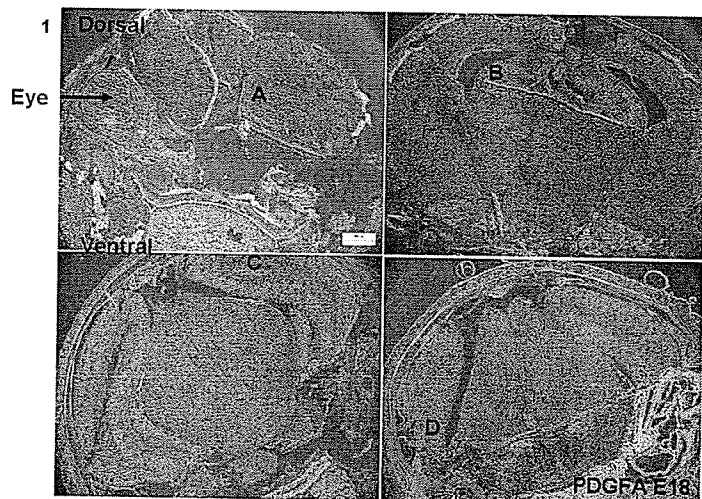


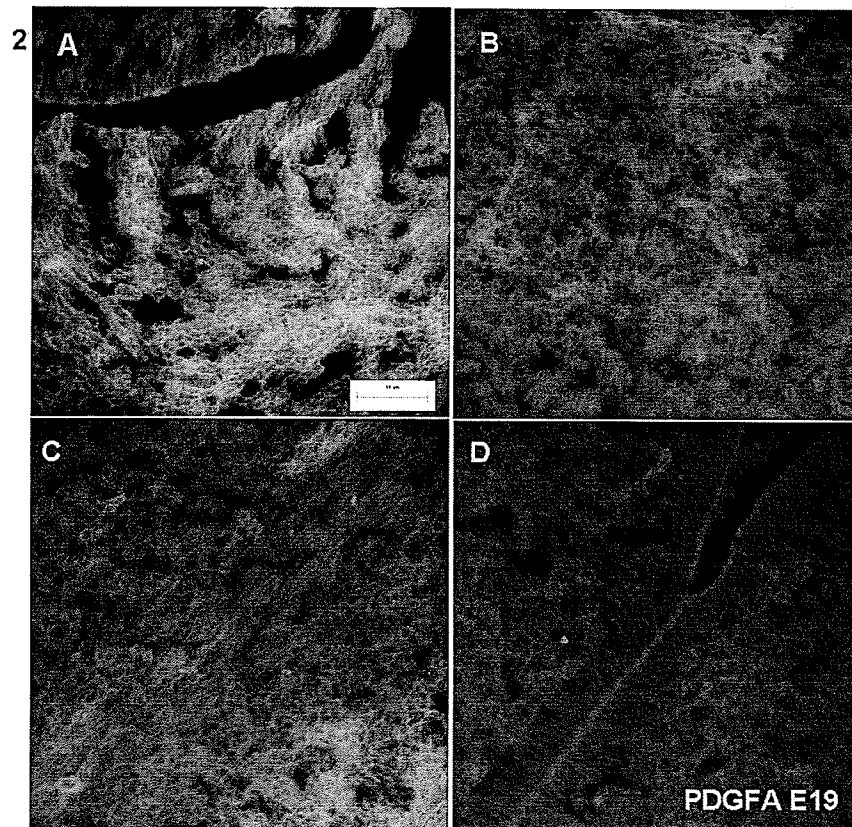
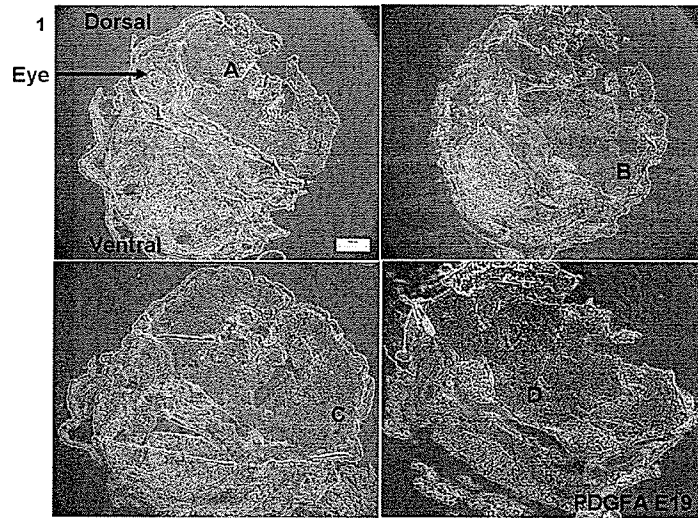
Figure 5.7. PDGF-A expression at E19.5 in the mouse brain:

Panel 1 – Phase contrast photomicrograph of an E19 mouse brain section showing four regions of the brain: anterior (top left, top right panels), in the middle (bottom left) and posterior (bottom right) (10×). Areas shown at higher magnification are labeled A-D. Bar = 500 μm .

Panel 2 – Immunohistochemistry showing PDGF-A (green) expression in the different regions of mouse brain (60×). Cells are counterstained with DAPI (blue).

A – Area from subventricular zone besides lateral ventricle showing PDGF-A expression. B – Area from olfactory tubercle showing PDGF-A expression. C – The conjunction of caudate putamen and cerebral cortex showing PDGF-A expression. D – Area from medial preoptic area showing PDGF-A expression. Bar = 50 μm .

E19.5



PDGF-R α Expression Pictures from E11 to P7

Figure 5.8. PDGF-R α expression at E11.5 in the mouse brain:

Panel 1 – Phase contrast photomicrograph of an E11 mouse brain section showing three regions of the brain: anterior (left and middle panels) and in the middle (right panel) (10 \times). Areas shown at higher magnification are labeled A-D. Bar = 500 μ m.

Panel 2 – Immunohistochemistry showing PDGF-R α (green) expression in the different regions of mouse brain (60 \times). Cells are counterstained with DAPI (blue).

A – Area from pallidum showing no PDGF-R α expression. B – Area from hypothalamus showing no PDGF-R α expression. C – Area from mesencephalic tegmentum besides aqueduct showing PDGF-R α expression. D – Area from anterior thalamus besides 3rd ventricle showing PDGF-R α expression. Bar = 50 μ m.

E11.5

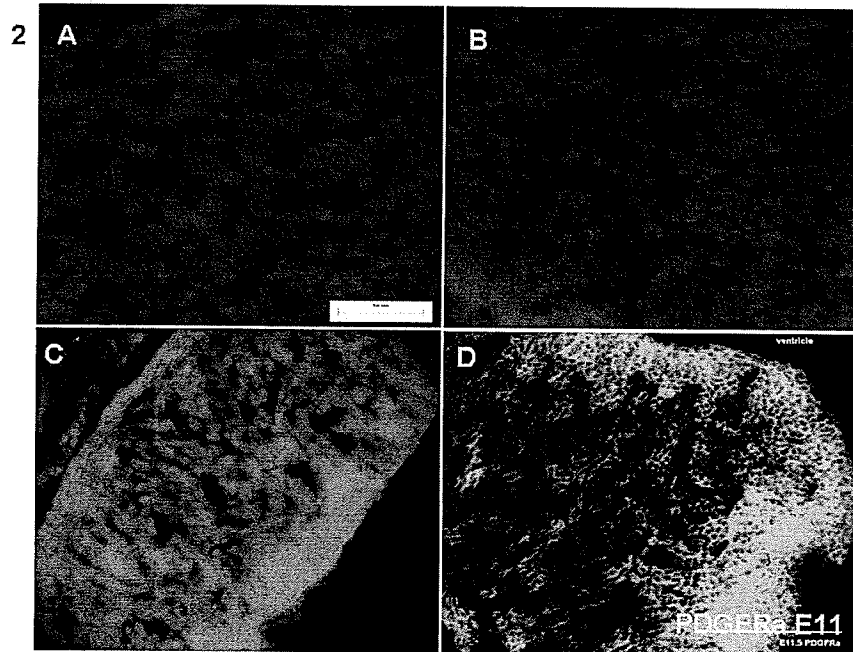
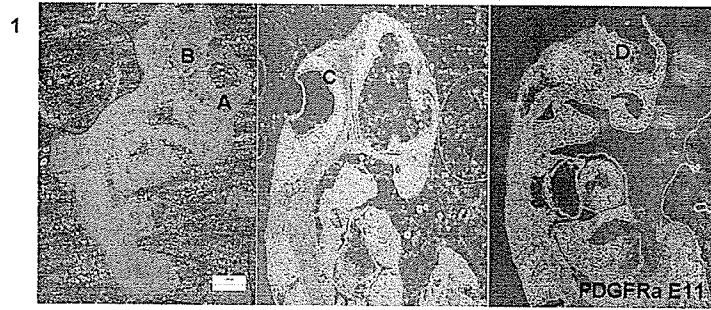


Figure 5.9. PDGF-R α expression at E12.5 in the mouse brain:

Panel 1 – Phase contrast photomicrograph of an E12 mouse brain section showing one region of the brain: in the middle (10 \times). Areas shown at higher magnification are labeled A-D. Bar = 500 μ m.

Panel 2 – Immunohistochemistry showing PDGF-R α (green) expression in the different regions of mouse brain (60 \times). Cells are counterstained with DAPI (blue).

A – Area from posterior thalamus besides 3rd ventricle showing PDGF-R α expression.

B and C – The conjunction of posterior thalamus and hypothalamus showing no

PDGF-R α expression. D – Area from hypothalamus showing no PDGF-R α

expression. Bar = 50 μ m.

E12.5

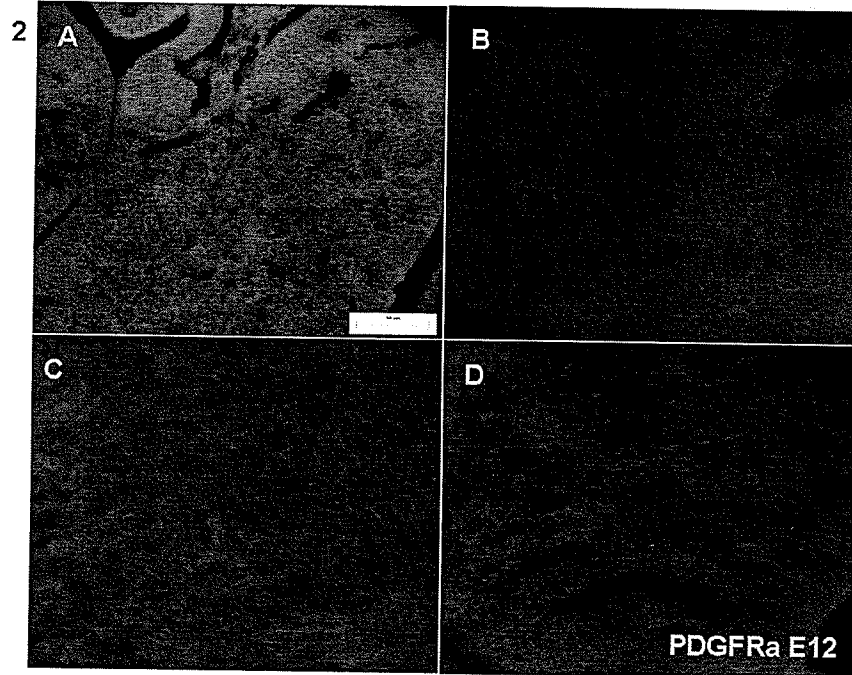
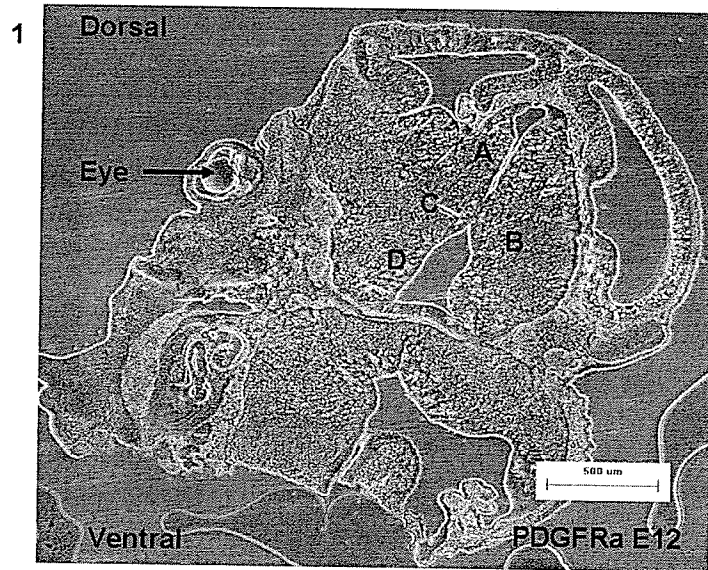


Figure 5.10. PDGF-R α expression at E13.5 in the mouse brain:

Panel 1 – Phase contrast photomicrograph of an E13 mouse brain section showing one region of the brain: in the middle (10 \times). Areas shown at higher magnification are labeled A-D. Bar = 500 μ m.

Panel 2 – Immunohistochemistry showing PDGF-R α (green) expression in the different regions of mouse brain (60 \times). Cells are counterstained with DAPI (blue).

A – Area from thalamic eminence showing no PDGF-R α expression. B – Area from dorsal thalamus showing PDGF-R α expression. C – Area from dorsal thalamus showing PDGF-R α expression. D – Area from thalamic eminence showing no PDGF-R α expression. Bar = 50 μ m.

E13.5

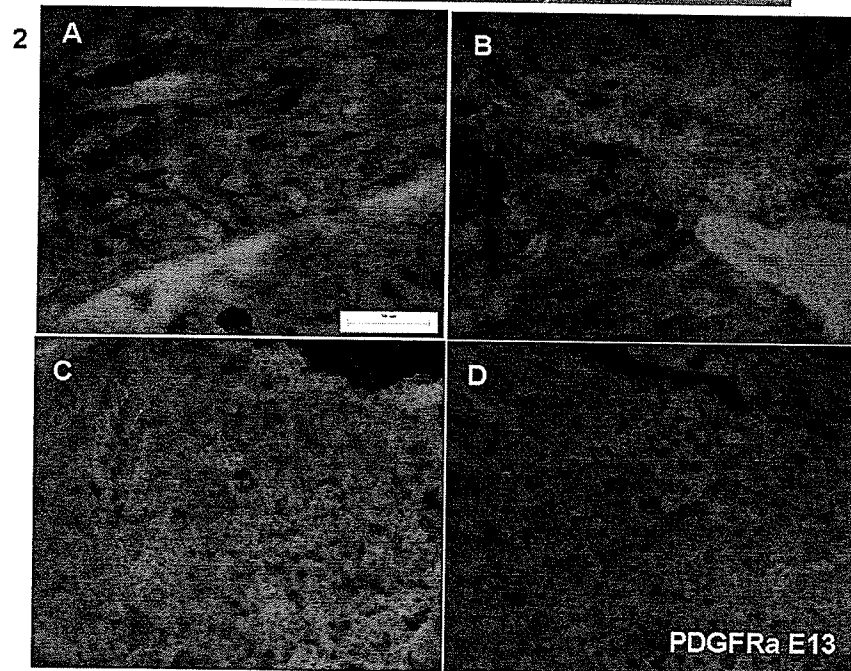
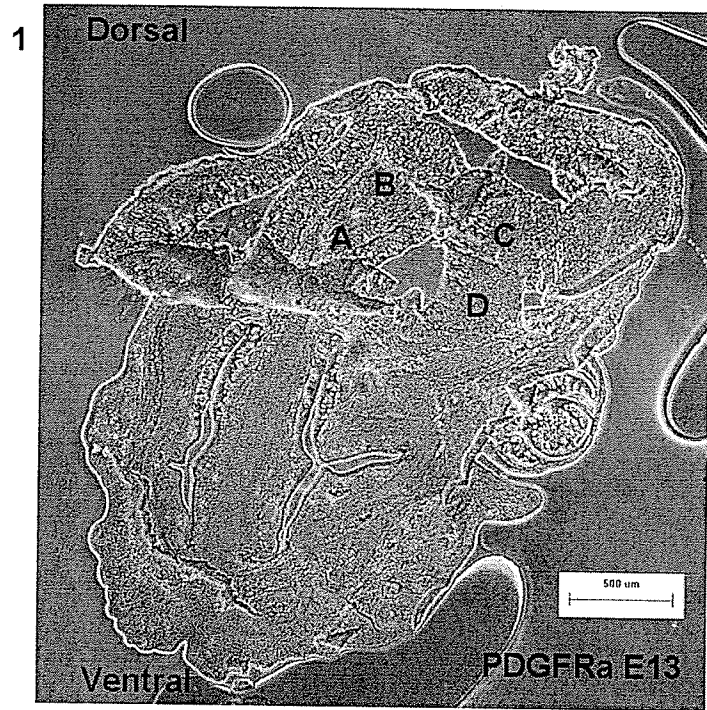


Figure 5.11. PDGF-R α expression at E14.5 in the mouse brain:

Panel 1 – Phase contrast photomicrograph of an E14 mouse brain section showing two regions of the brain: posterior (left and right panels) (10 \times). Areas shown at higher magnification are labeled A-D. Bar = 500 μ m.

Panel 2 – Immunohistochemistry showing PDGF-R α (green) expression in the different regions of mouse brain (60 \times). Cells are counterstained with DAPI (blue).

A – Area from cerebral cortex besides lateral ventricle showing PDGF-R α expression.

B – Area from dorsal thalamus showing PDGF-R α expression. C – Area from

thalamic eminence showing no PDGF-R α expression. D – Area from cerebral

cortex showing PDGF-R α expression. Bar = 50 μ m.

E14.5

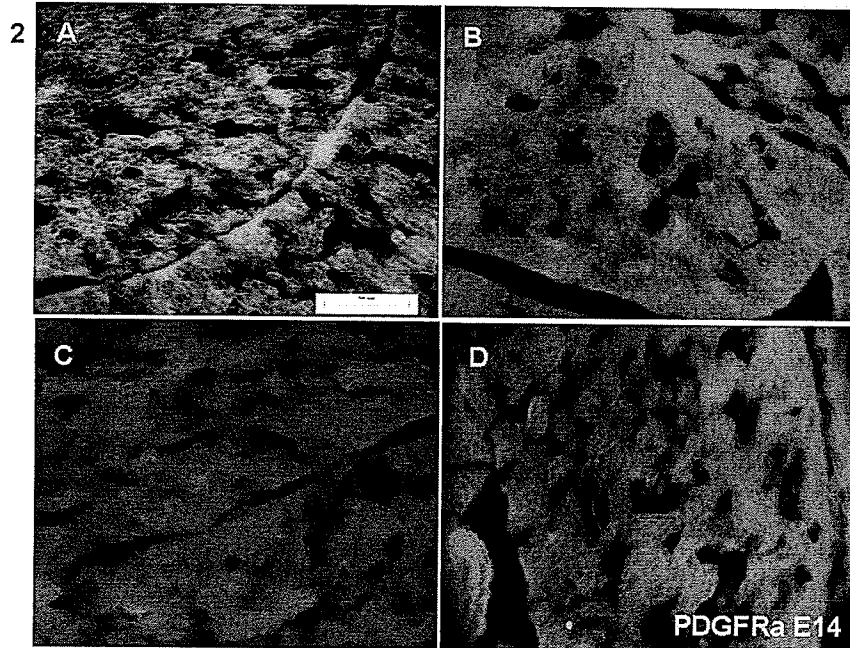
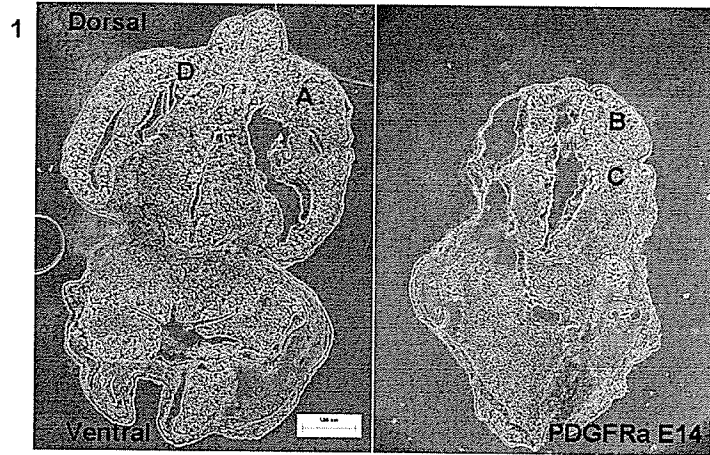


Figure 5.12. PDGF-R α expression at E16.5 in the mouse brain:

Panel 1 – Phase contrast photomicrograph of an E16 mouse brain section showing three regions of the brain: anterior (bottom left and bottom right panels) and in the middle (top panel) (10 \times). Areas shown at higher magnification are labeled A-D. Bar = 500 μ m.

Panel 2 – Immunohistochemistry showing PDGF-R α (green) expression in the different regions of mouse brain (60 \times). Cells are counterstained with DAPI (blue).

A – Area from subventricular zone showing PDGF-R α expression. B – Area from subventricular zone showing no PDGF-R α expression. C – Area from subventricular zone (olfactory bulb) showing PDGF-R α expression. D – Area from subventricular zone (olfactory bulb) showing PDGF-R α expression. Bar = 50 μ m.

E16.5

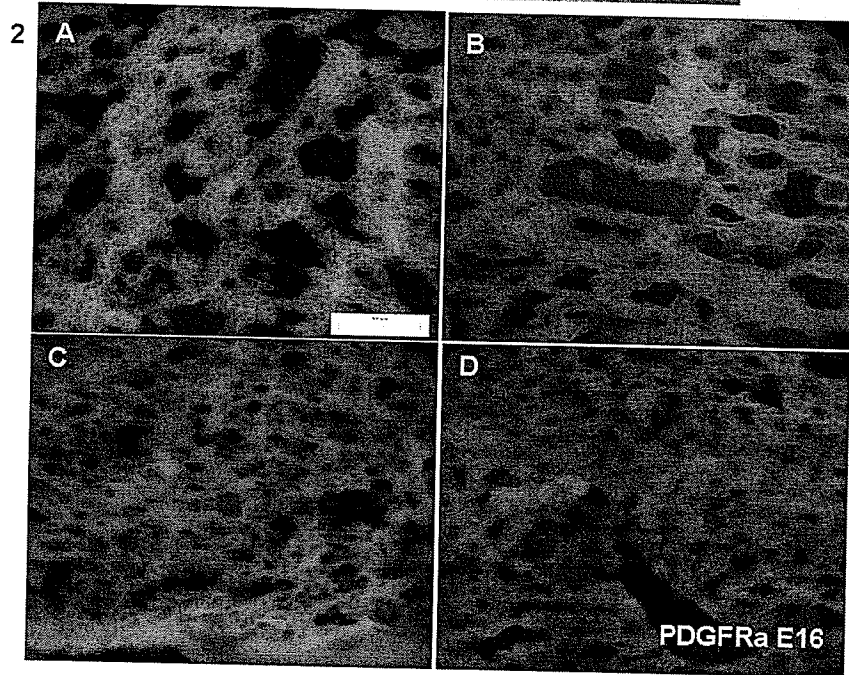
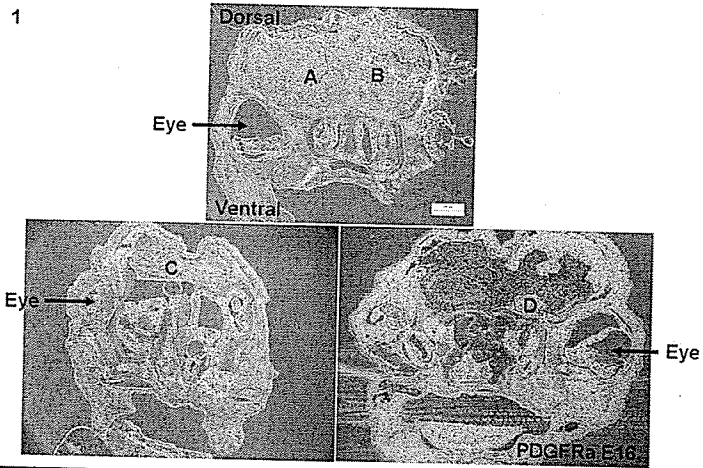


Figure 5.13. PDGF-R α expression at E17.5 in the mouse brain:

Panel 1 – Phase contrast photomicrograph of an E17 mouse brain section showing three regions of the brain: in the middle (left and middle panels) and posterior (right panel) (10 \times). Areas shown at higher magnification are labeled A-D. Bar = 500 μ m.

Panel 2 – Immunohistochemistry showing PDGF-R α (green) expression in the different regions of mouse brain (60 \times). Cells are counterstained with DAPI (blue). A – Area from subventricular zone showing PDGF-R α expression. B – Area from caudate putamen showing PDGF-R α expression. C – Area from cerebral cortex showing PDGF-R α expression. D – Area from caudate putamen showing PDGF-R α expression. Bar = 50 μ m.

E17.5

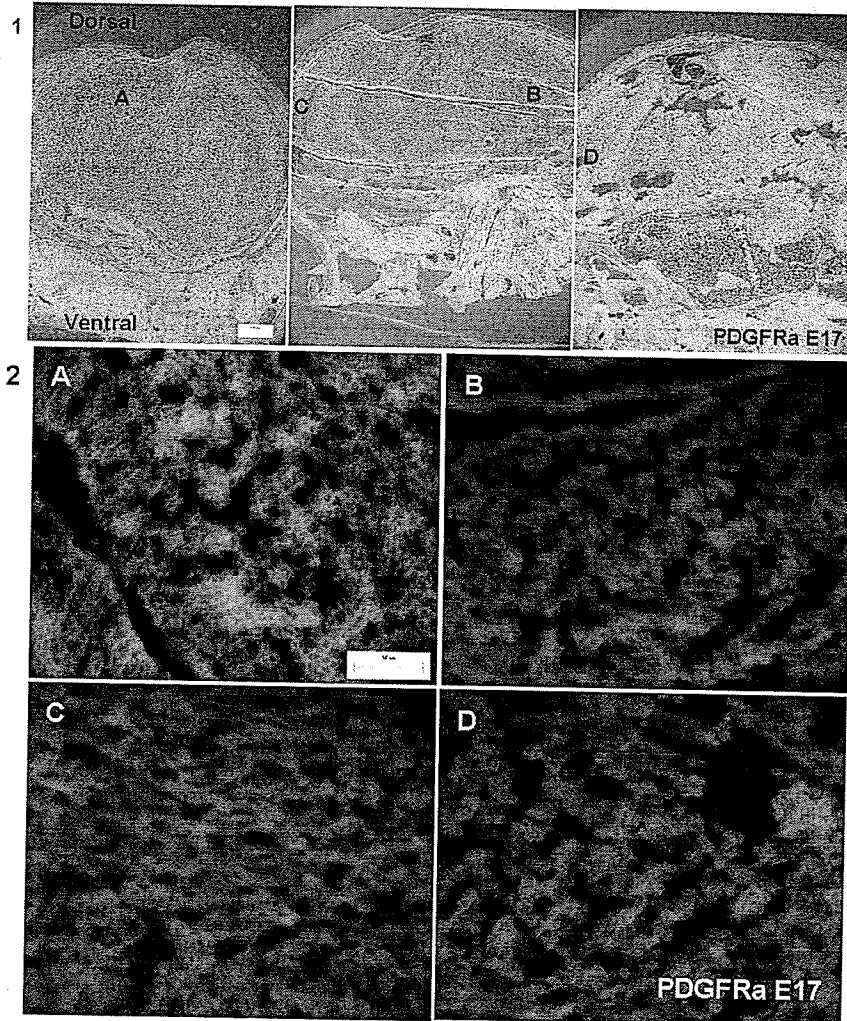


Figure 5.14. PDGF-R α expression at E18.5 in the mouse brain:

Panel 1 – Phase contrast photomicrograph of an E18 mouse brain section showing two regions of the brain: in the middle (left and right panels) (10 \times). Bar = 500 μ m.

Panel 2 – Immunohistochemistry showing PDGF-R α (green) expression in the different regions of mouse brain (60 \times). Cells are counterstained with DAPI (blue).

A – Area from paraventricular thalamus showing PDGF-R α expression. B – Area from cerebral cortex showing PDGF-R α expression. C – Area from cerebral cortex showing PDGF-R α expression. D – Area from cerebral cortex showing PDGF-R α expression. Bar = 50 μ m.

E18.5

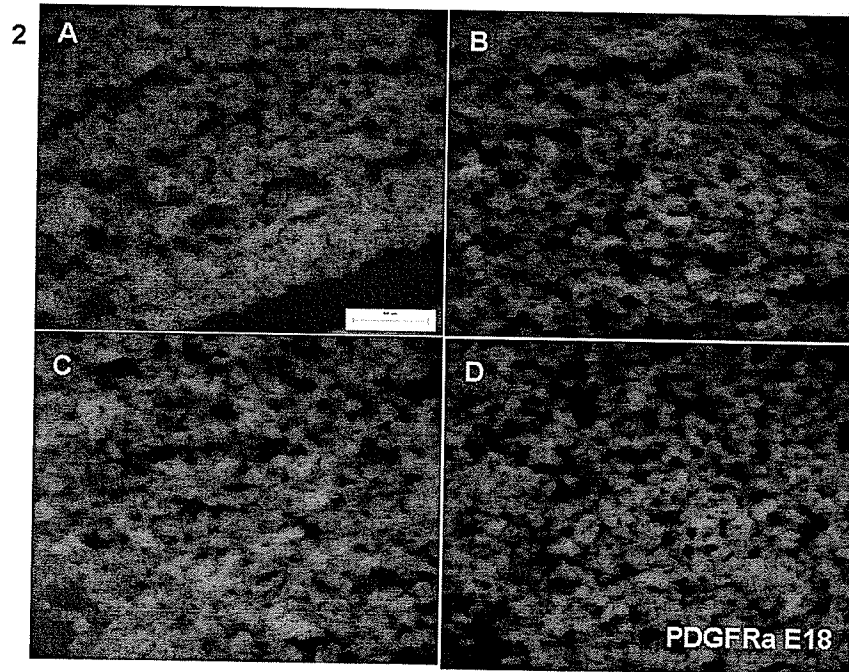
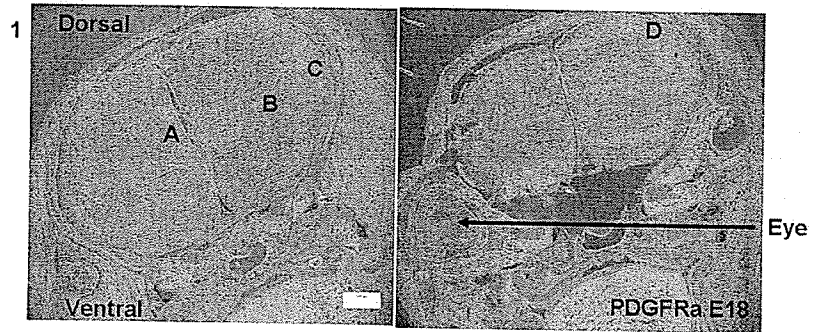


Figure 5.15. PDGF-R α expression at E19.5 in the mouse brain:

Panel 1 – Phase contrast photomicrograph of an E19 mouse brain section showing three regions of the brain: in the middle (bottom left and bottom right panels) and posterior (top panel) (10 \times). Areas shown at higher magnification are labeled A-D.

Bar = 500 μ m.

Panel 2 – Immunohistochemistry showing PDGF-R α (green) expression in the different regions of mouse brain (60 \times). Cells are counterstained with DAPI (blue).

A – Area from caudate putamen besides ventricle showing PDGF-R α expression. B

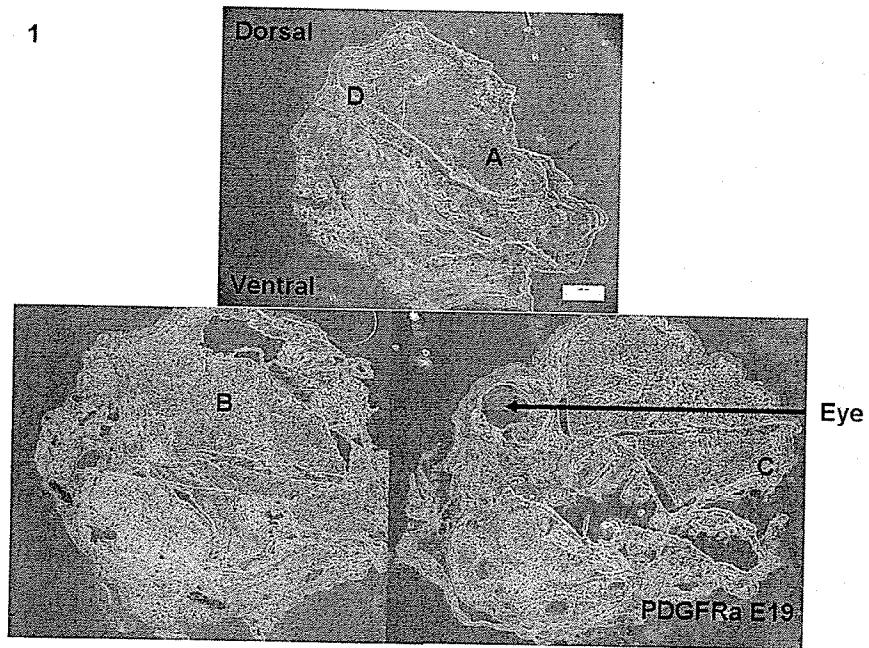
– Area from fornix showing PDGF-R α expression. C – Area from cerebral cortex

showing PDGF-R α expression. D – Area from cerebral cortex showing PDGF-R α

expression. Bar = 50 μ m.

E19.5

1



2

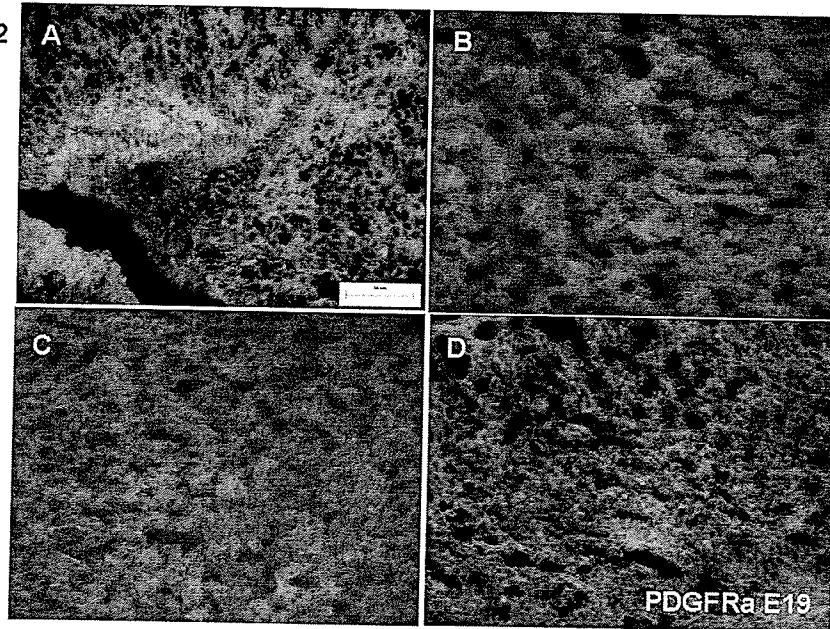


Figure 5.16. PDGF-R α expression at P2 in the mouse brain:

Panel 1 – Phase contrast photomicrograph of P2 mouse brain section showing three regions of the brain: in the middle (top, bottom left and bottom right panels) (10 \times).

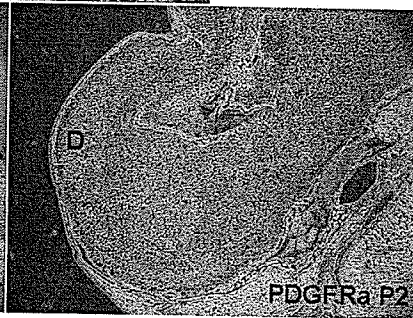
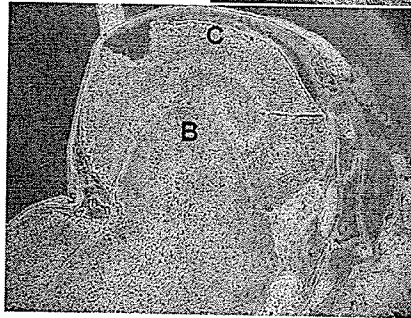
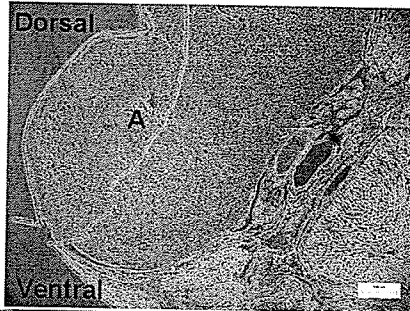
Areas shown at higher magnification are labeled A-D. Bar = 500 μ m.

Panel 2 – Immunohistochemistry showing PDGF-R α (green) expression in the different regions of mouse brain (60 \times). Cells are counterstained with DAPI (blue).

A – Area from caudate putamen showing PDGF-R α expression. B – Area from hippocampus showing PDGF-R α expression. C – Area from primary auditory cortex showing PDGF-R α expression. D – Area from primary somatosensory cortex showing PDGF-R α expression. Bar = 50 μ m.

P2

1



2

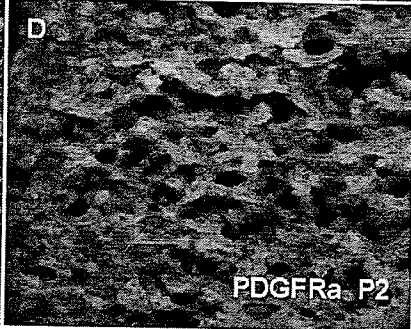
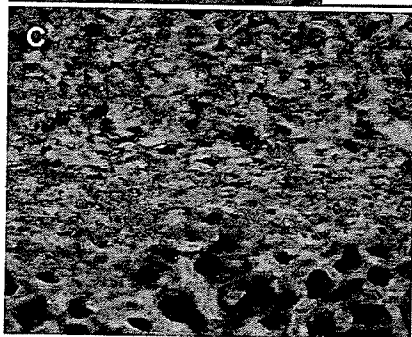
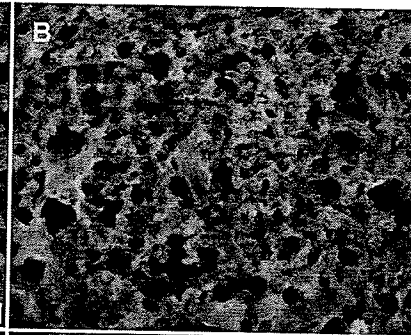
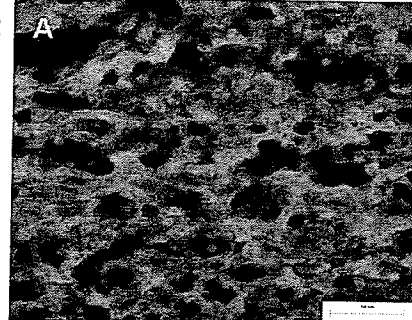


Figure 5.17. PDGF-R α expression at P3 in the mouse brain:

Panel 1 – Phase contrast photomicrograph of a P3 mouse brain section showing two regions of the brain: anterior (left panel) and in the middle (right panel) (10 \times). Areas shown at higher magnification are labeled A-D. Bar = 500 μ m.

Panel 2 – Immunohistochemistry showing PDGF-R α (green) expression in the different regions of mouse brain (60 \times). Cells are counterstained with DAPI (blue).

A – Area from olfactory bulb showing PDGF-R α expression. B – Area from caudate putamen showing PDGF-R α expression. C – Area from secondary somatosensory cortex showing PDGF-R α expression. D – The conjunction of caudate putamen and piriform cortex showing PDGF-R α expression. Bar = 50 μ m.

P3

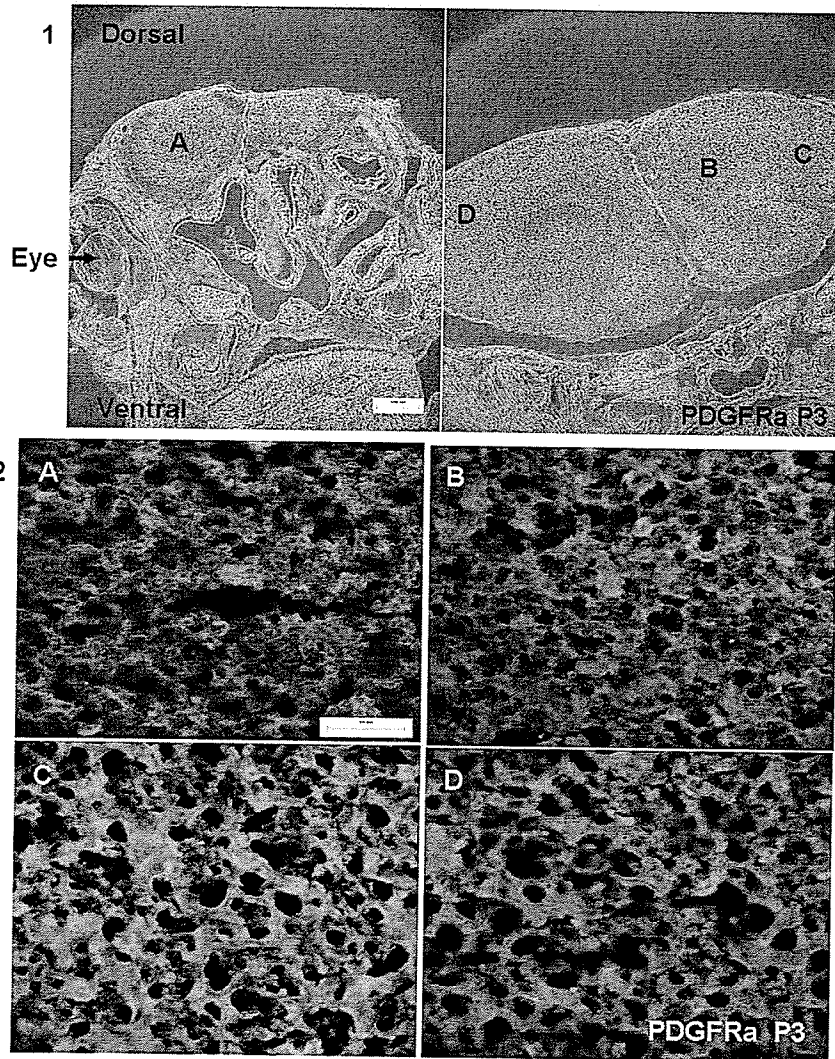


Figure 5.18. PDGF-R α expression at P4 in the mouse brain:

Panel 1 – Phase contrast photomicrograph of a P4 mouse brain section showing four regions of the brain: anterior (top left panel) and posterior (top right, bottom left and bottom right panels) (10 \times). Areas shown at higher magnification are labeled A-D.

Bar = 500 μ m.

Panel 2 – Immunohistochemistry showing PDGF-R α (green) expression in the different regions of mouse brain (60 \times). Cells are counterstained with DAPI (blue).

A – Area from olfactory bulb showing PDGF-R α expression. B – Area from caudate putamen showing PDGF-R α expression. C – Area from lateral hypothalamic area showing PDGF-R α expression. D – Area from piriform cortex showing PDGF-R α expression. Bar = 50 μ m.

P4

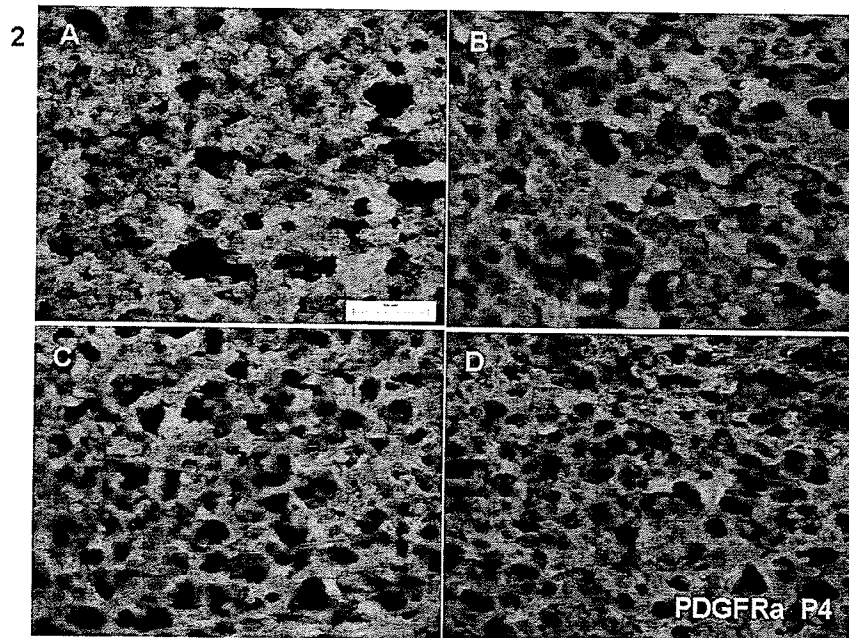
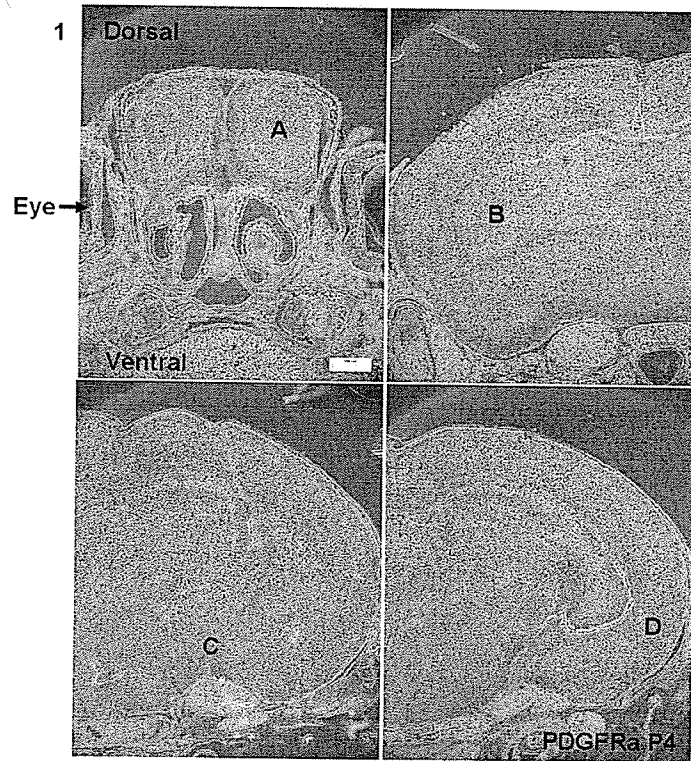


Figure 5.19. PDGF-R α expression at P5 in the mouse brain:

Panel 1 – Phase contrast photomicrograph of a P5 mouse brain section showing three regions of the brain: anterior (left panel) and posterior (middle and right panels) (10 \times). Areas shown at higher magnification are labeled A-D. Bar = 500 μ m.

Panel 2 – Immunohistochemistry showing PDGF-R α (green) expression in the different regions of mouse brain (60 \times). Cells are counterstained with DAPI (blue).

A – Area from olfactory bulb showing PDGF-R α expression. B – Area from caudate putamen showing PDGF-R α expression. C – Area from accumbens nucleus showing PDGF-R α expression. D – Area from accumbens nucleus showing PDGF-R α expression. Bar = 50 μ m.

P5

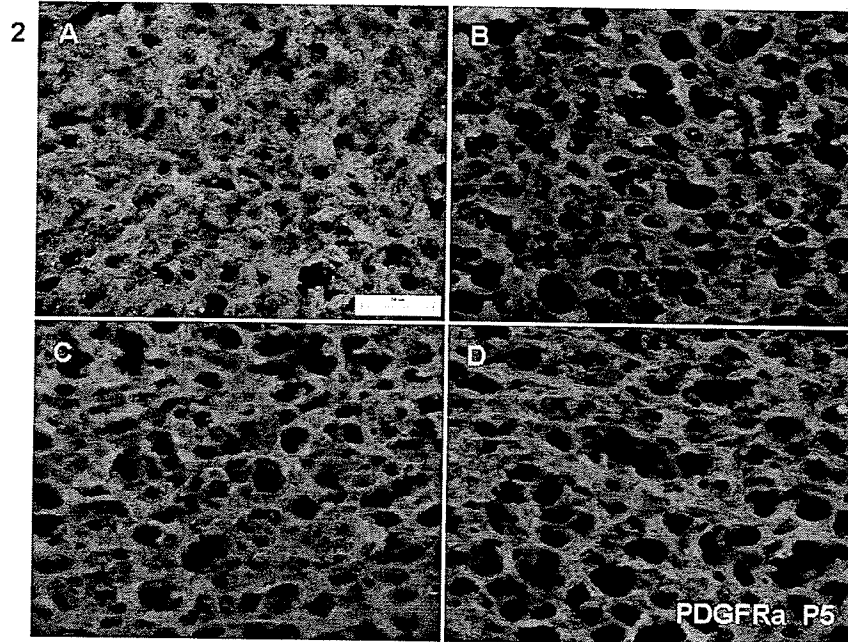
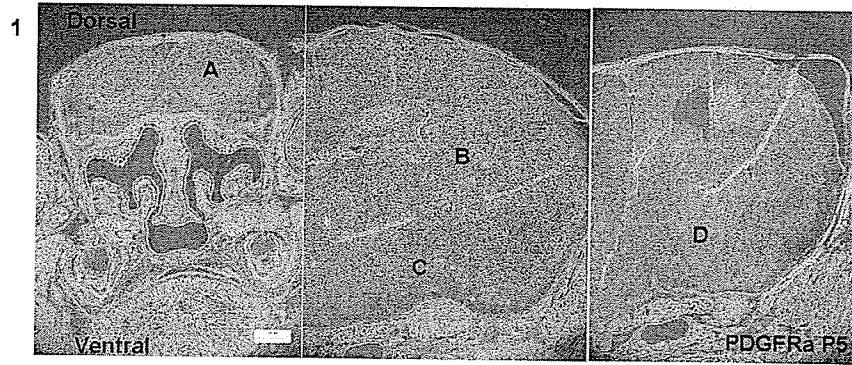


Figure 5.20. PDGF-R α expression at P6 in the mouse brain:

Panel 1 – Phase contrast photomicrograph of a P6 mouse brain section showing four regions of the brain: anterior (top left panel) and posterior (top right, bottom left and bottom right panels) (10 \times). Areas shown at higher magnification are labeled A-D.

Bar = 500 μ m.

Panel 2 – Immunohistochemistry showing PDGF-R α (green) expression in the different regions of mouse brain (60 \times). Cells are counterstained with DAPI (blue).

A – Area from olfactory bulb showing PDGF-R α expression. B – Area from caudate putamen showing PDGF-R α expression. C – Area from accumbens nucleus showing PDGF-R α expression. D – Area from secondary motor cortex showing PDGF-R α expression. Bar = 50 μ m.

P6

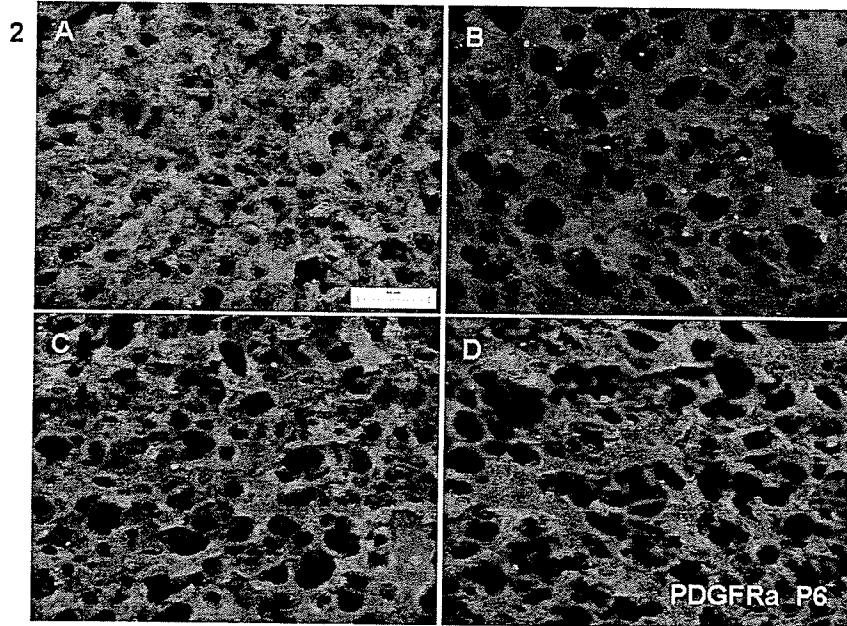
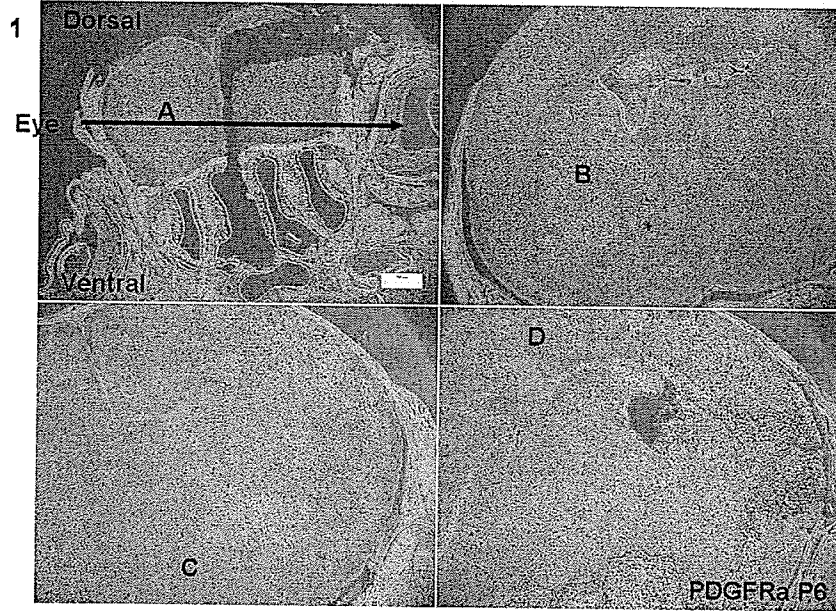


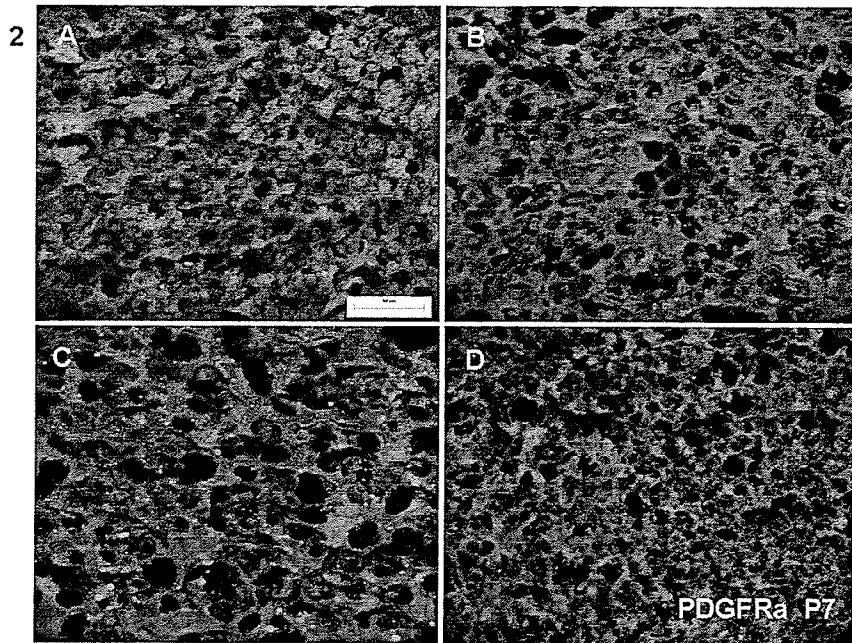
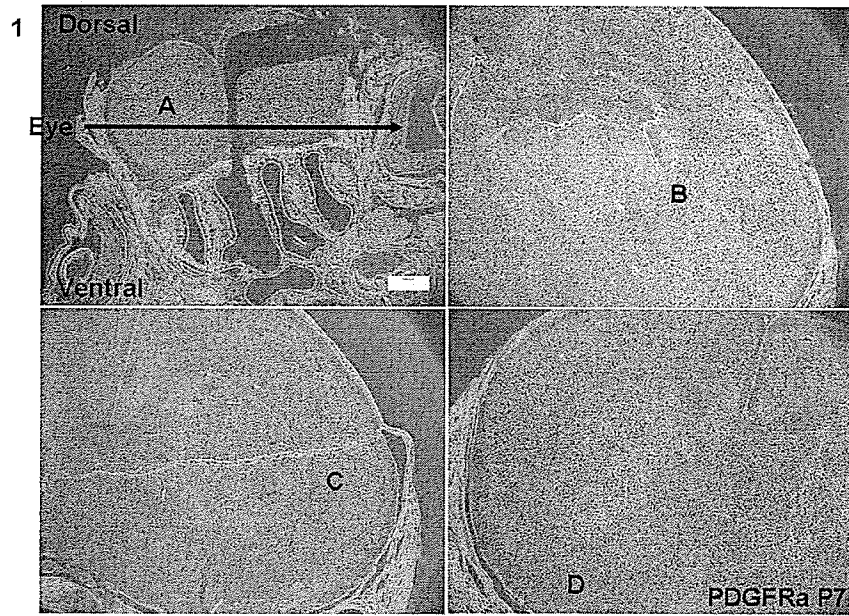
Figure 5.21. PDGF-R α expression at P7 in the mouse brain:

Panel 1 – Phase contrast photomicrograph of a P7 mouse brain section showing four regions of the brain: anterior (top left panel), in the middle (bottom left and bottom right panels) and posterior (top right) (10 \times). Areas shown at higher magnification are labeled A-D. Bar = 500 μ m.

Panel 2 – Immunohistochemistry showing PDGF-R α (green) expression in the different regions of mouse brain (60 \times). Cells are counterstained with DAPI (blue).

A – Area from olfactory bulb showing PDGF-R α expression. B – Area from caudate putamen showing PDGF-R α expression. C – Area from agranular insular cortex showing PDGF-R α expression. D – Area from piriform cortex showing PDGF-R α expression. Bar = 50 μ m.

P7



Results

The current study examined PDGF-A and PDGF-R α expression all over the brain at both embryonic and postnatal stages. The results showed that PDGF-R α immunoreactivity is restricted to the germinal matrix, where the ventricular zone and SVZ are located, at the earliest stage of brain development. As the brain develops, PDGF-R α immunoreactivity is seen at an increasing distance from the germinal matrix. PDGF-R α expression pattern, therefore, changes in correlation to expected movement of OPs in the developing brain.

On the other hand, PDGF-A protein expression is ubiquitous. The immunoreactivity of PDGF-A is seen everywhere throughout the developing mouse brain. Further, the extent of the PDGF-A expression is the same at the different stages.

Chapter VI

CXCL1 Expression in the Developing Mouse Brain

Introduction

The CXC chemokines are a group of chemokines that have the two conserved cysteine residues separated by one amino acid residue. CXCL1 is a high affinity ligand for CXCR2. In the CNS, CXCL1 is largely expressed by astrocytes (Tsai et al., 2002). In contrast, its receptor CXCR2 is expressed by a variety of cells: immature OPs, mature OLs, neurons, microglia cells and astrocytes (Tsai et al., 2002; Fillpovic and Zecevic, 2008; Omari et al., 2006).

To date, the role of chemokines in regulating OL lineage and myelination is not fully understood. Previous studies have shown that CXCL1, in combination with PDGF, plays an important role in the regulation of OP dispersal in the developing CNS (Robinson et al., 1998; Tsai et al., 2002; Fillpovic and Zecevic, 2008). CXCL1 is known to regulate OPs migration, proliferation and myelination in the rodent CNS (Robinson et al., 1998; Tsai et al., 2002; Fillpovic and Zecevic, 2008). It is important to note that its receptor, CXCR2, is also essential for the OL development, distribution as well as myelination in the CNS (Robinson et al., 1998; Tsai et al., 2002; Padovani-Claudio et al., 2006). Further, CXCR2s bind some other chemokines, such as IL-8 and CXCL8 which may also regulate OP proliferation (Fillpovic and Zecevic, 2008).

In the developing spinal cord, CXCL1 contributes to the distribution of OPs by inhibiting PDGF induced OPs migration (Tsai et al., 2002). Further, this effect is rapid and reversible (Tsai et al., 2002). However, the mechanism by which CXCL1 inhibits OPs migration is currently unclear. In addition, CXCL1 initiates

proliferation in human and rodent OPs (Robinson et al., 1998; Fillpovic and Zecevic, 2008). Robinson et al first discovered that CXCL1 induces the OPs proliferative response in synergy with PDGF in rats (Robinson et al., 1998). One recent study also found that CXCL1 promotes OPs proliferation in the human fetal brain (Fillpovic and Zecevic, 2008). Fillpovic and Zecevic further revealed that this effect is achieved by activating the ERK1/2 pathway and releasing IL-6 from astrocytes in the human fetal brain (Fillpovic and Zecevic, 2008). Moreover, one in vitro study demonstrated that CXC chemokines, such as CXCL1, IL-8, and stromal cell-derived factor-1 alpha (SDF-1 α), are able to increase OL proliferation, MBP synthesis, as well as enhance myelin sheath formation (Kadi et al., 2006).

A few studies have examined the CXCL1 expression in the rat spinal cord and brain. Robinson et al detected CXCL1 expression at the postnatal stage, both in the rat spinal cord and brain (Robinson et al., 1998; Robinson and Franic, 2001). Tsai et al further confirmed the above finding in the rat spinal cord (Tsai et al., 2002). Due to the few published studies focusing on the role of expression in the developing brain, this study's purpose was proposed to clarify the pattern of expression of CXCL1.

CXCL1 Expression in the Mouse Brain

The expression of CXCL1 was hypothesized that it is expressed after OPs migration and proliferation, but prior to differentiation, which is at the postnatal stage (personal communication with Dr. Emma, Frost). Therefore, sequential sections of mice brains from P2 to P7 were used to investigate CXCL1 expression in the developing mouse brain. The fluorescent secondary antibodies were not as robust as

was required, and photobleaching of the staining occurred. Therefore, AEC which is a permanent, enzymatic visualization and a robust reliable procedure was used to assess immunoreactivity.

The sections were photographed under bright-field microscopy using Image Pro 6.0. The age of the tissue is denoted at the lower right and the higher magnification images are derived from the boxes in phase contrast images.

The protein expression was analyzed throughout the brain, including SVZ, lateral ganglion eminence and cortical regions. Representative pictures are shown as follows.

CXCL1 Expression Pictures from P2-P7

Figure 6.1. CXCL1 expression at P2 in the mouse brain:

Panel 1 – Phase contrast photomicrograph of a P2 mouse brain section showing two regions of the brain: anterior (left panel) and in the middle (right panel) (10×). Areas shown at higher magnification are labeled A-D. Bar = 500 μm .

Panel 2 – High magnification bright field photomicrograph of P2 mouse brain section showing CXCL1 expression (60×). A – Area from olfactory bulb showing no detectable CXCL1 expression. B – Area from caudate putamen showing no detectable CXCL1 expression. C – Area from primary motor cortex showing no detectable CXCL1 expression. D – Area from primary motor cortex showing no detectable CXCL1 expression. The arrow indicated red cell which is from the blood vessel. Bar = 50 μm .

P2

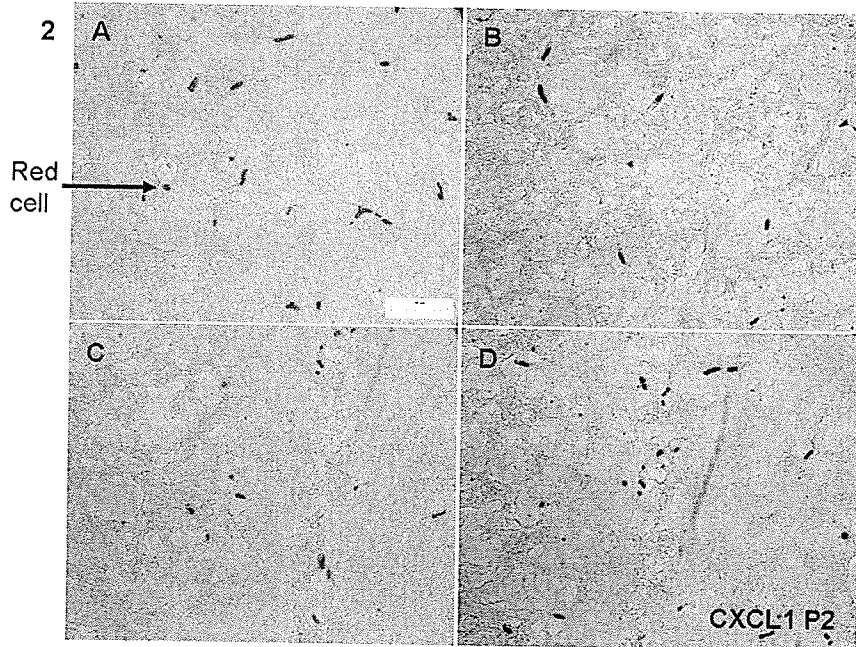
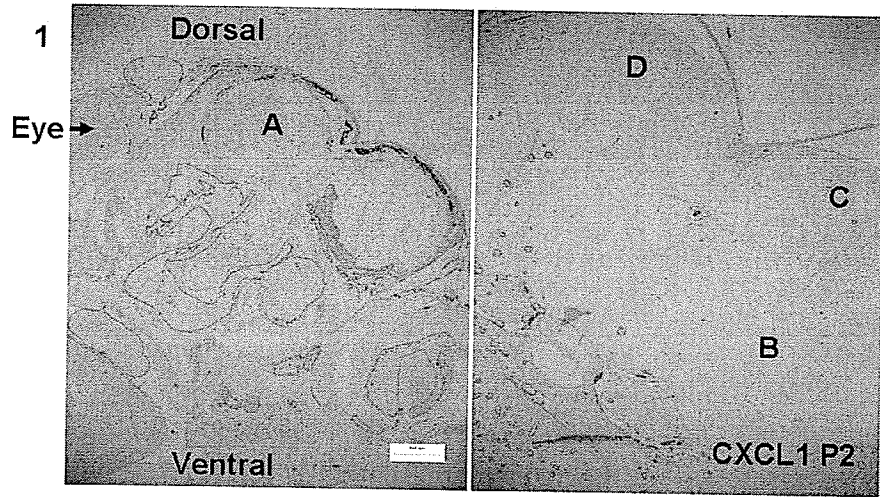


Figure 6.2. CXCL1 expression at P3 in the mouse brain:

Panel 1 – Phase contrast photomicrograph of a P3 mouse brain section showing two regions of the brain: anterior (left panel) and in the middle (middle and right panels) (10×). Areas shown at higher magnification are labeled A-D. Bar = 500 μm .

Panel 2 – High magnification bright field photomicrograph of P3 mouse brain section showing CXCL1 expression (60×). A – Area from olfactory bulb showing no detectable CXCL1 expression. B – Area from caudate putamen showing no detectable CXCL1 expression. C – Area from primary motor cortex and secondary motor cortex showing no detectable CXCL1 expression. D – Area from primary somatosensory cortex showing no detectable CXCL1 expression. Bar = 50 μm .

P3

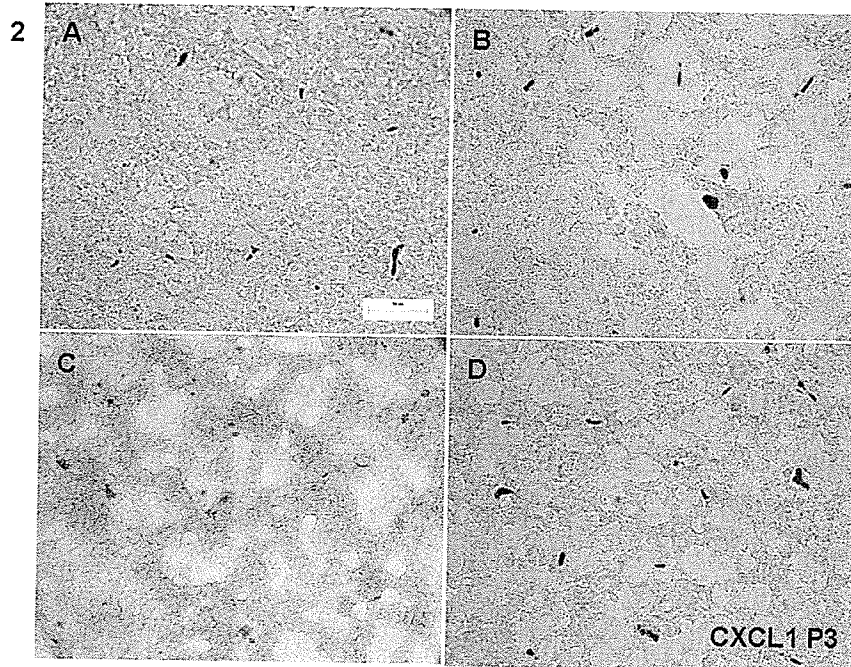
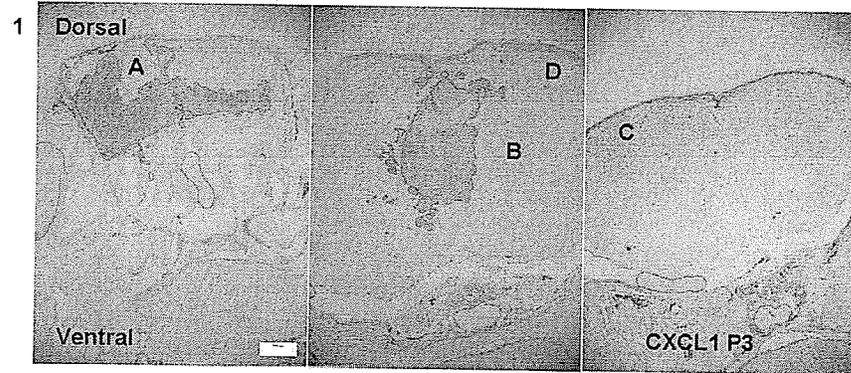


Figure 6.3. CXCL1 expression at P4 in the mouse brain:

Panel 1 – Phase contrast photomicrograph of a P4 mouse brain section showing three regions of the brain: anterior (left panel), in the middle (middle and right panels) (10×). Areas shown at higher magnification are labeled A-D. Bar = 500 μm .

Panel 2 – High magnification bright field photomicrograph of P4 mouse brain section showing CXCL1 expression (60×). A – Area from olfactory bulb showing no detectable CXCL1 expression. B – Area from the conjunction of lateral orbital cortex and ventral orbital cortex showing no detectable CXCL1 expression. C – Area from caudate putamen showing no detectable CXCL1 expression. D – Area from secondary motor cortex showing no detectable CXCL1 expression. Bar = 50 μm .

P4

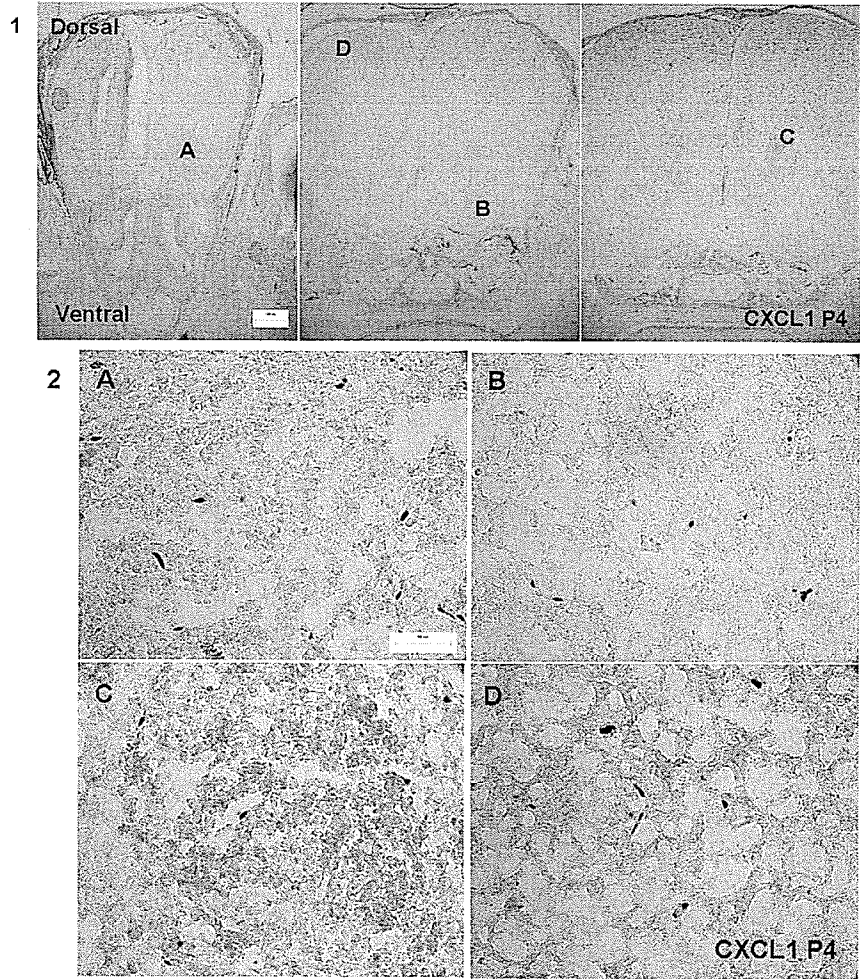


Figure 6.4. CXCL1 expression at P5 in the mouse brain:

Panel 1 – Phase contrast photomicrograph of a P5 mouse brain section showing three regions of the brain: anterior (left panel), in the middle (middle panel) and posterior (right panel) (10×). Areas shown at higher magnification are labeled A-D. Bar = 500 μm .

Panel 2 – High magnification bright field photomicrograph of P5 mouse brain section showing CXCL1 expression (60×). A – Area from olfactory bulb showing no detectable CXCL1 expression. B – Area from caudate putamen showing no detectable CXCL1 expression. C – Area from piriform cortex showing no detectable CXCL1 expression. D – Area from the conjunction of primary motor cortex and primary somatosensory cortex showing no detectable CXCL1 expression. Bar = 50 μm .

P5

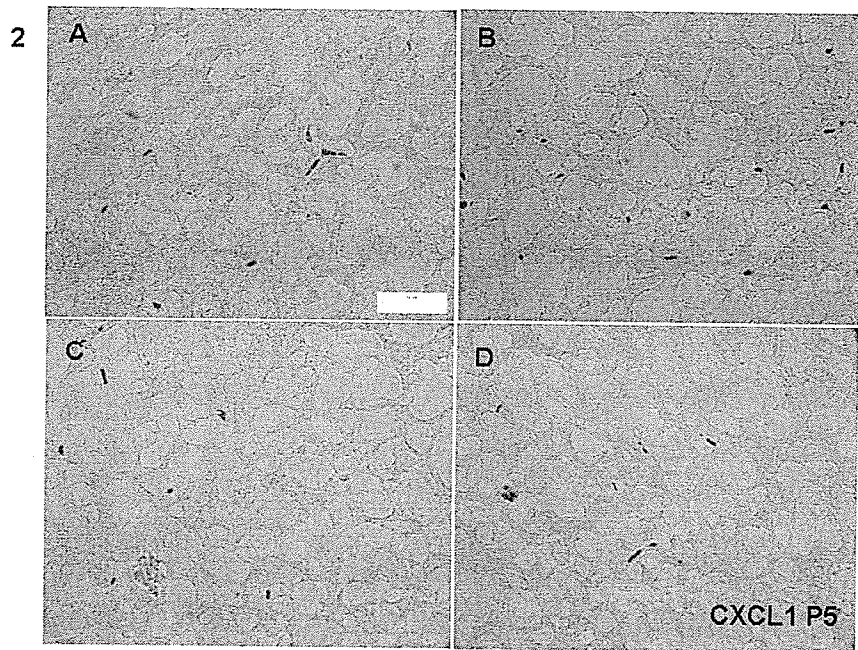
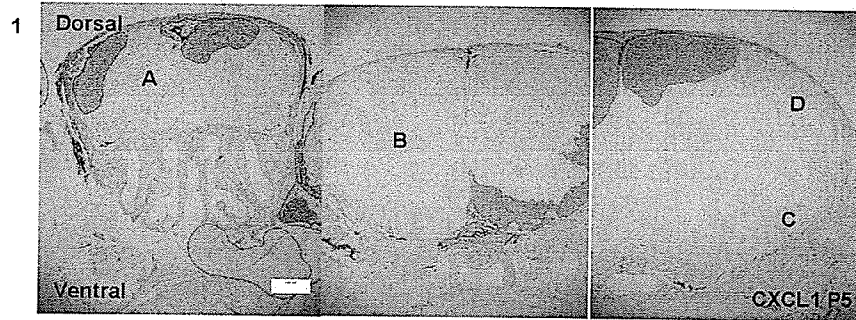


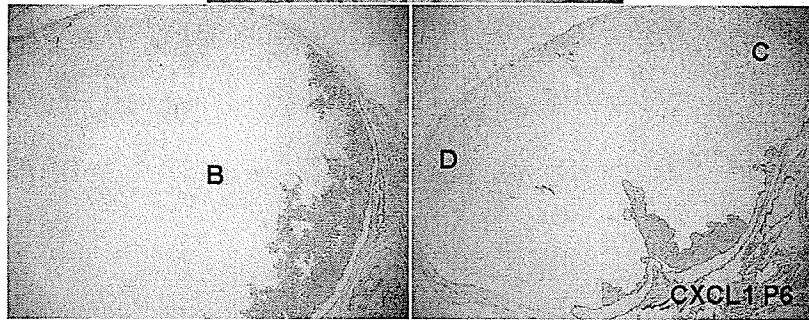
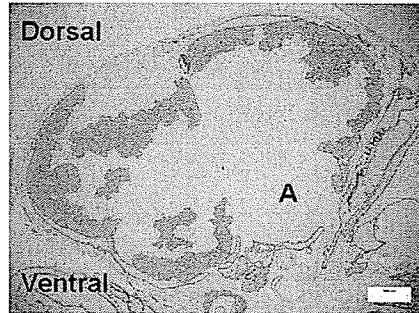
Figure 6.5. CXCL1 expression at P6 in the mouse brain:

Panel 1 – Phase contrast photomicrograph of a P6 mouse brain section showing three regions of the brain: in the middle (top panel) and posterior (bottom left and bottom right panels) (10×). Areas shown at higher magnification are labeled A-D. Bar = 500 μm .

Panel 2 – High magnification bright field photomicrograph of P6 mouse brain section showing CXCL1 expression (60×). A – Area from anterior olfactory nucleus showing no detectable CXCL1 expression. B – Area from caudate putamen showing no detectable CXCL1 expression. C – Area from primary somatosensory cortex showing no detectable CXCL1 expression. D – Area from primary somatosensory cortex showing no detectable CXCL1 expression. Bar = 50 μm .

P6

1



2

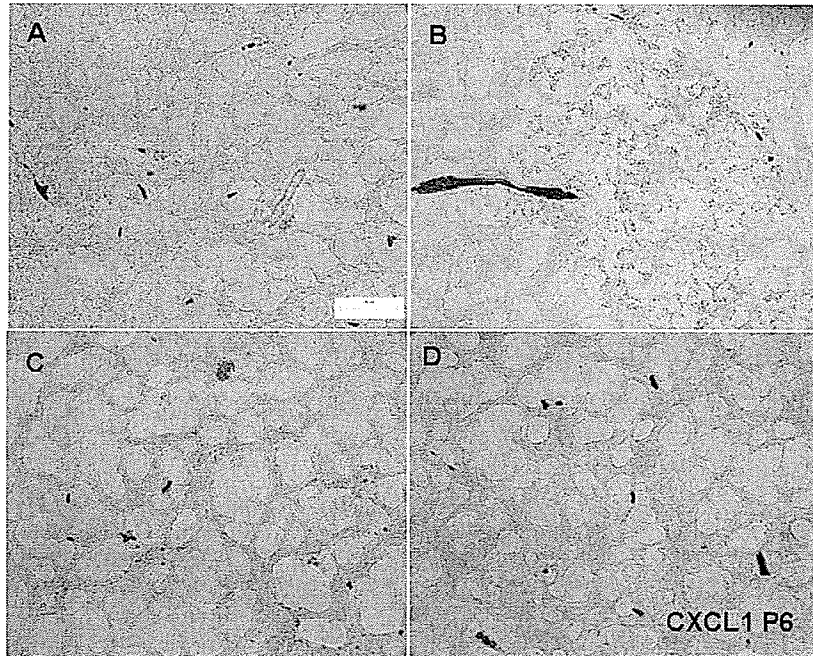
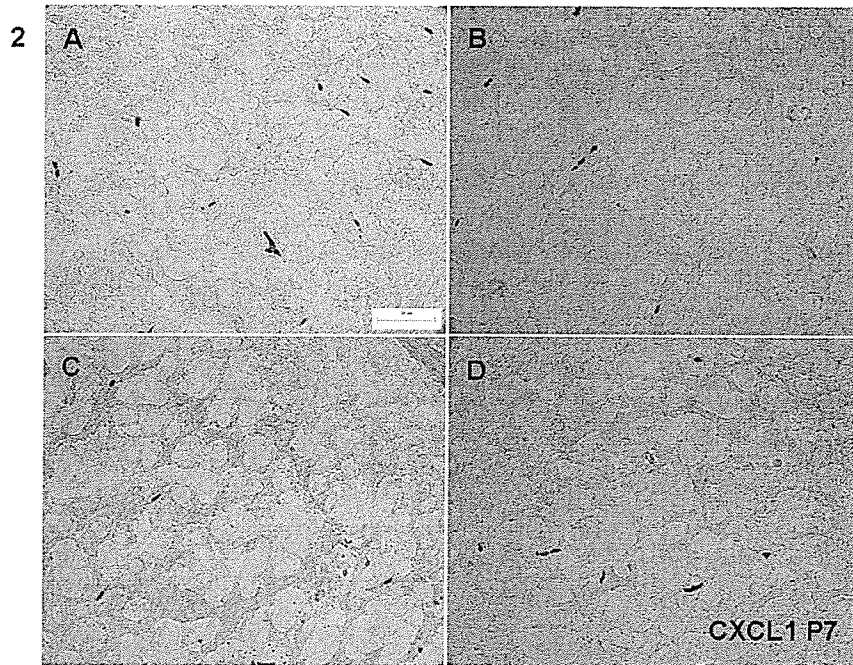
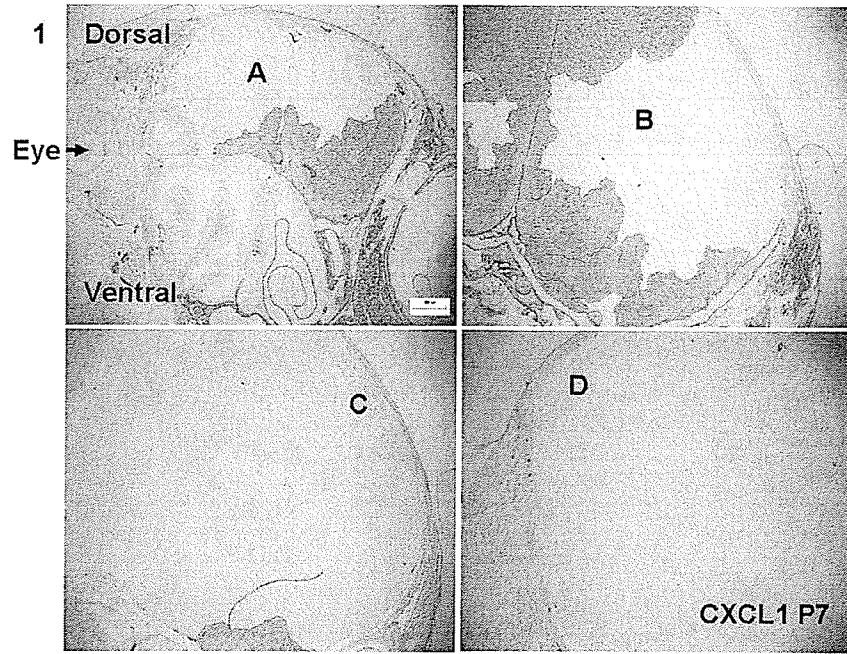


Figure 6.6. CXCL1 expression at P7 in the mouse brain:

Panel 1 – Phase contrast photomicrograph of a P7 mouse brain section showing three regions of the brain: anterior (top left panel) and in the middle (top right, bottom left and bottom right panels) (60×). Areas shown at higher magnification are labeled A-D. Bar = 500 μ m.

Panel 2 – High magnification bright field photomicrograph of P7 mouse brain section showing CXCL1 expression (60×). A – Area from olfactory bulb showing no detectable CXCL1 expression. B – Area from caudate putamen showing no detectable CXCL1 expression. C – Area from primary motor cortex showing no detectable CXCL1 expression. D – Area from primary motor cortex showing no detectable CXCL1 expression. Bar = 50 μ m.

P7



Results

From postnatal stage P2 to P7, CXCL1 expression is undetectable throughout this stage of brain development. However, positive control study was not conducted prior to this study. The reason is that I have difficulty to find suitable tissue or organ to test the antibody. Therefore, further study needs to be performed before drawing conclusions.

Chapter VII

Discussion

In the CNS, OLs play an important role in the formation and maintenance of the myelin sheath. An intact myelin system is essential for the efficient conduction of nerve impulses. As previously mentioned, OPs initially appear in discrete areas of the developing CNS, such as the embryonic ependymal zone (Rakic and Zecevic, 2003), the ganglionic eminences (Kessaris et al., 2006) and the SVZ, or sub-ependymal zone (Miller, 1996). Subsequently, OPs proceed through a complex lineage series of events, including migration, proliferation, differentiation and myelination.

The development of OLs is associated with several growth factors that appropriately govern OL migration, proliferation and differentiation, ultimately leading to the assembly of myelin sheath. Therefore, to achieve a clear understanding of the growth factors that regulate OL development, it would be greatly beneficial to explore these intricate mechanisms. Of these growth factors, PDGF-A is known to act as a powerful motogen for OPs, as well as being an important factor for regulating OPs migration, proliferation, differentiation and survival (Calver et al., 1998; Armstrong et al., 1991; Frost et al., 1996; Frost et al., 2008; Barres et al., 1993; Noble et al., 1988). CXCL1 has been shown to synergize with PDGF-A to regulate OPs migration, proliferation and myelination (Robinson et al., 1998; Tsai et al., 2002; Fillpovic and Zecevic, 2008).

Early hypotheses suggested that a gradient of PDGF-A concentrations exists to drive OPs migration away from their site of origin. However, such concentration gradient has never been experimentally identified. Therefore, this study was designed to answer the question “Is there a concentration gradient of PDGF-A in the

developing mouse brain?”

In the study presented in this thesis, novel finding includes short term exposure (30 minutes) to PDGF-A is able to induce OPs migration for up to 72 hours without increasing cell number or causing cell death. Further, another novel finding of this study is that ERK signaling pathway is responsible for the PDGF-A stimulated OP migration. As the first to analyze the OL specific proteins expression in daily succession during both embryonic and postnatal development, this study showed that PDGF-R α immunoreactivity is restricted to the germinal matrix at the earliest stage, and then as the brain develops, is seen at an increasing distance from the germinal matrix. In contrast, PDGF-A expression is ubiquitous, which is in accordance with the previous studies (Calver et al., 1998; Hutchins and Jefferson, 1992). Furthermore, there is no detectable CXCL1 expression at the postnatal stage, differing from the previous studies (Robinson et al., 1998; Robinson and Franic, 2001; Tsai et al., 2002).

Previous studies have shown that PDGF is indispensable for normal OL development (Fruttiger et al., 1999; Soriano, 1997) and plays a critical role in regulating OP migration (Armstrong et al., 1991; Frost et al., 1996; Milner et al., 1997). Based on the present study, the results are consistent with the previous studies that PDGF is a key factor to initiate OPs migration. In addition, this study does not support a PDGF-A concentrations gradient both in vivo and in vitro. In vivo study proved that PDGF-A expression is ubiquitous. In vitro study further revealed that OP does not require such concentration gradient in order to migrate.

Transient Exposure to PDGF-A Induces OPs Migration for up to 72 Hours

Previous studies looked at OPs migration by exposing OPs to PDGF continuously (Armstrong et al., 1991; Frost et al., 1996; Milner et al., 1997), while this study investigated OPs migration in response to transient PDGF exposure. The results showed that OPs treated with 10 ng/ml PDGF-A for 30 minutes migrate as far as cells exposed to PDGF-A continuously throughout the 72 hours duration of the experiment. This novel finding indicates that OP does not need to expose to PDGF-A continuously, in other words, OP does not require a PDGF-A concentration gradient in order to migrate. In addition, PDGF-A is confirmed to be critical in inducing and maintaining OPs migration.

Further, transient exposure to 10 ng/ml PDGF-A for up to 120 minutes does not initiate OPs proliferation, in contrast to the PDGF-A incubation for 24 hours which does induce proliferation. This was also confirmed by AMPA, which proved that inhibition of OPs proliferation does not affect OPs migration in response to PDGF-A. According to the migration assay, the cell density, on the other hand, appeared to be lower when OPs were exposed to PDGF-A for only 30 minutes.

A study by Dyson and Gurdon revealed that cells can detect morphogen concentration, followed by changing receptor occupancy from below to above 50% (Dyson and Gurdon, 1998). In addition, another previous study showed that ligand and receptor tyrosine kinase binding duration plays an important role in activation of different downstream signaling pathways (Stork, 2002). For example, transient and

continuous ERK activation may result in proliferation and differentiation, respectively (Stork, 2002). Further, Heldin and his co-workers reported that the binding of ligand and receptor for at least 8 hours is required to activate cell cycle progression (Heldin et al., 1998). In the current study, transient PDGF-A exposure for up to 120 minutes does not stimulate OPs proliferation, which is consistent with the previous study (Heldin et al., 1998). Therefore, transient PDGF-A exposure only activates OPs migratory capacity, but not proliferation (Frost et al., 2008).

PDGF Withdrawal

In this study, there is no significant increase of activated caspase-3 in OPs 72 hours after PDGF-A withdrawal. As stated, PDGF-A is essential to regulate OP survival (Calver et al., 1998). Tokumoto et al used RT-PCR to investigate the effect of PDGF withdrawal on mRNAs encoding cyclin D and E which is necessary for cell progression through G1 phase and into S phase (Tokumoto et al., 1999). They found that PDGF withdrawal resulted in a decrease in cyclin D2 mRNA and an increase in cyclin D3 mRNA (Tokumoto et al., 1999). In addition, they also used RT-PCR to examine the induction of several immediate early genes in OPs in response to PDGF withdrawal. The mRNAs of two genes: c-fos and NGFI-A/Krox-23 were found decreasing rapidly, suggesting that such change plays a role in facilitating cells to arrest from cell cycle and differentiate (Tokumoto et al., 1999). However, the data presented in this study differ from the previous study.

An explanation for the difference is the different techniques used. The current standard technique for culturing OP includes the addition of PDGF and FGF to

increase cell numbers prior to analysis. Consequently, removal of the PDGF leads to cell death. In contrast, OPs in this study are not exposed to PDGF-A prior to running experiment. Further, Baron showed that when PDGF at the physiological concentration, OPs proliferation depends on the growth factor and the $\alpha v\beta 3$ integrin binding to PDGF-R α (Baron et al., 2002). Thus, we (personal communication with Dr. Emma Frost) hypothesized that PDGF dependency occurs only after PDGF exposure. Further experiments are required to clarify this hypothesis.

ERK Signaling Regulates PDGF Induced OPs Migration

ERK signaling activation is one of the most rapid cellular responses to growth factor and other external stimuli (Bhat and Zhang, 1996). The current study deals with the characterization of the activation of ERK signaling in response to PDGF-A, using the agarose drop migration assay and Western blot analysis.

The results indicated that ERK signaling pathway is activated in OPs upon PDGF-A stimulation and is a necessary requirement for PDGF-A induced OPs migration. Further, this study shows that U0126, an inhibitor for both ERK1 and ERK2, reduced PDGF-A stimulated OPs migration at both 5 and 10 μ M in a concentration-dependent manner.

In a recent study, Kato et al investigated the expression of the activated form of ERK, phosphorylated ERK, in the developing chick spinal cord and dorsal root ganglia. They showed that expression of pERK is in a spatio-temporal pattern, supporting the role of ERK in the regulation of OPs migration (Kato et al., 2005).

The finding from this previous study also supports the results presented from the current study that the ERK signaling pathway is involved in the PDGF-A stimulated OPs migration.

PDGF Ligand and Receptor Expression in the Developing Mouse Brain

Accumulating evidence demonstrates that both PDGF-A and PDGF-R α are crucial in the development of OL (Fruttiger et al., 1999; Soriano, 1997). Previous studies have shown that PDGF-R α is expressed exclusively or predominantly on OL pre-progenitor cells and OPs (Pringle et al., 1992). PDGF-A is ubiquitously distributed in the developing CNS (Calver et al., 1998). Mercola and colleagues showed that PDGF-A mRNA, but not PDGF-B mRNA is detectable at both E 6.5 and E 7.5 (Mercola et al., 1990). In addition, they also demonstrated that transcripts encoding receptor α were more abundant than those encoding receptor β in embryos from E 6.5 to E 8.5 (Mercola et al., 1990). Another study using Western blot showed that PDGF-A protein expression becomes detectable at E11, peaks at E18 and disappears at P14 (Hutchins and Jefferson, 1992).

Previous studies showed that PDGF-R α expression is time dependent and location specific. Using in situ hybridization, Pringle et al showed that a few PDGF-R α positive cells are expressed inferior to the lateral ventricles outside of the rat SVZ at E16 (Pringle et al., 1992). The PDGF-R α positive cells distribute widely throughout the brain and increase in numbers with time until P 10 (Pringle et al., 1992).

Levison et al examined the patterns or pathways of OPs migration in rats, using a retroviral expression vector (Levison, Chuang et al., 1993). The retroviral labeling study has the ability to integrate the recombinant retrovirus into the host genome stably. Further, the labeled cells can be easily visualized. They found that the majority of the labeled cells were restricted to the SVZ, and the remainders were located close to the SVZ at postinjection day 2 (Levison, Chuang et al., 1993). The labeled cells then decreased in the SVZ with time, while more cells appeared in the white matter adjacent to the SVZ. They concluded that the cells had migrated from the SVZ (Levison, Chuang et al., 1993).

The results outlined here corroborate the earlier studies, showing that the developmental pattern of PDGF-R α is temporally and spatially regulated. I also found that PDGF-R α expression is restricted to the germinal matrix at the earliest stage. As the brain develops, PDGF-R α expression is seen at an increasing distance from the germinal matrix. Therefore, PDGF-R α is expressed in a pattern that correlates to hypothesized movement of OPs in the developing rodent brain, which concurred with a previous study by Levison in 1993 (Levison, Chuang et al., 1993).

In contrast, PDGF-A, which is synthesized by neurons, astrocytes and OLs (Fruttiger et al., 1999; Heldin and Westermark, 1999), is expressed everywhere throughout the developing mouse brain. Early hypotheses suggested that there is a chemotactic gradient of PDGF-A driving OP migration. However, the current findings do not support such hypotheses. Further, future experiments using *in situ* hybridization will be conducted to map the distribution of mRNA of both PDGF-A

and PDGF-R α . This will provide information on differential expression patterns of the genes, further clarifying the role of PDGF-A expression in the regulation of OPs, which is indispensable to make a complete and full descriptive study.

CXCL1 Expression in the Developing Mouse Brain

The responsiveness of OPs can be altered by interacting with a variety of other mediators. The chemokine, CXCL1 is an ideal candidate. CXCL1 is crucial for the OL development, which is evident by the CXCR2 knockout mouse. The absence of CXCR2 leads to reduced numbers of OL, hypomyelination and a decreased size of OL distribution in the spinal cord white matter (Tsai et al., 2002). It has been clearly demonstrated that CXCL1 plays an essential role in patterning the developing spinal cord (Tsai et al., 2002).

Previous studies showed that CXCL1 synergizes with PDGF to promote OP proliferation as well as to inhibit OP migration in the rodent spinal cord (Robinson et al., 1998; Tsai et al., 2002). However, no clear mechanism underlying the CXCL1 inhibiting OPs migration has been determined.

Several investigators described that the CXCL1 is expressed in the developing spinal cord and brain of the rat. Robinson et al used 3,3'-diaminobenzidine (DAB) staining to detect CXCL1 positive cells from P1 to P8 in the rat spinal cord (Robinson et al., 1998). This group using the same method showed that the CXCL1 expression is temporally and spatially regulated in the neonatal rat brain (Robinson and Franic, 2001). Tsai et al also found that CXCL1 expression appears at postnatal stages in

the rat spinal cord (Tsai et al., 2002).

In the current study, there is no detectable CXCL1 expression throughout the brain from postnatal stage P2 to P7. The results differ widely from the previous studies. This perhaps stems from the varying methodologies or techniques applied. For example, monoclonal anti-human GRO α from Sigma-Aldrich, Inc. was used in the previous studies, while polyclonal goat-anti-GRO α from Santa Cruz Biotechnology, Inc. was used in the present study. Further, positive control study was not tested in the present study. Moreover, slides are 12 μ m, in contrast to the 50 μ m and 200 μ m of the previous studies. Thus, it is essential for a further study to be conducted to confirm the validity of the current study, using the previous methods. An alternate approach could be transient focal CXCL 1 expression. In such a hypothesis, CXCL1 is transiently expressed by astrocytes only when OPs migrate to the presumptive white matter (Tsai et al., 2002).

Chapter VIII

Conclusions

Early hypotheses suggested that a chemotactic gradient of PDGF-A exists to drive the OPs migration. However, the novel findings presented in this study do not support such a gradient. In the current study, OPs do not require a chemotactic gradient in order to migrate. As shown, OPs exposed to PDGF-A for 30 minutes undergo continued active migration. Further, the equivalent extent of migration was reached by OPs exposed to PDGF-A transiently as well as exposed to PDGF-A continuously. In addition, there was no increase in cell numbers when OPs were treated transiently with PDGF-A. Moreover, a 30 minutes PDGF-A exposure is demonstrated to be sufficient to activate ERK signaling pathway. Therefore, the present study has provided unique evidence that PDGF-A acts as an inducer to initiate OPs migration through the activation of ERK signaling.

Further, this study provides novel data demonstrating that the immunoreactivity of PDGF-A is seen everywhere throughout the developing mouse brain, and the expression level remains consistent at all developmental stages. In contrast, a marker of OPs, PDGF-R α immunoreactivity is restricted to the putative location of the migrating OPs at the earliest stage of brain development. As the brain develops, PDGF-R α is seen at increasingly larger distances from the germinal matrix.

Based on the above novel findings, this study, therefore, will provide valuable and basic information for future research on the role of different proteins in the regulation of the different stages of OL lineage.

CXCL1 has been demonstrated to play a pivotal role in patterning the developing spinal cord (Tsai et al., 2002). However, I was unable to detect CXCL1

immunoreactivity during development of the mouse brain in the current study.

Therefore, it is surely evident that further study needs to be performed prior to

drawing conclusions.

Chapter IX

Future Directions

Future directions include:

1. Identify positive control for CXCL1 and do the CXCR2 study.
2. Further study the role of ERK signaling using knockdown and specific pharmacological inhibitor.
3. Study the signaling pathway interaction.

Chapter X

References

- Alessi, DR., Cuenda, A., Cohen, P., Dudley, DT., Saltiel, AR. (1995). PD098059 is a specific inhibitor of the activation of mitogen-activated protein kinase kinase in vitro and in vivo. *J Biol Chem.* 270: 27489-27494
- Amiri, KI. and Richmond, A. (2003). Fine tuning the transcriptional regulation of the CXCL1 chemokine. *Progress in Nucleic Acid Research and Molecular Biology.* 74: 1-36
- Armstrong, RC., Harvath, L., Dubois-Dalcq, M. (1991). Astrocytes and O-2A progenitors migrate toward distinct molecules in a microchemotaxis chamber. *Ann N Y Acad Sci.* 633: 520-522
- Armstrong, RC. (1998). Isolation and characterization of immature oligodendrocyte lineage cells. *Methods.* 16: 282-292
- Aston, C., Jiang, L., Sokolov, BP. (2005). Transcriptional profiling reveals evidence for signaling and oligodendroglial abnormalities in the temporal cortex from patients with major depressive disorder. *Mol Psychiatry.* 10:309-322
- Bajramovic, JJ., Brok, HP., Ouwering, B., Jagessar, SA., van Straalen, L., Kondova, I., Bauer, J., Amor, S., t Hart, BA., Ben-Nun, A. (2008). Oligodendrocyte –specific protein is encephalitogenic in rhesus macaques and induces specific demyelination of the optic nerve. *Eur J Immunol.* 38: 1452-1464
- Baron, W., Shattil, JS. and ffrench-Constant, C. (2002). The oligodendrocyte precursor mitogen PDGF stimulates proliferation by activation of $\alpha v\beta 3$ integrins. *EMBO. J.* 21: 1957-1966

- Barres, BA., Jacobson, MD., Schmid, R., Sendtner, M., Raff, MC. (1993). Does oligodendrocyte survival depend on axons? *Curr Biol.* 3(8): 489-497
- Baumann, N. and Pham-Dinh, D. (2001). Biology of oligodendrocyte and myelin in the mammalian central nervous system. *Physiol Rev.* 81: 871-927
- Bhat, NR. and Zhang, P. (1996). Activation of mitogen-activated protein kinases in oligodendrocyte. *J. Neurochem.* 66: 1986-1994
- Bjartmar, C., Hildebrand, C., Loinder, K. (1994). Morphological heterogeneity of rat oligodendrocytes: electron microscopic studies on serial sections. *Glia.* 11:235-244
- Bozzali, M. and Wrabetz, L. (2004). Axonal signals and oligodendrocyte differentiation. *Neurochem Res.* 29: 979-988
- Budihardjo, I., Oliver, H., Lutter, M., Luo, X., Wang, X. (1999). Biochemical pathways of caspase activation during apoptosis. *Annu Rev Cell Dev Biol.* 15: 269-290
- Campagnoni, AT. and Skoff, RP. (2001). The pathobiology of myelin mutants reveal novel biological functions of the MBP and PLP genes. *Brain Pathol.* 11: 74-91
- Calver, AC., Hall, AC., Yu, WP., Walsh, FS., Heath, JK., Betsholtz, C., Richardson, WD. (1998). Oligodendrocyte population dynamics and the role of PDGF in vivo. *Neuron.* 20: 869-882
- Chen, MS., Huber, AB., van der Haar, ME., Frank, M., Schnell, L., Spillmann, AA., Christ, F., Schwab, ME. (2000). Nogo-A is a myelin-associated neurite

outgrowth inhibitor and an antigen for monoclonal antibody IN-1. *Nature*.
403:434-439

de Castro, F. and Bribian, A. (2005). The molecular orchestra of the migration of
oligodendrocyte precursors during development. *Brain Res Rev.* 49: 227-241

Duchala, CS., Asotra, K., Macklin, WB. (1995). Expression of cell surface markers
and myelin proteins in cultured oligodendrocytes from neonatal brain of rat and
mouse: a comparative study. *Dev Neurosci.* 17(2):70-80

Dyer, CA. (2002). The structure and function of myelin: from inert membrane to
perfusion pump. *Neurochem Res.* 27(11):1279-1292

Dyson, S. and Gurdon, J.B. (1998). The interpretation of position in a morphogen
gradient as revealed by occupancy of activin receptors. *Cell.* 93: 557-568

Favata, MF., Horiuchi, KY., Manos, EJ., Daulerio, AJ., Stradley, DA., Feeser, WS.,
Van Dyk, DE., Pitts, WJ., Earl, RA., Hobbs, F., Copeland, RA., Magolda, RL.,
Scherle, PA., Trzaskos, JM. (1998). Identification of a novel inhibitor of
mitogen-activated protein kinase kinase. *J Biol Chem.* 273: 18623-18632

Fields, RD. (2008). White matter in learning, cognition and psychiatric disorders.
Trends Neurosci. 31(7):361-370

Filipovic, R. and Zecevic, N. (2008). The effect of CXCL1 on human fetal
oligodendrocyte progenitor cells. *Glia.* 56:1-15

Fitzner, D., Schneider, A., Kippert, A., Mobius, W., Willig, KI., Hell, SW., Bunt, G.,
Gaus, K., Simons, M. (2006). Myelin basic protein-dependent plasma
membrane reorganization in the formation of myelin. *EMBO. J.* 25: 5037-5048

- Fredriksson, L., Li, H. and Eriksson, U. (2004). The PDGF family: four gene products form five dimeric isoforms. *Cytokine & growth factor rev.* 15: 197-204
- Frost, EE., Kiernan, BW., Faissner, A., French-Constant, C. (1996). Regulation of oligodendrocyte precursor migration by extracellular matrix evidence for substrate-specific inhibition of migration by tenascin-C. *Dev Neurosci.* 18(4): 266-273
- Frost, EE., Milner, R., French-Constant, C. (2000). Migration assays for oligodendrocyte precursor cells. *Methods Mol Biol.* 139: 265-278
- Frost, EE., Nielsen, JA., Le, TQ., Armstrong, RC. (2003). PDGF and FGF2 regulate oligodendrocyte progenitor responses to demyelination. *J Neurobiol.* 54(3): 457-472
- Frost, EE., Zhou, Z., Krasnesky, K., Armstrong, RC. (2008). Initiation of oligodendrocyte progenitor cell migration by a PDGF-A activated extracellular regulated kinase (ERK) signaling pathway. *Neurochem Res.* Epub ahead of print
- Fruttiger, M., Karlsson, L., Hall, AC., Abramsson, A., Calver, AR., Bostrom, H., Willetts, K., Bertold, CH., Heath, JK., Betsholtz, C., Richardson, WD. (1999). Defective oligodendrocyte development and severe hypomyelination in PDGF-A knockout mice. *Development.* 126: 457-467
- Garbern, JY. (2007). Pelizaeus-Merzbacher disease: Genetic and cellular pathogenesis. *Cell Mol Life Sci.* 64(1): 50-65

- Giedd, JN. (2004). Structural magnetic resonance imaging of the adolescent brain.
Ann N Y Acad Sci. 1021: 77-85
- Hakak, Y., Walker, JR., Li, C., Wong, WH., Davis, KL., Buxbaum, JD., Haroutunian, V., Fienberg, AA. (2001). Genome-wide expression analysis reveals dysregulation of myelinatin-related genes in chronic schizophrenia. Proc Natl Acad Sci USA. 98:4746-4751
- Harauz, G., Ishiyama, N., Hill, CM., Bates, IR., Libich, DS., Fares, C. (2004). Myelin basic protein-diverse conformational states of an intrinsically unstructured protein and its roles in myelin assembly and multiple sclerosis. Micron. 35: 503-542
- Heldin, CH., Ostman, A., Ronnstrand, L. (1998). Signal transduction via platelet-derived growth factor receptors. Biochim Biophys Acta. 1378(1):F79-113
- Heldin, CH. and Westermark, B. (1999). Mechanism of action and in vivo role of platelet-derived growth factor. Physiol Rev. 79: 1283-1316
- Hinman, JD. and Abraham, CR. (2007). What's behind the decline? The role of white matter in brain aging. Neurochem Res. 32: 2023-2031
- Hutchins, JB. and Jefferson, VE. (1992). Developmental distribution of platelet-derived growth factor in the mouse central nervous system. Dev Brain Res. 67: 121-135
- Huxley, AF. and Stampfli, R. (1949). Evidence for saltatory conduction in peripheral myelinated fibres. J Physiol. 108: 315-339

- Juraska, JM. and Kopcik, JR. (1988). Sex and environmental influences on the size and ultrastructure of the rat corpus callosum. *Brain Res.* 450: 1-8
- Kadi, L., Selvaraju, R., de Lys, P., Proudfoot, AE., Wells, TN., Boschert, U. (2006). Differential effects of chemokines on oligodendrocyte precursor proliferation and myelin formation in vitro. *J Neuroimmunol.* 174: 133-146
- Kakita, A. and Goldman, JE. (1999). Patterns and dynamics of SVZ cell migration in the postnatal forebrain: monitoring living progenitors in slice preparations. *Neuron.* 23: 461-472
- Kaplan, MR., Meyer-Franke, A., Lambert, S., Bennett, V., Duncan, ID., Levinson, SR., Barres, BA. (1997). Induction of sodium channel clustering by oligodendrocytes. *Nature.* 386: 724-728
- Kato, T., Ohtani-Kaneko, R., Ono, K., Okado, N., Shiga, T. (2005). Developmental regulation of activated ERK expression in the spinal cord and dorsal root ganglion of the chick embryo. *Neurosci Res.* 52: 11-19.
- Kessaris, N., Fogarty, M., Iannarelli, P., Grist, M., Wegner, M., Richardson, WD. (2006). Competing waves of oligodendrocytes in the forebrain and postnatal elimination of an embryonic lineage. *Nat Neurosci.* 9(2):173-179
- Kinney, HC., Brody, BA., Kloman, AS., Gilles, FH. (1988). Sequence of central nervous system myelination in human infancy. II. Patterns of myelination in autopsied infants. *J Neuropathol Exp Neurol.* 47: 217-234

- Klinghoffer, RA., Muetting-Nelsen, PF., Faerman, A., Shani, M., Soriano, P. (2001).
The two PDGF receptors maintain conserved signaling in vivo despite
divergent embryological function. *Mol Cell*. 7: 343-354
- Koeppen, AH. and Robitaille Y. (2002). Pelizaeus-Merzbacher disease. *J Neuropathol*
Exp Neurol. 61: 747-759
- Kujala, P., Portin, R., Ruutinen, J. (1997). The progress of cognitive decline in
multiple sclerosis. A controlled 3-year follow-up. *Brain*. 120: 289-297
- Levi, G., Aloisi, F., Wilkin, GF. (1987). Differentiation of cerebellar bipotential glial
precursors into oligodendrocytes in primary culture: developmental profile of
surface antigens and mitotic activity. *J Neurosci Res*. 18(3): 407-417
- Levison, SW., Chuang, C., Abramson, BJ., Goldman, JE. (1993). The migrational
patterns and developmental fates of glial precursors in the rat subventricular
zone are temporally regulated. *Development*. 119:611-622
- Levison, SW. and Goldman, JE. (1993). Both oligodendrocytes and astrocytes develop
from progenitors in the subventricular zone of postnatal rat forebrain. *Neuron*.
10(2): 201-212
- Li, C., Tropak, MB., Gerlai, R., Clapoff, S., Abramow-Newerly, W., Trapp, B.,
Peterson, A., Roder, J. (1994). Myelination in the absence of myelin-associated
glycoprotein. *Nature*. 369: 747-750
- Lin, T., Xiang, Z., Cui, L., Stallcup, W., Reeves, SA. (2006). New mouse
oligodendrocyte precursor (mOP) cells for studies on oligodendrocyte
maturation and function. *J Neurosci Methods*. 157: 187-194.

- Looney, GA. and Elberger, AJ. (1986). Myelination of the corpus callosum in the cat: time course, topography, and functional implications. *J Comp Neurol.* 248: 336-347
- Lyon, G., Fattal-Valevski, A., Kolodny, EH. (2006). Leukodystrophies: clinical and genetic aspects. *Top Magn Reson Imaging.* 17: 219-242
- McKerracher, L., David, S., Jackson, DL., Kottis, V., Dunn, RJ., Braun, PE. (1994). Identification of myelin-associated glycoprotein as a major myelin-derived inhibitor of neurite growth. *Neuron.* 13:805-811
- Menn, B., Garcia-Verdugo, JM., Yaschine, C., Gonzalez-Perez, O., Rowitch, D., Alvarez-Buylla, A. (2006). Origin of oligodendrocytes in the subventricular zone of the adult brain. *J Neurosci.* 26: 7907-7918
- Mercola, M., Wang, CY., Kelly, J., Brownlee, C., Jackson-Grusby, L. (1990). Selective expression of PDGF A and its receptor during early mouse embryogenesis. *Dev Biol.* 138: 114-122
- Miller, RH. (1996). Oligodendrocyte origins. *Trends Neurosci.* 19(3):92-96
- Miller, RH. (2002). Regulation of oligodendrocyte development in the vertebrate CNS. *Prog Neurobiol.* 67: 451-467
- Miller, RH. and Bai, L. (2007). Cellular approaches for stimulating CNS remyelination. *Regen Med.* 2: 817-829
- Milner, R., Anderson HJ., Rippon, RF., McKay, JS., Franklin, RJ., Marchionni, MA., Reynolds, R. and French-Constant, C. (1997). Contrasting effects of mitogenic growth factors on oligodendrocyte precursor cell migration. *Glia.* 19: 85-90

- Mikoshiha, K., Okano, H., Tamura, T., Ikenaka, K. (1991). Structure and function of myelin protein genes. *Annu Rev Neurosci.* 14: 201-217
- Ndubaku, U. and de Bellard, ME. (2008). Glial cells: old cells with new twists. *Acta histochem.* 110:182-195
- Newton, R., Cambridge, L., Hart, LA., Stevens, DA., Lindsay, MA., Barnes, PJ. (2000). The MAP kinase inhibitors, PD098059, U0126 and SB203580, inhibit IL-1beta- dependent PGE (2) release via mechanistically distinct processed. *Br J Pharmacol.* 130: 1353-1361
- Nishiyama, A., Lin, XH., Giese, N., Heldin, CH., Stallcup, WB. (1996). Co-localization of NG2 proteoglycan and PDGF alpha-receptor on O2A progenitor cells in the developing rat brain. *J Neurosci Res.* 43(3):299-314
- Noble, M., Murray, K., Stroobant, P., Waterfield, MD., Riddle, P. (1988). Platelet-derived growth factor promotes division and motility and inhibits premature differentiation of the oligodendrocyte/type-2 astrocyte progenitor cell. *Nature.* 333(6173): 560-562.
- Omari, KM., John, G., Lango, R., Raine, CS. (2006). Role for CXCR2 and CXCL1 on glia in multiple sclerosis. *Glia.* 53: 24-31
- Oumesmar, BN., Vignais, L., Baron-Van Evercooren, A. (1997). Developmental expression of platelet-derived growth factor alpha-receptor in neurons and glial cells of the mouse CNS. *J. Neurosci.* 17(1): 125-139

- Padovani-Claudio, DA., Liu, L., Ransohoff, RM., Miller, RH. (2006). Alterations in the oligodendrocyte lineage, myelin, and white matter in adult mice lacking the chemokine receptor CXCR2. *Glia*. 54: 471-483
- Polito, A. and Reynolds, R. (2005). NG2-expressing cells as oligodendrocyte progenitors in the normal and demyelinated adult central nervous system. *J Anat*. 207: 707-716
- Pringle, NP. and Richardson, WD. (1993). A singularity of PDGF alpha-receptor expression in the dorsoventral axis of the neural tube may define the origin of the oligodendrocyte lineage. *Development*. 117(2): 525-533
- Pringle, NP., Mudhar, HS., Collarini, EJ., Richardson, WD. (1992). PDGF receptors in the rat CNS: during late neurogenesis, PDGF alpha-receptor expression appears to be restricted to glial cells of the oligodendrocyte lineage. *Development*. 115: 535-551
- Privat, A., Jacque, C., Bourre, JM., Dupouey, P., Baumann, N. (1979). Absence of the major dense line in myelin of the mutant mouse "shiverer". *Neurosci Lett*. 12: 107-112
- Raff, MC., Abney, ER., Cohen, J., Lindsay, R., Noble, M. (1983). Two types of astrocytes in cultures of developing rat white matter: differences in morphology, surface gangliosides, and growth characteristics. *J Neurosci*. 3(6): 1289-1300
- Rakic, S. and Zecevic, N. (2003). Early oligodendrocyte progenitor cells in the human fetal telencephalon. *Glia*. 41(2):117-127

- Robinson, S. and Franic, LA. (2001). Chemokine GRO1 and the spatial and temporal regulation of oligodendrocyte precursor proliferation. *Dev neurosci.* 23: 338-345
- Robinson, S., Tani, M., Strieter, RM., Ransohoff, RM., Miller, RH. (1998). The chemokine growth-regulated oncogene-alpha promotes spinal cord oligodendrocyte precursor proliferation. *J Neurosci.* 18: 10457-10463
- Schachner, M., Kim, SK., and Zehnle, R. (1981). Developmental expression in central and peripheral nervous system of oligodendrocyte cell surface antigens (O antigens) recognized by monoclonal antibodies. *Dev Biol.* 83: 328-338.
- Simons, M. and Trotter, J. (2007). Wrapping it up: the cell biology of myelination. *Curr Opin Neurobiol.* 17: 533-540
- Simpson, PB. and Armstrong, RC. (1999). Intracellular signals and cytoskeletal elements involved in oligodendrocyte progenitor migration. *Glia.* 26: 22-35
- Soriano, P. (1997). The PDGF receptor is required for neural crest cell development and for normal patterning of the somites. *Development.* 124: 2691-2700
- Stariha, RL. and Kim, SU. (2001). Protein kinase C and mitogen-activated protein kinase signalling in oligodendrocytes. *Microsc Res Tech.* 52: 680-688
- Storch, M. and Lassmann, H. (1997). Pathology and pathogenesis of demyelinating diseases. *Curr Opin Neurol.* 10: 186-192
- Stork, PJ. (2002). ERK signaling : duration, duration, duration. *Cell Cycle.* 1(5):315-317

- Suzuki, SO. and Goldman, JE. (2003). Multiple cell populations in the early postnatal subventricular zone take distinct migratory pathways: a dynamic study of glial and neuronal progenitor migration. *J Neurosci.* 23: 4240-4250
- Szalay, F. (2001). Development of the equine brain motor system. *Neurobiology.* 9: 107-135
- Tkachev, D., Mimmack, ML., Ryan, MM., Wayland, M., Freeman, T., Jones, PB., Starkey, M., Webster, MJ., Yolken, RH., Bahn, S. (2003). Oligodendrocyte dysfunction in schizophrenia and bipolar disorder. *Lancet.* 362: 798-805
- Tokumoto, YM., Durand, B., Raff, MC. (1999). An analysis of the early events when oligodendrocyte precursor cells are triggered to differentiate by thyroid hormone, retinoic acid, or PDGF withdrawal. *Dev Biol.* 213: 327-339
- Trajkovic, K., Dhaunchak, AS., Goncalves, JT., Wenzel, D., Schneider, A., Bunt, G., Nave, KA, Simons, M. (2006). Neuron to glia signaling triggers myelin membrane exocytosis from endosomal storage sites. *J Cell Biol.* 172: 937-948
- Tsai, HH., Frost, EE., To, V., Robinson, S., French-Constant, C., Geertman, R., Ransohoff, RM., Miller, RH. (2002). The chemokine receptor CXCR2 controls positioning of oligodendrocyte precursors in developing spinal cord by arresting their migration. *Cell.* 110: 373-383
- Tsai, HH., Tessier-Lavigne, M. and Miller, RH. (2003). Netrin 1 mediates spinal cord oligodendrocyte precursor dispersal. *Development.* 130(10): 2095-2105

- Vincze, A., Mazlo, M., Seress, L., Komoly, S., Abraham, H. (2008). A correlative light and electron microscopic study of postnatal myelination in the murine corpus callosum. *Int J Dev Neurosci.* 26:575-584
- Wang, X., Zhu, C., Qiu, L., Hagberg, H., Sandberg, M., Blomgren, K. (2003). Activation of ERK1/2 after neonatal rat cerebral hypoxia-ischaemia. *J Neurochem.* 86: 351-362.
- Wiggins, RC. and Gottesfeld, Z. (1986). Restraint stress during late pregnancy in rats elicits early hypermyelination in the offspring. *Metab Brain Dis.* 1: 197-203
- Windebank, AJ., Wood, P., Bunge, RP., Dyck, PJ. (1985). Myelination determines the caliber of dorsal root ganglion neurons in culture. *J Neurosci.* 5: 1563-1569
- Zalc, B. and Fields, RD. (2000). Do action potentials regulate myelination? *Neuroscientist.* 6(1): 5-13
- Zalc, B., Goujet, D. and Colman, D. (2008). The origin of the myelination program in vertebrates. *Curr Biol.* 18(12): R511-512
- Zujovic, V., Bachelin, C. and Baron-Van Evercooren, A. (2007). Remyelination of the central nervous system: a valuable contribution from the periphery. *Neuroscientist.* 13: 383-391